CANADIAN THESES ON MICROFICHE

THÈSES CANADIENNES SUR MICROFICHE

National Library of Canada
Collections Development Branch

Canadian Theses on
Microfiche Service

Ottawa, Canada
K1A 0N4

Bibliothèque nationale du Canada
Direction du développement des collections

Service des thèses canadiennes
sur microfiche

NOTICE

The quality of this microfiche is heavily dependent upon the quality of the original thesis submitted for microfilming. Every effort has been made to ensure the highest quality of reproduction possible.

If pages are missing, contact the university which granted the degree.

Some pages may have indistinct print especially if the original pages were typed with a poor typewriter ribbon or if the university sent us an inferior photocopy.

Previously copyrighted materials (journal articles, published tests, etc.) are not filmed.

Reproduction in full or in part of this film is governed by the Canadian Copyright Act, R.S.C. 1970, c. C-30. Please read the authorization forms which accompany this thesis.

AVIS

La qualité de cette microfiche dépend grandement de la qualité de la thèse soumise au microfilmage. Nous avons tout fait pour assurer une qualité supérieure de reproduction.

S'il manque des pages, veuillez communiquer avec l'université qui a conféré le grade.

La qualité d'impression de certaines pages peut laisser à désirer, surtout si les pages originales ont été dactylographiées à l'aide d'un ruban usé ou si l'université nous a fait parvenir une photocopie de qualité inférieure.

Les documents qui font déjà l'objet d'un droit d'auteur (articles de revue, examens publiés, etc.) ne sont pas microfilmés.

La reproduction, même partielle, de ce microfilm est soumise à la Loi canadienne sur le droit d'auteur, SRC 1970, c. C-30. Veuillez prendre connaissance des formules d'autorisation qui accompagnent cette thèse.

THIS DISSERTATION
HAS BEEN MICROFILMED
EXACTLY AS RECEIVED

LA THÈSE A ÉTÉ
MICROFILMÉE TELLE QUE
NOUS L'AVONS REÇUE

Canada

NL 339 (r. 88/09)

D 315-19416-2

National Library of Canada | Bibliothèque nationale du Canada

Canadian Theses Division | Division des thèses canadiennes

Ottawa, Canada
K1A 0N4

67324

PERMISSION TO MICROFILM — AUTORISATION DE MICROFILMER

• Please print or type — Écrire en lettres moulées ou dactylographier

Full Name of Author — Nom complet de l'auteur

Nelson Gordon Curdk

Date of Birth — Date de naissance

Sept. 30, 1943

Country of Birth — Lieu de naissance

Canada

Permanent Address — Résidence fixe

10533 – 29A Ave
Edmonton, Alberta

Title of Thesis — Titre de la thèse

Measurement and Analysis of Electrical [redacted]
Slow Wave Activity of the Colon.

University — Université

University of Alberta.

Degree for which thesis was presented — Grade pour lequel cette thèse fut présentée

Ph. D. in Electrical Engineering

Year this degree conferred — Année d'obtention de ce grade

1983

Name of Supervisor — Nom du directeur de thèse

Y. J. Kingma

Permission is hereby granted to the NATIONAL LIBRARY OF CANADA to microfilm this thesis and to lend or sell copies of the film.

The author reserves other publication rights, and neither the thesis nor extensive extracts from it may be printed or otherwise reproduced without the author's written permission.

L'autorisation est, par la présente, accordée à la BIBLIOTHÈQUE NATIONALE DU CANADA de microfilmer cette thèse et de prêter ou de vendre des exemplaires du film.

L'auteur se réserve les autres droits de publication; ni la thèse ni de longs extraits de celle-ci ne doivent être imprimés ou autrement reproduits sans l'autorisation écrite de l'auteur.

Date

Aug. 21/85

Signature

N. G. Curdk

NL-91 (4/77)

THE UNIVERSITY OF ALBERTA

MEASUREMENT AND ANALYSIS OF ELECTRICAL SLOW WAVE ACTIVITY OF THE COLON

by

NELSON GORDON DURDLE

A THESIS

SUBMITTED TO THE FACULTY OF GRADUATE STUDIES AND RESEARCH

IN PARTIAL FULFILLMENT OF THE REQUIREMENTS FOR THE DEGREE

OF DOCTOR OF PHILOSOPHY

DEPARTMENT OF ELECTRICAL ENGINEERING

EDMONTON, ALBERTA

SPRING, 1983

THE UNIVERSITY OF ALBERTA

RELEASE FORM

NAME OF AUTHOR Nelson Gordon Durdle

TITLE OF THESIS Measurement and Analysis of Electrical Slow Wave Activity of the Colon

DEGREE FOR WHICH THESIS WAS PRESENTED Doctor of Philosophy

YEAR THIS DEGREE GRANTED 1983

Permission is hereby granted to THE UNIVERSITY OF ALBERTA LIBRARY to reproduce single copies of this thesis and to lend or sell such copies for private, scholarly or scientific research purposes only.

The author reserves other publication rights, and neither the thesis nor extensive extracts from it may be printed or otherwise reproduced without the author's written permission.

(Signed) N. G. Durdle

PERMANENT ADDRESS:
10533 - 29A Avenue
Edmonton, Alberta

DATED April 21, 1983

THE UNIVERSITY OF ALBERTA

FACULTY OF GRADUATE STUDIES AND RESEARCH

The undersigned certify that they have read, and recommend to the Faculty of Graduate Studies and Research, for acceptance, a thesis entitled MEASUREMENT AND ANALYSIS OF THE ELECTRICAL SLOW WAVE ACTIVITY OF THE COLON submitted by NELSON G. DURDLE in partial fulfillment of the requirements for the degree of Doctor of Philosophy.

.....

.....

Supervisors

.....

.....

.....

External Examiner

Date ..April 6, 1983.....

DEDICATION

to my wife, son and daughter
whose sacrifice made this work
a reality.

ABSTRACT

The electrical slow wave activity of the colon was studied using in vitro muscle strips of canine colon. Recordings were obtained using both extracellular pressure electrodes and intracellular microelectrodes. Electrical coupling between regions was studied using multisite measurements on each side of the intact muscle wall and on each side of isolated circular and longitudinal muscle layers. Coupling and intrinsic oscillator frequencies were also studied by calculating frequencies and phase angles before and after cutting the tissue between recording sites. The origin of the slow wave and the roles played by the individual muscle layers in the generation of the slow wave were studied using the simultaneous application of extracellular electrodes to both sides of the intact muscle wall and isolated muscle layers. The above points were also examined using intracellular microelectrode measurements. Also, the intracellular-to-extracellular transduction mechanism was examined using simultaneous intracellular and extracellular measurements and intracellular measurements in cells directly below simultated pressure electrodes. Computer programs were written to manipulate, process and display experimental results.

The results may be summarized as follows:

1. The electrical slow wave originates at the boundary of the inner circular layer and the submucosa, and the integrity of the circular muscle-to-submucosa interface is essential for the existence of the slow wave.
2. The slow wave is not generated by cells of the longitudinal muscle layer.

3. The mean resting potential and slow wave amplitude of cells in the circular muscle layer was -77.8 ± 6.8 mV and 28.9 ± 5.5 mV respectively.
4. The mean resting potential of longitudinal muscle cells was -52.6 ± 7.0 mV.
5. With regard to electrical coupling between oscillatory regions in the circular and longitudinal directions:
   (a) Coupling was better in the circular direction than in the longitudinal direction. The mean phase angle for an electrode spacing of 2.5 mm in the circular direction was 29.0 ± 23.2 as compared to 117.3 ± 51.0 degrees in the longitudinal direction.
   (b) No gradient of intrinsic oscillator frequencies existed in the longitudinal direction but a frequency gradient was present in the circular direction with respect to the mesenteric border.
6. With respect to the intracellular-to-extracellular transduction mechanism:
   (a) The results do not support the generally accepted pressure electrode hypothesis proposed by Bortoff (1967).
   (b) Contrary to this theory the application of a pressure electrode resulted in a reduction in the intracellular potential of the slow wave trough but did not change the intracellular potential of the slow wave plateau.

ACKNOWLEDGEMENTS

The author would like to express his sincere gratitude to his supervisor Prof. Y.J. Kingma for his guidance and valuable suggestions throughout the course of this work and to Dr. K.L. Bowes for useful advice and moral support.

The physiological measurements were conducted in the Surgical Medical Research Institute and the author wishes to thank its director Dr. G. Scott and his staff for their support.

The support received from the supervisor and staff of the electrical engineering machine shop is also gratefully appreciated.

Financial support for this work was provided in part by both the Medical Research Council and the National Science and Engineering Research Council.

TABLE OF CONTENTS

CHAPTER		PAGE
1.	INTRODUCTION	1
	1.1 MOTIVATION	1
	1.2 SCOPE OF THE PRESENT WORK	2
	1.3 THESIS ORGANIZATION	5
2.	ANATOMY OF THE COLON	7
	2.1 INTRODUCTION	7
	2.2 GROSS ANATOMY AND FUNCTION	7
	2.3 THE MUSCLE COAT	11
	2.4 CONTROL OF CONTRACTIONS	15
3.	SLOW WAVE ACTIVITY	18
	3.1 INTRODUCTION	18
	3.2 SLOW WAVES IN THE COLON AND SMALL INTESTINE	18
	3.2.1 Electrical Characteristics	18
	3.2.2 Relationship to Mechanical Activity	19
	3.2.3 Site of Origin of Slow Wave Activity	21
	3.2.4 The Ionic Basis for Slow Waves	22
	3.3 MODELLING WITH COUPLED RELAXATION OSCILLATORS	23
	3.3.1 Introduction	23
	3.3.2 Modelling of Slow Wave Activity in the Canine Colon	27
	3.3.3 Modelling of Slow Wave Activity in the Canine Small Intestine	27
	3.4 INTRACELLULAR-TO-EXTRACELLULAR SIGNAL TRANSDUCTION	30
	3.4.1 Introduction	30

CHAPTER PAGE

3.4.2 The Injury Potential Theory 31
3.4.3 An Extension of Gillespie's Model 33
3.5 SLOW WAVE ACTIVITY IN THE COLON 35
3.5.1 Introduction 35
3.5.2 Slow Waves in the Human Colon 36
3.5.3 Slow Waves in the Cat Colon 36
3.5.4 Slow Waves in the Canine Colon 37

4. OBJECTIVES, METHODS, AND MATERIALS 39
4.1 INTRODUCTION 39
4.2 THE DESIGN AND STUDY OF A NEW PRESSURE ELECTRODE 40
4.2.1 Electrode Description 41
4.2.2 Electrode Impedance Minimization 42
4.2.3 Electrode Impedance Measurement 44
4.3 EXTRACELLULAR STUDIES 46
4.3.1 Multisite Electrode Studies on the Intact Muscle Wall 46
4.3.2 Phase Angles as a Function of Electrode Spacing 49
4.3.3 The Cutting Experiments 51
4.3.4 Studies on Isolated Muscle Layers 52
4.3.5 Separation and Study of Longitudinal and Circular Muscle Layers 53
4.3.6 Dual Chamber Studies 55
4.4 INTRACELLULAR STUDIES 57
4.4.1 Introduction 57
4.4.2 The Measurement System 58
4.4.3 Circular Muscle Measurements 61
4.4.4 Longitudinal Muscle Measurements 62
4.5 STUDIES OF THE INTRACELLULAR-TO-EXTRACELLULAR TRANSDUCTION PROCESS 64
4.5.1 Introduction 64

CHAPTER PAGE

4.5.2 A Comparison of Intracellular and Extracellular Electrode Potentials 64
4.5.3 Injury Potential Measurement 65
4.6 COMPUTER ANALYSIS 67

5. EXPERIMENTAL RESULTS 69
5.1 INTRODUCTION 69
5.2 ELECTRODE CHARACTERISTICS 69
5.2.1 An Electrode Model 70
5.2.2 Consideration of Signal Distortion Due to Electrode Characteristics 75
5.3 EXTRACELLULAR RESULTS 78
5.3.1 Phase Angles as a Function of Electrode Spacing 78
5.3.2 Interpretation of Results 82
5.3.3 The Results from the Cutting Experiments 87
5.3.4 Results from the Studies of Isolated Muscle Layers 91
5.3.5 The Submucosal Layer 92
5.3.6 Results from the Dual Chamber Studies 101
5.4 INTRACELLULAR RESULTS 110
5.4.1 Circular Muscle Measurements on the Intact Muscle 110
5.4.2 Measurements on Isolated Circular Muscle 113
5.4.3 Longitudinal Muscle Measurements 116
5.5 RESULTS FROM STUDIES OF THE INTRACELLULAR-TO-EXTRACELLULAR TRANSDUCTION PROCESS 119
5.5.1 A Comparison of Simultaneous Intracellular and Extracellular Measurements 119
5.5.2 Injury Potential Measurement 121

CHAPTER PAGE

6. CONCLUSIONS 128

6.1 INTRODUCTION 128

6.2 SLOW WAVE ORIGIN 128

6.3 INTRACELLULAR SLOW WAVE CHARACTERISTICS 132

6.4 ELECTRICAL COUPLING WITHIN THE COLON 134

6.5 PRESSURE ELECTRODE SIGNAL TRANSDUCTION 134

6.6 A PROPOSED THEORY FOR SLOW WAVE GENERATION AND PRESSURE ELECTRODE SIGNAL GENERATION 136

6.7 AN EXAMINATION OF THE ROLES PLAYED BY THE INDIVIDUAL MUSCLE LAYERS IN THE GENERATION OF SLOW WAVE ACTIVITY 142

6.7.1 The Circular Layer 142

6.7.2 The Longitudinal Layer 143

6.8 FUTURE WORK 145

REFERENCES 146

APPENDIX A 153

APPENDIX B 222

LIST OF TABLES

TABLE		PAGE
5.1	Phase angle between recording sites as a function of electrode spacing.	84
5.2	Cutting experiment results for longitudinally oriented strips. NC is defined as Not Coupled.	88
5.3	Cutting experiment results for circularly oriented strips. NC is defined as Not Coupled.	90
5.4	Intracellular Results on the Intact Muscle.	114
5.5	A summary of intracellular results from isolated longitudinal and circular layers.	115
5.6	Results from experiments to determine the affect of extracellular electrode force on intracellular potential.	123
5.7	Summary of the results of Table 5.6 arranged in order of increasing electrode force.	125

LIST OF FIGURES

FIGURE		PAGE
2.1	Attachment of the human colon to the dorsal wall via the mesentery.	9
2.2	Diagrammatic cross-section showing the structure of the canine colon wall.	10
2.3	Diagram of a longitudinal section through the smooth muscle of the dog intestine.	12
2.4	Cross-section of the human colon wall.	13
2.5	The arrangement of smooth muscle cells in a muscle bundle of the guinea-pig vas deferens.	14
2.6	Model of a gap junction.	16
3.1	Microelectrode recordings from the musculature of cat intestine.	20
3.2	Block diagram illustrating the arrangement of oscillators in the intestinal model.	26
3.3	Arrangement of oscillators in the gastric ECA model.	28
3.4	Diagram showing the intrinsic frequency gradients of the dog stomach.	29
3.5	The injury potential generated by an extracellular electrode, and an equivalent circuit of the extracellular signal generation.	32
3.6(a)	A schematic drawing of a pressure electrode measurement.	
(b)	An equivalent circuit.	34
4.1	Pressure Electrode Details.	43
4.2	Electrode impedance as a function of chloriding levels and frequency.	45
4.3	Multisite electrode experiments designed to examine coupled oscillator characteristics.	47

FIGURE		PAGE
4.4	Experiments designed to determine the origin of the slow wave signal.	48
4.5	The constant temperature bath and extracellular measurement apparatus.	50
4.6	Histology slides showing (a) the intact muscle wall, (b) the isolated longitudinal layer, and (c) the isolated circular layer.	54
4.7	The dual chambered measurement system.	56
4.8	The intracellular measurement system.	59
4.9	Details of the intracellular measurement system.	60
4.10	Tissue mounting configurations.	63
4.11	Apparatus simulating the application of the pressure electrode to an intact muscle specimen.	66
4.12	The Hewlett-Packard 21 MX/E computer system.	68
5.1	The real and reactive components of the impedance of a typical electrode plotted as a function of frequency.	71
5.2	Real and reactive components of the impedance of a twelve-day-old electrode.	72
5.3	Electrode Noise (a) Normal Electrode (b) Unchlorided Electrode	73
5.4	Electrode impedance model.	74
5.5	Slow wave measurement circuit.	77
5.6	A recording from four pressure electrodes applied to the mucosal side of the intact muscle wall.	79
5.7	Output from the fourier transform program "PSPT".	80

FIGURE		PAGE
5.8	Output from the zero-crossing program "PHSE".	81
5.9	Output from the x-correlation program "XCORR".	83
5.10	Four pressure electrode signals from the serosal side of isolated longitudinal muscle.	93
5.11(a)	Slow waves from the mucosal side of isolated circular muscle.	94
5.11(b)	Slow waves from the longitudinal side of isolated circular muscle.	95
5.12	Histology slides showing (a) the circular muscle before the removal of the submucosal layer, (b) the circular muscle after the removal of the submucosal layer, and (c) the submucosal layer.	97
5.13(a)	Slow waves recorded from the mucosal side of the intact muscle wall before removal of the submucosa.	98
5.13(b)	Slow waves recorded from the mucosal side of the intact muscle wall after removal of the submucosa from half of the specimen.	99
5.14	A recording from the mucosal side of the intact muscle wall after complete removal of the submucosal layer.	100
5.15	Typical signals from an intact muscle specimen in the dual chambered bath.	102
5.16(a)	Dual chamber recording with normal Krebs-Ringer solution.	104
5.16(b)	KCl concentration changed to 30 mM on the mucosal side of the bath.	105
5.16(c)	Tissue washed with normal Krebs-Ringer solution.	106

FIGURE		PAGE
5.16(d)	KCl concentration changed to 30 mM on the longitudinal side of the bath.	107
5.17	Dual chamber study of isolated circular muscle.	108
5.18	Burst activity recorded from isolated longitudinal muscle.	109
5.19	Recordings of the potential of the circular reference electrode with respect to the longitudinal reference electrode in the presence of (a) an intact muscle specimen, and (b) an isolated circular muscle specimen.	111
5.20	A typical intracellular recording from a circular muscle cell.	112
5.21	A typical intracellular recording from a longitudinal cell.	117
5.22	Burst activity recorded intracellularly from a longitudinal cell penetration.	118
5.23	Simultaneous recording of intracellular and extracellular signals.	120
5.24	Intracellular potentials in the presence of an extracellular pressure electrode.	122
5.25	Normalized slow wave amplitude versus extracellular electrode application force.	127
6.1	Model of the smooth muscle membrane.	139
6.2	Extracellular pressure electrode slow wave generation.	141
6.3	A model showing a possible arrangement of oscillators in the colon wall.	144
A-2-1	Flow chart of FLOCT.	158
A-2-2	Program listing of DWRI and table showing disc file organization.	164

FIGURE		PAGE
A-3-1	Flow chart of TDSPL.	173
A-4-1	Flow chart of PLOT.	179
A-4-2	Typical single channel output of subroutine PLOT.	181
A-5-1	Flow chart of program FILTR.	187
A-6-1	Flow chart of program PSPT.	194
A-6-2	Typical single channel output from program PSPT.	196
A-7-1	Flow chart of program PHSE.	202
A-7-2	Typical output from the program PHSE.	204
A-8-1	Flow chart of program XCORR.	211
A-8-2	Typical output of program XCORR.	212

LIST OF PROGRAM LISTINGS

PROGRAM LISTING	PROGRAM	PAGE
A-2-1	FLOCT	159
A-2-2	STPT	167
A-2-3	DREA	169
A-2-4	RDPT	171
A-3-1	TDSPL	174
A-3-2	GRID	176
A-4-1	PLOT	182
A-5-1	FILTR	188
A-5-2	BPASS	189
A-5-3	DCAC	191
A-6-1	PSPT	197
A-6-2	SMTH	200
A-7-1	PHSE	205
A-7-2	LFIT	209
A-8-1	XCORR	213
A-9-1	MAIN	219

CHAPTER 1

INTRODUCTION

1.1 MOTIVATION

Electrical signals are known to play a major role in the control of many physiological systems. The majority of these signals may be placed into one of two categories. Either they are of a pulsatile nature such as the action potentials which permit communication within the nervous system or they are cyclic oscillatory signals of the type generated by the sinoatrial node of the heart.

It has been known since 1922 (Alverez and Mahoney) that the gastrointestinal tract is electrically active. It has been shown since that time that both action potentials and slow oscillatory type signals generated within the organs themselves play a role in the control of contractions in the stomach (Sarna, 1971), small intestine (Sarna, 1971), and colon (Shearin et. al., 1979). These electrical signals and their control function are best understood in the stomach and least understood in the colon.

The purpose of this work is to increase the understanding of the electrical activity and its control function in the human colon. The immediate incentive for persuing this is the acquisition of information which will lead to improved clinical treatment of colonic dysfunction.

1.2 SCOPE OF THE PRESENT WORK

The study of the electrical activity of the colon could be pursued in a number of different ways. One could study the intrinsic cyclic electrical activity generated by the smooth muscle of the colon wall, the neural control of the organ, or the integration of both the intrinsic and neural signals in the control of colon function. The first of these approaches was adopted by this present work.

The intrinsic cyclic electrical activity of the gastrointestinal tract has been referred to as slow waves, electrical control potentials, and basic electrical rhythm (Bass, 1968; Connor, 1979; Szurszewski, 1981). The term slow waves will be used in this thesis. The principal objectives of this work are (1) the definition of the origin of the slow wave activity in the colon, (2) the definition of the role played by each of the muscle layers in the generation of the slow wave, and (3) the determination of the basic electrical characteristics of this signal. The last of these will require an examination of the intracellular resting potentials and slow wave amplitudes as well as an examination of the phase relationships of signals recorded from different sites.

A number of alternative ways of attaining these objectives were considered. One method was to study the electrical activity in vivo in humans using surgically implanted electrodes. An alternative to this was the study of the activity in vitro from organ specimens removed during required surgery. Another approach was the study of the colonic electrical activity in animals using either in vivo or in vitro recording techniques.

The first of the above methods was seriously considered because it would examine the electrical activity of the human colon under close-to-normal physiological conditions. However, a number of difficulties existed with this approach. The first of these difficulties was in finding a sufficient number of subjects for the study. Electrodes could only be placed in patients who required abdominal surgery and who gave informed consent. The availability of such subjects would require a long period of time to obtain sufficient data. Since this study would be on post operative patients, many of whom were being treated for some colon disfunction, the normality of the data might be suspect. In addition to this, currently available in vivo electrodes produce very poor quality signals. These electrodes usually consist of stainless steel or platinum wires inserted into the colon muscle wall. The signals obtained from such electrodes are of very low amplitude and contain large noise components due to electrode movement.

The second approach considered was the study of human colonic muscle in vitro. This approach has advantages in comparison to in vivo studies because it does not have to contend with electrode movement artifacts and because signals obtained from in vitro electrodes are usually larger in amplitude than in vivo signals. However, this type of study is hindered by the lack of availability of healthy human tissue. Specimens are only available from patients who require colonic surgery. Therefore, these specimens are obtained from abnormal organs. Because the surgeon's primary concern is for his patient, and not for the health of the specimen, the viability of such specimens would be questioned.

The third method of study considered was the in vitro and in vivo study of slow wave activity in an animal with colon and colonic function similar to man. The major advantage of this approach was the adequate supply of animals and animal tissue. However, animal in vivo studies have electrode and movement artifact problems similar to their human counterparts. In vitro animal studies have the disadvantages (1) that the tissue is not maintained in exactly the same physiological state as it would be in vivo and (2) that the tissue under study is not human tissue. Species differences could make the results inapplicable to the human organ. However, studies of the electrical activity of the canine stomach and small intestine have greatly increased the understanding of the electrical activity in the corresponding human organs (Sarna, 1971; El-Sharkawy et. al., 1978; Szurszewski, 1981).

In vitro studies have the advantages of (1) a ready supply of tissue, (2) few movement artifacts, (3) larger signals from electrodes which are better understood than in vivo electrodes, and (4) the facility to permit changes in the ionic composition and the application of hormonal agents at the measurement site. For the above reasons, and because in vitro canine studies have proven very useful in many other gastrointestinal studies, the research described in this thesis is based entirely on studies of in vitro strips of canine colon. The work uses both extracellular silver-silverchloride pressure electrodes (Kingma, et. al., 1982) and intracellular microelectrodes. Because the relationship between extracellular pressure electrode signals and their associated intracellular potential variations has not been adequately defined, it was necessary to investigate the pressure electrode transduction mechanism. Also, because the

characteristics of silver-silverchloride electrodes were not known for the very low frequencies (4 to 7 cycles/minute) found in the colon, it was necessary to measure the electrode impedance versus frequency characteristics.

The extracellular studies included multisite measurements on strips of both the intact colonic muscle wall and of isolated muscle layers. Also, they included simultaneous measurements on opposite sides of the intact muscle wall as well as on opposite sides of isolated muscle layers.

The microelectrode studies involved the recording of intracellular potentials from cells in both muscle layers of the colonic wall. These measurements were also used to compare extracellular and intracellular signals and to investigate the mechanism responsible for the generation of the extracellular pressure electrode signal.

1.3 THESIS ORGANIZATION

Because of the interdisciplinary nature of this work it is expected that it will be read by both engineers and medical scientists. To make the work more easily understood by the engineering reader Chapter 2 provides a description of the anatomy of the colon. Chapter 3 provides a review of studies of electrical slow wave activity conducted on the stomach, small intestine, and colon. This chapter also includes a description of the currently accepted theory of pressure electrode signal generation and of slow wave modelling using relaxation oscillators. Chapter 4 describes the research objectives as well as providing a detailed description of the experiments conducted

to attain these objectives. Chapter 5 provides the results of all experiments and Chapter 6 includes a discussion of the results and of the conclusions which can be deduced from these results.

CHAPTER 2

ANATOMY OF THE COLON

2.1 INTRODUCTION

This chapter is included to provide the reader with a basic knowledge of the anatomy and function of the colon. This will facilitate a better understanding of the motives and significance of the research described in this thesis. It will also define physiological terms using in the following chapters.

Much of the data provided is from animals other than man, but where possible data from the human colon is included. Since the canine colon is to be used in this work the differences and similarities of human and canine colon are particularly noted.

2.2 GROSS ANATOMY AND FUNCTION

The colon or large intestine is the portion of the gastrointestinal tract extending from the ileocecal value to the rectum. The functions of the colon are (1) storage of fecal matter and (2) absorption of water and electrolytes. The proximal half of the colon is concerned principally with absorption and the distal half with storage. The caliber of the organ is greatest at the proximal end and its diameter reduces towards the rectum. As shown in Figure 2.1 there is an alteration of fixed and mobile parts due to variations in the degree of fusion to the dorsal body wall by means of a membranous fold called the mesentery (Schofield, 1968).

A diagrammatic cross section of the alimentary canal illustrating

structures typical of the canine colon is shown in Figure 2.2. As can be seen from this figure the colon wall is composed of a number of distinct layers. The outer lining which is continuous with the mesentery is called the serosa. The muscle wall shown immediately inside the serosa consists of two smooth muscle layers, one oriented in the longitudinal direction and the other in the circular direction. The muscle wall facilitates movement and mixing of bowel contents to improve absorption of fluids. Also the muscle coat is responsible for the mass movement of wastes to the distal end of the colon and for final evacuation of these wastes. As seen in Figure 2.2 the longitudinal muscle coat of the canine colon is continuous around the complete circumference of the organ. However, in the human the longitudinal muscle coat is gathered mainly into distinctive bands or taenia coli. The mucosa or inner lining of the colon is responsible for the absorption of fluids and electrolytes. Associated with the mucosa is another thin smooth muscle layer, the muscularis mucosae. This muscle layer causes movement of the mucosa to maximize fluid absorption. There is a high density of nerves in the colon wall. The majority of these nerves is found in two nerve networks or plexuses. Auerbach's plexus is a network of nerves and ganglia located between the longitudinal and circular muscle layers. Meissner's plexus is located in the submocosa which is a connective tissue layer between the mucosa and the circular muscle layer. These nerve networks form a sophisticated system controlling colon function. This control system combines both local reflex loops in the colon wall and extrinsic inputs from the spinal cord and higher centers to control absorption, muscle contraction and mass movement.

Page 9 has been removed due to copyright restrictions.

It contained a figure entitled, "Figure 2.1 Attachment of the human colon to the dorsal wall via the mesentery".

This figure was obtained from, "Anatomy of muscular and neural tissues in the alimentary canal", by G.C. Schofield, pp. 1579-1628, Handbook of Physiology, ed. C.F. Code, Am. Physiological Society, 1968.

Page 10 has been removed due to copyright restrictions.

It contained a figure entitled, "Figure 2.2 Diagrammatic cross section showing the structure of the alimentary canal".

This figure was obtained from, "Anatomy of muscular and neural tissues in the alimentary canal", by G.C. Schofield, pp. 1579-1628, Handbook of Physiology, ed. C.F. Code, Am. Physiological Society, 1968.

2.3 THE MUSCLE COAT

There is much species variation in the structure of the smooth muscle layers. However, all species studied have both longitudinal and circular muscle layers composed of long thin spindle-like cells ranging in diameter from 4 to 6 μm and in length from 200 to 400 μm (Bennett & Rogers, 1967; McGeachie, 1975; Prosser et. al., 1960; and Schofield, 1968). A connective tissue sheath, the epimysium, completely surrounds the smooth muscle of each layer. Thin septa extend inward from the epimysium to form the perimysium which contains collagenous and elastic fibres as well as fibroblasts, capillaries, and nerves. An example of this arrangement in the longitudinal muscle of the dog intestine is shown in Figure 2.3. The perimysium divides the muscle into bundles of smooth muscle cells. This formation of descrete bundles has been observed in the guinea-pig and cat (Prosser et. al., 1960), the dog (Cajal, 1933), and the human (Schofield, 1968). Transverse sections through the muscle bundles show that they vary in outline from rectangular to circular and are 20 to 200 μm wide. A cross section of muscle bundles in the circular muscle layer of human colon is shown in Figure 2.4. The muscle bundles can be traced in serial transverse sections through a smooth muscle, before they lose their identity by anastomosing with adjacent bundles. Because it is difficult to define where one bundle ends and the next begins, no concensus exists on the length of these bundles.

The packing of smooth muscle cells into a bundle is shown in cross section in Figure 2.5. Each cell in the bundle has about five close neighbours. These cells are separated by a protein-polysaccharide-filled gap of 50 to 80 nm. The three-dimensional relationship between

Page 12 has been removed due to copyright restrictions.

It contained a figure entitled, "Figure 2.3 Diagram of a longitudinal section through the smooth muscle of the dog intestine; the muscle bundles *(b)* and the perimysium *(P)* are clearly shown; the perimysium consists of collagenous and elastic fibres as well as capillaries and nerves; at irregular intervals adjacent bundles fuse or small bundles *(I)* interconnect larger bundles".

This figure was obtained from, "Histology", by S. Cajal, Bailliere, Tindall, & Co., London, 1933.

Page 13 has been removed due to copyright restrictions.

It contained a figure entitled, "Figure 2.4 Cross section of the human colon wall showing the smooth muscle bundles in the circular muscle layer".

This figure was obtained from, "Anatomy of muscular and neural tissues in the alimentary canal", by G.C. Schofield, pp. 1579-1628, Handbook of Physiology, ed. C.R. Code, Am. Physiological Society, 1968.

Page 14 has been removed due to copyright restrictions.

It contained a figure entitled, "Figure 2.5 The arrangement of smooth muscle cells in a muscle bundle of the guinea-pig vas deferens. Electron micrograph montage of a very small muscle bundle *(Bo)* in the longitudinal muscle coat. Note that the muscle bundle is clearly separated by a layer of connective tissue *(c)*, the perimysium, from the neighbouring muscle bundles *B1* and *B2*. Each muscle cell *(M)* at the centre of the bundle is surrounded by about five other muscle cells; *a*, axons; *S*, Schwann cell".

This figure was obtained from, "Autonomic neuromuscular transmission", by M.R. Bennett, Cambridge University Press, 1972.

muscle cells in a bundle has been determined from studies of the guinea-pig (Bennett & Rogers, 1967) and the mouse (Taxi, 1965). In these animals each cell is closely apposed by approximately twelve cells at any point along its length. Approximately equal numbers of cells overlap at either end of any given cell.

The muscle cells within the bundles are connected to each other at points along their lengths by three different types of structures called tight junctions, desmosomes, and gap junctions (Staehelin & Hull, 1978). The main function of tight junctions is to enable the group of cells to maintain an internal environment that is different from the external one. Desmosomes are the mechanical links which hold the tissue together. Gap junctions are believed to play a role in cellular chemical and electrical communication. A broad correlation exists between the appearance of gap junctions and the transmission of action potentials with a tissue (Dewey & Barr, 1962). A model of a gap junction is shown in Figure 2.6. These junctions consist of a 2 nm gap between the apposed outer lamella of adjoining cell membranes which is bridged by an hexagonal array of structures joining the membranes together. It is probable that these structures which bridge the 2 nm gap provide a low resistance pathway between cells (Brightman & Reese, 1969).

2.4 CONTROL OF CONTRACTIONS

Muscle contraction is generally controlled by nerves. In skeletal muscle the effector unit, the smallest unit controlled by the nervous system, is the single muscle fibre. A propagating wave of depolarization (an action potential) arrives at the end of a nerve causing the release of a chemical transmitter substance. For skeletal muscle

Page 16 has been removed due to copyright restrictions.

It contained a figure entitled, "Figure 2.6 Model of a Gap Junction depicts the structural elements that allow the exchange of nutrients and signal molecules between cells without loss of material into the intercellular space. The communicating "pipes" are formed by pairs of abutting particles, which are in turn composed of six dumbbell-shaped protein subunits that span the lipid bilayer of each cell membrane. The channel passing through the cylindrical particles is about 20 angstroms in diameter, limiting the size of the molecules that can pass through it. Unlike the tight junction, fluids and tracers in the intercellular space can permeate the gap junction: they flow around the pipes".

This figure was obtained from, "Junctions between living cells", by L.A. Staehelin, & B.E. Hull, Sci. Am., 238(5):140-152, 1978.

the nerve ending is in close proximity to the muscle fibre it controls. The transmitter substance depolarizes an area of the muscle fibre membrane to a threshold level initiating an action potential in the muscle fibre. This action potential causes the fibre to contract.

In smooth muscle, nerves are not closely associated with specific muscle fibres. The effector unit is not the single muscle cell. It has been shown by Bennett (1972) that it is difficult or impossible to initiate an action potential in a single muscle cell. The response of most smooth muscles to depolarization of their surface membranes is a passive electrotonic depolarization (Kuriyama & Tomita, 1965 and Bennett & Merrillees, 1966). In smooth muscle the effector unit is the smooth muscle bundle. It has been shown by Bennett (1967) and Tomita (1967) that a propagating action potential can be initiated if a large area of the muscle is simultaneously depolarized, either by stimulating the nerves to the muscle or by passing current across the muscle with large extracellular electrodes. The area of muscle which must be simultaneously depolarized in order to initiate a propagating action potential indicates that the effector unit is the muscle bundle. The nervous system causes the release of transmitter substance in the general area of a muscle bundle. When the cells in the bundle have been depolarized to a threshold level, action potentials are initiated and the bundle contracts.

CHAPTER 3

SLOW WAVE ACTIVITY

3.1 INTRODUCTION

The majority of studies of slow waves have been done on the stomach and small intestine. This chapter will first review what is currently known about the slow waves occurring in these organs. It will also discuss the use of coupled oscillator models to simulate the spatial organization of the slow wave activity. Because of the importance of pressure electrode measurements to the work described in this thesis, a discussion is included of the currently accepted theory of how these electrodes work. Finally, the current knowledge of slow wave activity in the human, cat, and dog colons is presented.

3.2 SLOW WAVES IN THE STOMACH AND SMALL INTESTINE

3.2.1 Electrical Characteristics

The slow waves which occur in the smooth muscle wall of the stomach have a single frequency of one to three cycles per minute in man in vivo. Intracellular recordings from stomach smooth muscle show an electrical complex consisting of a rapid depolarization followed by a plateau upon which spikes are sometimes imposed. In vitro measurements by El-Sharkawy et. al. (1978) showed a cellular resting potential in canine and human stomach averaging -69 to -74 mV as the recording location moved from the orad side of the corpus to the terminal antrum. The slow wave amplitude increased in the aboral direction from 21 to 31 mV.

Slow waves in the small intestine of the human, cat, and dog have a frequency in the range of 7 - 20 cycles/minute (Connor, 1979). Intracellular micro-electrode studies from the small intestine of the rabbit showed a mean resting potential -54.8 ± 0.3 mV and a slow wave amplitude of 17.9 ± 0.2 mV (El-Sharkawy and Daniel, 1975 a). The corresponding measurements for the cat are -67.0 ± 7.0 mV and 30.0 ± 5.0 mV (Connor et. al., 1977). Characteristic slow wave activity from the cat small intestine is illustrated in Figure 3.1.

3.2.2 Relationship to Mechanical Activity

It has been shown (Daniel et. al., 1960; Daniel and Chapman, 1963) that spike potentials in the stomach and small intestine most frequently occur during the plateau phase of the slow wave as shown in Figure 3.1). Although contractions can occur without spike potentials (Daniel and Irwin, 1968; Szurszewski, 1981), these potentials always correspond with contractions. Therefore contractions occur most frequently during the plateau portion of the slow wave.

Many studies employing multisite in vivo recordings (Bass, 1968; Kelly et. al., 1969; Kelly and Code, 1971) have demonstrated that slow waves are responsible for the highly coordinated contractile activity of the stomach. Slow waves are phase locked over the stomach from the corpus to the antrum, and the frequency and relative phase lag of these waves determine the frequency and velocity of peristaltic contractions in this organ.

The relationship of the small intestine electrical activity to the role of the intestine musculature, mixing and propelling material, is not as straightforward as in the stomach. The basic element of

Page 20 has been removed due to copyright restrictions.

It contained a figure entitled, "Figure 3.1 Microelectrode recordings from the musculature of cat intestine. (A) Two examples of records taken from longitudinal layer cells. (B) Activity in circular muscle recorded from a 1 mm area from which the longitudinal layer had been dissected. Calibrations are the same in all records".

This figure was obtained from, "On exploring the basis for slow potential oscillations in the mamalian stomach and intestine", by J.A. Connor, J. Exp. Biol., 81:153-173, 1979.

contractile activity in the small intestine is the contraction of a ring of circular muscle fibers a few centimeters wide. During a peristaltic wave, a ring of strong contraction travels down the intestine at the velocity of the slow wave. More commonly, rings of contraction occur nearly simultaneously at several stationary or slowly moving locations, dividing the active length of the intestine into segments (Cannon, 1902). The contractions recur at the slow wave frequency and it has been suggested that the wavelength[+] of the periodic slow waves determines the segment lengths (Code et. al., 1968).

3.2.3 Site of Origin of Slow Wave Activity

There are inconsistencies in the findings of various investigators from studies designed to determine the cellular origin of slow waves in the stomach and small intestine. These differences probably arise because of the different ways used to prepare measurement specimens.

In the cat small intestine the longitudinal and circular muscle layers separate easily as confirmed by light and electron microscopy (Connor et. al., 1974; Prosser, 1974; Taylor et. al., 1977). In the rabbit, the dissection techniques employed separate the musculature within the circular muscle layer (Daniel & Sarna, 1978). Studies of isolated circular and longitudinal layers from the cat intestine have shown that the circular layer is quiescent while the longitudinal layer generates slow waves (Connor et. al., 1977; Kobayashi et. al., 1966). These findings have been contrasted with data taken from the rabbit

---

[+]Wavelength = $\frac{\text{Slow wave propagation velocity}}{\text{Slow wave frequency}}$

intestine by (El-Sharkawy and Daniel, 1974) and (Daniel and Sarna, 1978). In these studies slow waves were found in both isolated circular and longitudinal muscle.

In the stomach there is agreement that the slow wave activity originates in the longitudinal muscle layer (Szurszewski, 1981).

3.2.4 The Ionic Basis for Slow Waves

There is considerable evidence supporting the hypothesis that an electrogenic Na-K pumping mechanism is responsible for part of the resting potential of smooth muscle cells in the gut (Szurszewski, 1981). For example, the measured membrane potential in guinea pig taenia coli ranges from -51 to -55 mV while the membrane potential calculated from the Goldman equation (Goldman, 1943) is -35 mV (Casteels, 1970). This difference in measured and calculated values is caused by the flow of pump current across the membrane resistance. In addition to the Na-K pump there is evidence of other metabolic pumping mechanisms responsible for the active transfer of Cl^- and Ca^{++} across the cell membrane (Brading, 1979; Casteels & Van Breeman, 1975). These two mechanisms may also contribute to the difference between calculated and measured membrane potentials.

It is generally agreed that the Na-K pump is responsible for slow wave generation in the small intestine (Szurszewski, 1981), but the particular ionic mechanism responsible is in dispute. There are two hypotheses: The first states that the slow wave results from

the oscillatory activity of the Na-K pump. The pump turns off to generate the positive phase of the slow wave and on again to return the membrane to its resting potential. Evidence in support of this theory has been obtained by Connor and Prosser (1974) and Connor et. al. (1974). The second hypothesis states that slow waves result from cyclic changes in membrane permeability. Studies supporting this hypothesis have been reported by Mills and Taylor (1971) and El-Sharkawy and Daniel (1975 b). Additional work is required to determine which of these hypotheses is correct.

3.3 MODELLING WITH COUPLED RELAXATION OSCILLATORS

3.3.1 Introduction

The Hodgkin-Huxley model (Hodgkin & Huxley, 1952) was very successful in explaining the nerve action potential in terms of regenerative feedback through voltage controlled conductances. This supported the use of relaxation type oscillators in explaining cardiac electrical activity (Roberge & Nadeau, 1966). It was therefore natural that this type of oscillator would be chosen to model gastrointestinal electrical activity (Nelsen & Becker, 1968).

Relaxation type oscillators were first used to model cardiac electrical activity (Van der Pol & Van der Mark, 1928). The equation describing the Van der Pol oscillator is as follows:

$$\ddot{x} - \alpha(1 - x^2)\dot{x} + \omega^2 x = 0 \qquad 3.1$$

where x is the independent variable representing the amplitude of the oscillation, α is the damping coefficient, ω is the natural frequency

in radians per second, and $\dot{x}$ and $\ddot{x}$ are the first and second derivatives of x respectively. Fitzhugh (1961) used Lienard's transformation to obtain a system of two first order differential equations as follows:

let $$y = \frac{\dot{x}}{\alpha} + \frac{x^3}{3} - x \qquad 3.2$$

then $$\dot{y} = \frac{\ddot{x}}{\alpha} + x^2\dot{x} - \dot{x} \qquad 3.3$$

using equation 3.1

$$\dot{y} = -\frac{\omega^2 x}{\alpha} \qquad 3.4$$

Terms were then added to equation 3.4 to give

$$\dot{y} = -\frac{1}{\alpha}(\omega^2 x - a + by) \qquad 3.5$$

Also from equation 3.2

$$\dot{x} = \alpha(y + x - \frac{x^3}{3}) \qquad 3.6$$

Equations 3.5 and 3.6 are the Fitzhugh system of equations. Sarna et. al. (1971) further generalized these equations introducing other coefficients and higher powers of x as follows:

$$\dot{x} = \alpha(cy + fx + gx^2 + hx^3) \qquad 3.7$$

$$\dot{y} = -\frac{1}{\alpha}(by + \omega^2 x + cx^2 + dx^3 - a) \qquad 3.8$$

The smooth muscle of the gastrointestinal tract does not function as a syncytium such as cardiac muscle where the electrical activity of the complete muscle is controlled from a single pacemaker site. Instead, any small region of the smooth muscle wall of the stomach, small intestine and colon generates slow wave activity. The muscle

can be considered to consist of islands of electrically oscillating tissue electrically coupled to other surrounding regions which are also electrically active. As a consequence of this the electrical activity of the stomach and small intestine has been modelled using an array of coupled relaxation oscillators as shown in Figure 3.2 where the nth oscillator is described by the following equations (Sarna et. al., 1971, 1972):

$$\dot{x}_n = k(a_1 y_n + a_2 x_n + a_3 x_n^2 + a_4 x_n^3 + I_n) \qquad 3.9$$

$$\dot{y}_n = -\frac{1}{k}(b_1 y_n + b_2 x_n + b_3 x_n^2 + b_4 x_n^3 - b_0) \qquad 3.10$$

where I_n represents the resultant of all other oscillators feeding into the nth oscillator.

When any two of these oscillators with different intrinsic frequencies are coupled together a number of different results are possible depending on the oscillator and coupling parameters. The two coupled oscillators could oscillate at a frequency (1) higher than either of the intrinsic frequencies, or (2) equal to the higher of the two frequencies, or (3) somewhere between the two intrinsic frequencies. In each of the above situations the two oscillators become phase locked with a fixed phase lag between the two oscillator outputs. If the degree of coupling is small, the two oscillators could oscillate at different frequencies making a fixed phase impossible. In this case the oscillator with the lower intrinsic frequency may have its frequency increased due to the coupling. This phenomena is referred to as "frequency pulling".

Page 26 has been removed due to copyright restrictions.

It contained a figure entitled, "Figure 3.2 Block diagram illustrating the arrangement of oscillators in the intestinal model".

This figure was obtained from, "Computer models of gastrointestinal electrical control activity", by S.K. Sarna, a thesis submitted to the Faculty of Graduate Studies, University of Alberta, 1971.

3.3.2 Modelling of Slow Wave Activity in the Canine Stomach

Slow wave activity in the canine stomach has been modelled using a two dimensional array of 16 bidirectionally coupled oscillators as shown in Figure 3.3 (Sarna et. al., 1972). The slow waves in the intact organ in vivo have a single frequency of 5.1 ± 0.52 cycles/minute. As seen in Figure 3.4 the intrinsic oscillator frequencies decrease from a maximum of 5.5 cycles/min. in the corpus to 2.5 cycles/min. near the pylorus. In the intact organ and in the model the slow wave signals were shown to be phase locked with the phase angle varying from 70 - 100^{o}/cm in the corpus to 8 - 20^{o}/cm near the pylorus. The degree of coupling between oscillating units increases distally to a maximum near the pylorus.

3.3.3 Modelling of Slow Wave Activity in the Canine Small Intestine

Several researchers have produced models of the slow wave activity of the canine small intestine (Nelsen & Becker, 1968; Diamant et. al., 1970; Sarna et. al., 1971). The proximal 60 to 80 cm of the small intestine produces slow waves of constant frequency in the range of 18.5 to 21.0 cycles/min. (Sarna et. al., 1971). In this plateau region of constant frequency, slow waves are phase locked with a phase lag of 10 - 15^{o}/cm. Distal to the plateau region the frequency gradually decreases to a minimum of 14 cyles/min. in the ileum. Coupling in the circular direction is good with slow waves appearing to be simultaneous at points around the circumference of the organ. Intrinsic frequencies in small intestine segments decrease exponentially as a function of distance from the pylorus, and the frequency of the intact plateau region

Page 28 has been removed due to copyright restrictions.

It contained a figure entitled, "Figure 3.3 Arrangement of oscillators in the gastric ECA model. Oscillators 1 to 6 represent the ECA of the greater curvature; oscillators 7 to 11 represent the ECA of the midline; and oscillators 10-13 represent the ECA near the lesser curvature. Numbers inside the boxes indicate the intrinsic frequencies of oscillators, and those between them indicate coupling factors".

This figure was obtained from, "Computer models of gastrointestinal electrical control activity", by S.K. Sarna, a thesis submitted to the Faculty of Graduate Studies, University of Alberta, 1971.

Page 29 has been removed due to copyright restrictions.

It contained a figure entitled, "Figure 3.4 Diagram showing the intrinsic frequency gradients along the greater curvature (—) and on the midline (--) of the dog stomach. Numbers refer to different electrodes".

This figure was obtained from, "Computer models of gastrointestinal electrical control activity", by S.K. Sarna, a thesis submitted to the Faculty of Graduate Studies, University of Alberta, 1971.

is higher than the highest intrinsic frequency from isolated segments (Sarna et. al., 1971). The model developed by Sarna et. al. (1971) consisted of a series string of bidirectionally coupled oscillators with intrinsic frequencies decreasing distally in the same manner as indicated by in vivo measurements. Coupling was also made to decrease as a function of the oscillator location in the string. The model was shown to exhibit the frequency and phase lag characteristics of the small intestine. In addition, the model was shown to predict the changes in slow wave activity produced by transection of the organ at various locations along its length.

3.4 INTRACELLULAR-TO-EXTRACELLULAR SIGNAL TRANSDUCTION

3.4.1 Introduction

Intracellular microelectrode measurements from smooth muscle cells are very difficult to obtain and multisite intracellular recordings have not been achieved in smooth muscle. For these reasons, the majority of in vitro slow wave studies has used pressure electrodes of the type described by Bortoff (1967). A large portion of the data in this thesis was obtained from pressure electrode measurements. A knowledge of the intracellular-to-extracellular transduction mechanism is necessary to relate these extracellular measurements to intracellular phenomena. It is generally believed that this mechanism results from the generation of an injury potential.

3.4.2 The Injury Potential Theory

In 1946 Graham and Gerard demonstrated that the impalement of muscle cells by large microelectrodes resulted in the measurement of an intracellular potential which was far less than the expected membrane potential. It was thought that an injury to the cell caused a drop in the intracellular potential and thus the measured potential was referred to as an "injury potential". This was again demonstrated for cardiac muscle by Woodbury et. al. (1951) who showed that the measured potential would fall to as low as 30% of the correct value. Later Gillespie (1962) reported a detailed study of this phenomena for the smooth muscle cells of the rabbit large intestine. He showed that in addition to measuring a reduced resting potential at the site of the injury, the action potential at this site was reduced by the same factor. He also showed that mechanical deformation of the cell due to stretching reduced the intracellular potential. From these observations he concluded that mechanical deformation of a cell by an electrode too large to penetrate it would cause depolization and produce an injury potential. He developed the simple model shown in Figure 3.5 to explain his results. In this model R_m is the normal cell membrane resistence and v_m is the normal intracellular potential. R_s is the shunt resistance existing between the interior and exterior of the electrode, and R_L is a variable membrane leakage resistance created by the injury. In the extreme case R_L will be zero. For this situation the measured potential v is given by the following equation:

$$v = \frac{R_s}{R_s + R_m} \cdot v_m \qquad 3.11$$

Page 32 has been removed due to copyright restrictions.

It contained a figure entitled, "Figure 3.5 The injury potential generated by an extracellular electrode, and an equivalent circuit of the extracellular signal generation".

This figure was obtained from, "Spontaneous mechanical and electrical activity of stretched and unstretched intestinal smooth muscle cells and their response to sympathetic nerve stimulation", by J.S. Gillespie, J. Physiol., 162:54-92, 1962.

Of course, if the intracellular potential has a time varying component, such as a slow wave, then v will contain a proportional time varying component.

Bortoff (1967) proposed that this same theory was applicable to the smooth muscle of the small intestine when deformed by large extracellular pressure electrodes.

3.4.3 An Extension of Gillespie's Model

Extracellular pressure electrodes are much bigger than the cells which are being studied. Figure 3.6(a) schematically shows the typical measurement situation. Figure 3.6(b) is the equivalent circuit. The components of this circuit no longer represent the parameters of a single cell as in Gillespie's model. They represent the equivalent parameters of many cells having the same characteristics. It is assumed that the membrane potential v_m is composed of a resting potential V_m and a slow wave component v_{sw}. From Gillespie's work it is assumed that the cells deformed by the electrode are depolarized by the creation of a membrane leakage resistance for each of these cells. R_L in Figure 3.6(b) represents the equivalent leakage resistance of all cell membranes deformed by the electrode. It is assumed that the internal resistances of the cells and of the extracellular fluid of the tissue bath are both negligible. R_s is the equivalent shunt leakage resistance existing between the measurement surface of the electrode and the extracellular fluid of the tissue bath. R_c is the equivalent coupling resistance existing between the injured and normal cells. In the extreme case the cells under the electrode will be completely depolarized and R_L will approach zero. In this case the measured potential v is

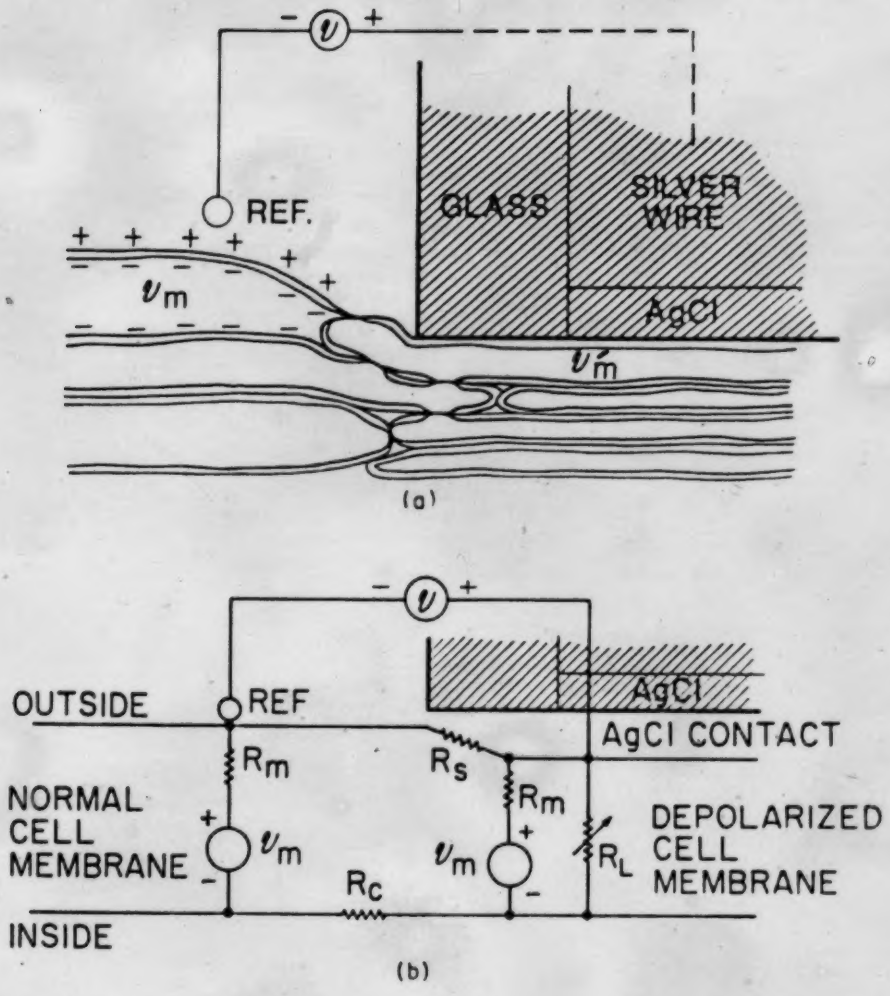

Figure 3.6 (a) A schematic drawing of a pressure electrode measurement.
(b) An equivalent circuit.

given by:

$$v = \frac{R_s}{R_m + R_c + R_s} \cdot (-v_m) \qquad 3.12$$

Since $v_m = V_m + v_{sw}$, the measured potential will have a time varying component proportional to v_{sw}, that is

$$v_{ac} = \frac{-R_s}{R_m + R_c + R_s} \cdot v_{sw} \qquad 3.13$$

where v_{ac} is the time varying component of v.

No direct comparisons of simultaneous intracellular and extracellular pressure electrode measurements have been reported to support this theory. However, part of the work described in this thesis shows that the theory described above does not directly apply to the smooth muscle of the colon. An alternative theory will be proposed in this thesis to explain the generation of pressure electrode signals.

3.5 SLOW WAVE ACTIVITY IN THE COLON

3.5.1 Introduction

Less is understood about the function of slow waves in the colon than in either the stomach or small intestine. Slow waves have been recorded from the colonic smooth muscle of the dog (El-Sharkawy, 1978), the cat (Christensen, 1975), the dog (Vanasin et. al., 1974; Bowes et. al., 1977) and the human (Vanasin et. al., 1974; Duthie, 1975; Sarna et. al., 1980; Chambers et. al., 1981). However many inconsistencies occur in these reports either due to species differences or differences in measurement procedures.

3.5.2 Slow Waves in the Human Colon

In vitro studies of human slow wave activity are hindered by the difficulty of obtaining healthy tissue specimens and in vivo studies are infrequently attempted because of the post operative risks to patients. There is lack of agreement on human colonic slow wave activity with respect to its omnipresence, its frequency, and frequency gradients. Taylor et. al. (1975) and Snape et. al. (1976) reported that the slow wave is intermittently present in the in vivo human colon. However, Provenzale and Pisano (1971) found that it was omnipresent. A number of researchers reported two distinct slow wave frequencies one of 3 and one of 12 cycles/minute (Vanasin et. al., 1974; Duthie, 1975; Stoddard et. al., 1979; Sarna et. al., (1980). However, Chambers et. al. (1981) report a single frequency of 2-9 cyles/minute. Vanasin et. al. (1974) reported the existence of two frequency gradients with the frequency decreasing distally in the ascending colon while increasing from transverse colon to rectum. However, Chambers et. al. (1981) report that no frequency gradient could be detected.

No data has been published concerning the intracellular slow wave characteristics or concerning the typical phase angle existing between oscillating regions in the human colon.

3.5.3 Slow Waves in the Cat Colon

The electrical activity of the cat colon has been extensively studied by Christensen et. al. (1969). In this animal the slow wave has been shown to originate in the circular muscle layer and to be

nonexistant in the longitudinal layer (Christensen et. al., 1969). This electrical activity is phase locked 67 percent of the time in the longitudinal direction and 95 percent of the time in the circular direction. The mean frequency in isolated muscle segments was determined to be 3.12 ± 1.62 cycles/minute (Christensen & Hauser, 1971 a; 1971 b). The phase lag between recording sites varies linearly with electrode spacing and the size of the oscillating regions is believed to be less than 0.5 mm (Christensen & Rasmus, 1972). The complete organ was studied in vitro by Christensen et. al. (1974). From this study it was found that a frequency gradient exists in the aboral direction with an intrinsic frequency of 7.3 cycles/minute at the distal end and 1.9 cycles/minute at the cecum. In addition to the slow wave, migrating spike bursts were also recorded. The spike bursts occurred every 74.3 seconds with a mean duration of 26.6 seconds and propagated distally over the complete organ.

3.5.4 Slow Waves in the Canine Colon

Less has been reported on the canine colon than on either the human or cat colon, and some of the reports have been contradictory. Vanasin et. al. (1974) reported the existence of a range of slow wave frequencies with a frequency gradient existing from the cecum to the rectum. However Shearin et. al. (1979) found no significant gradient of intrinsic frequencies. Coupling has been found to be better in the circular direction than in the longitudinal direction (El-Sharkawy, 1978; Shearin et. al., 1979). All researchers have found the slow waves to be omni-present with frequencies in the range from 4.1 to 6.2 cycles/minute.

Shearin et. al. (1979) determined mean phase angles between recording sites using visual and computer analysis. However, these results are to be questioned because there was not sufficient agreement between the visual and computer results.

There are a number of questions concerning slow waves in the canine colon which have not been answered in the literature. The site of origin of the slow wave is not known. What is the role played by each of the muscle layers in the generation of slow waves? Are slow waves present in the cells of both layers? In addition to these points, the intracellular characteristics of the slow wave in the canine colon have not been reported. The work described in this thesis addresses each of the above points.

It would have been most desirable to study human colonic muscle. However, the uncertainty concerning the availability of healthy specimens prevented this. As stated previously the dog has proven to be a most suitable animal for the study of stomach and small intestinal slow wave activity (Sarna et. al., 1971; 1972) and a base of knowledge had been obtained from previous studies in our laboratory on the canine colon (Shearin et. al., 1979; Bowes et. al., 1977). Thus, the dog was the obvious animal on which to base the present research.

CHAPTER 4

OBJECTIVES, METHODS, AND MATERIALS

4.1 INTRODUCTION

From initial preliminary studies on the canine colon it was determined that the distal colon was completely unpredictable in its ability to produce slow wave activity. Consequently, this work is based on specimens taken from the proximal one half to two thirds of the canine colon. The distal portion of the colon will require future study.

Healthy mongrel dogs weighing between 8 and 15 kilograms were anesthetized using pentobarbital, and the required sections of the colon were surgically removed. These sections were immediately placed in oxygenated Krebs-Ringer solution[≠] and cut open either along the mesenteric or antimesenteric border. These sections were carefully washed in three separate containers of Krebs-Ringer solution to insure the complete removal of fecal contents. The sections were then placed in a constant temperature bath of Krebs-Ringer solution and the mucosa and muscularis mucosa were removed using sharp dissection. The sections were then trimmed and cut into circularly or longitudinally oriented strips (10 mm x 40 mm) for specific experiments.

The objectives of the research are as follows:

1. The determination of the anatomical origin of colonic slow wave activity.
2. The definition of the role played by each of the muscle layers in

---

[≠]See Appendix B for composition.

the generation of slow wave activity.

3. A more accurate determination of the physical and electrical characteristics of slow wave activity. This will include an examination of intracellular potentials to determine the resting potentials and slow wave amplitudes. It will also include an examination of slow wave frequencies, of frequency gradients, of the size of oscillating regions, and of the relative phase angles existing between regions in the circular and longitudinal directions.

An additional objective resulting from the extensive use of pressure electrodes is to determine the relationship between pressure electrode signals and the intracellular potential variations of cells under these electrodes.

Extracellular pressure electrodes are essential to much of the work in this thesis. This chapter first includes a description of the development and study of the pressure electrode used in this work. This is followed by a detailed description of extracellular and intracellular experiments and of the computer processing used to analyze the results.

4.2 THE DESIGN AND STUDY OF A NEW PRESSURE ELECTRODE

The majority of slow wave studies have been completed using extracellular pressure electrodes (Bortoff, 1967; 1975; Christensen et. al., 1969; Shearin et. al., 1979). This is due to the fact that intracellular measurements are very difficult to obtain in comparison to extracellular measurements. Intracellular measurements are much more time consuming, require more sophisticated measurement apparatus, and require more

tedious measurement procedure. In addition to this, multisite intracellular measurements are very difficult to make whereas the number of simultaneous extracellular recordings is limited only by the size of the tissue and the availability of recording channels.

Nevertheless, extracellular measurements have a number of limitations. The most important of these is that no information can be obtained about the resting (dc) potentials existing in cells under the electrode. A second is that at present it is impossible to calibrate the electrode signals in terms of actual potential variations inside the cells. The pressure electrode theory outlined in the previous chapter has not yet been proven, and even if it were correct, it does not provide the necessary parameters to relate intracellular and extracellular potentials. In addition to the above problems, extracellular electrodes are limited by noise and low frequency drift. Most extracellular pressure electrodes utilize a silver-silverchloride layer as the signal transducer. The resistance and capacitance of this type of electrode increase as an inverse power of frequency. This characteristic could cause severe distortion of signals such as slow waves which have very low frequency components. Typical slow wave frequencies in the dog colon are in the range of 4 to 7 cycles/min. (0.067 to 0.117 Hz) in vitro.

4.2.1 Electrode Description

Our work on the colon started with a glass pore electrode of the type described by Christensen & Hauser (1971 a). However, this electrode was inadequate because of its high impedance, its large offset voltage and its low-frequency drift. Therefore, the development of a better

electrode was initiated. Silver-silverchloride electrodes have been used in many physiological applications (Geddes, 1972) and have been shown to have good impedance, noise, and drift characteristics (Geddes & Baker, 1968). These facts led to the design of an electrode using a chlorided silver wire as its transducing element.

The electrode is shown in Figure 4.1.[+] It consists of a 1 mm diameter silver wire inside a rigid glass capillary with an outside diameter of 2 mm. During electrode application the capillary provides a seal between the conducting extracellular fluid and the active electrode surface ensuring that the shunt resistance R_s is very large. As determined by equation 3.13 in Chapter 3, the larger the magnitude of R_s the larger the recorded signal and as a consequence the better the signal-to-noise ratio. The surface area of the electrode was maximized by roughening, and it was optimally chlorided to minimize electrode impedance and noise characteristics. The wire was fixed inside the capillary with epoxy resin.

4.2.2 Electrode Impedance Minimization

As stated above, the effective surface area of the electrode was increased before it is chlorided. This was accomplished by roughening the end surface of the silver wire. It was emperically determined that a maximum increase in effective surface area was obtained when the surface was roughened with an aluminium oxide abrasive with a mesh size of 240. It was difficult to measure the effective surface area, but by comparison of the capacitance of a roughened electrode to that of a polished electrode it was estimated that the area was increased by a factor of five or better.

[+]This electrode design was originally proposed by Prof. Y.J. Kingma.

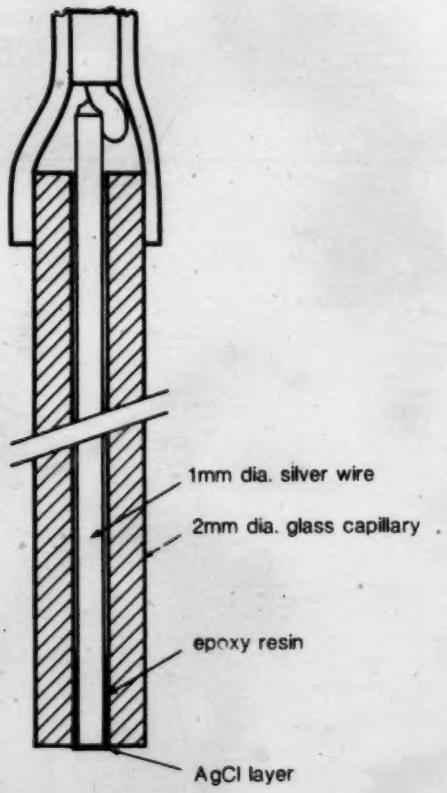

Figure 4.1 Pressure Electrode Details

Reports from the literature vary greatly with regard to the optimum chloriding levels required to produce minimum impedance silver-silver-chloride electrodes (Geddes, 1972). The applicability of these reports to our electrodes is questionable because these reports have been for much larger electrodes and for frequencies of 10 Hz and greater. Thus it was necessary to determine optimum chloriding levels and to measure the electrode impedance characteristics at low frequencies.

Figure 4.2 is a plot of impedance versus chloriding level for five different frequencies from 0.1 Hz to 10 KHz. The chloriding level is indicated as a product of chloriding current amplitude multiplied by the application time in seconds. For frequencies at 10 Hz and greater these results agree with data published by Geddes (1972). For 0.1 Hz the optimum chloriding level is 3 mA-seconds. This was chosen as the optimum level for the electrodes.

4.2.3 Electrode Impedance Measurement

To measure the impedance of the electrode it was placed in a 0.1 Normal saline solution at a fixed distance from a large silver-silver-chloride reference electrode of known negligible impedance. The impedance across the two electrodes was measured using two different methods of measurement for which the frequency ranges overlapped. For frequencies above 5 Hz a vector impedance meter was used. For frequencies in the range from 0.1 Hz to 20 Hz the impedance was determined by passing a sinusoidal current of peak density 25 $\mu A/cm^2$ through the electrode-reference pair.

The noise amplitude of the electrode was also measured with respect to a large silver-silverchloride reference electrode in a 0.1 Normal

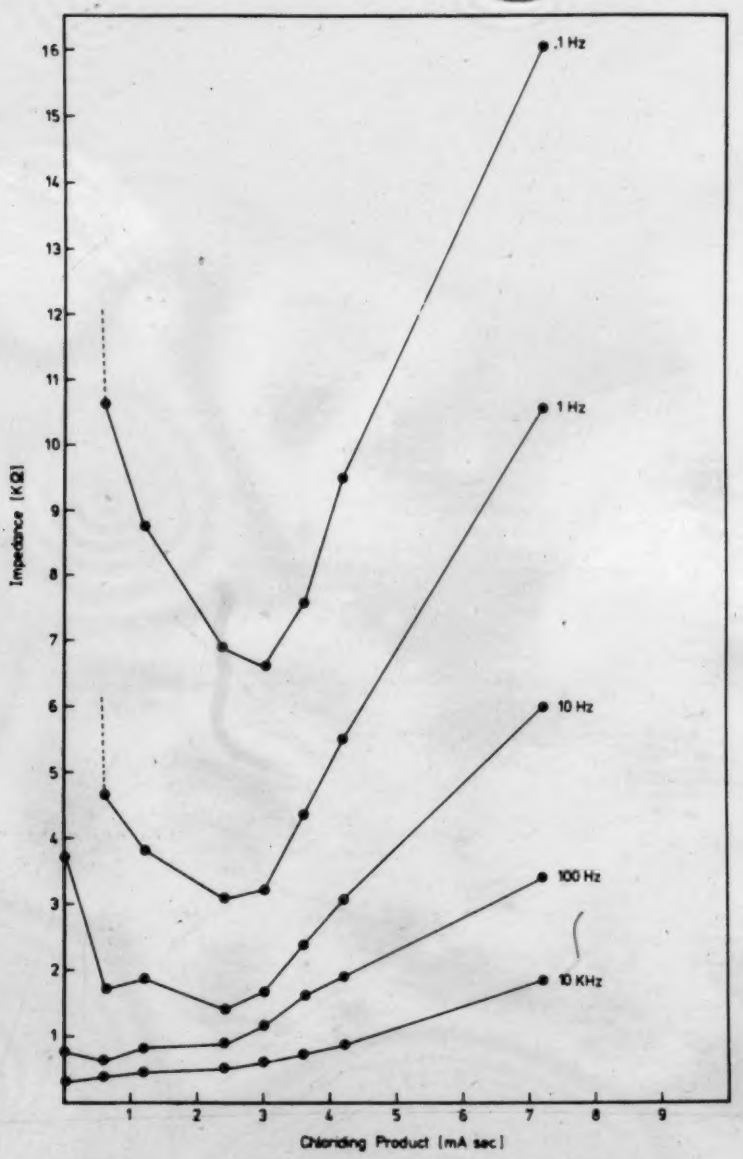

Figure 4.2 Electrode impedance as a function of chloriding levels and frequency.

saline bath.

4.3 EXTRACELLULAR STUDIES

The study of the oscillating regions of the colon and of their slow waves requires the simultaneous recording of electrical signals from a number of sites on the muscle wall. As stated previously, to obtain multisite measurements it was necessary to use the extracellular electrodes previously described.

Two sets of experiments were designed; one set to examine coupling characteristics between various oscillating regions and the other to examine the role played by each of the muscle layers in the generation of slow waves. The first set of experiments is summarized in Figure 4.3. This set of experiments is composed of two groups. One group of experiments, conducted to measure average relative phase angles as a function of electrode spacing, is described in sections 4.3 and 4.3.2. The second group, conducted to study frequencies and phase angles before and after tissue cuts, is described in section 4.3.3.

The second set of experiments, designed to study the role played by the individual muscle layers, is also composed of two groups of measurements as shown in Figure 4.4. The first group, isolated layer studies, is described in section 4.3.4, while the second group, the dual chamber studies, are described in section 4.3.6.

4.3.1 Multisite Electrode Studies on the Intact Muscle Wall

This set of experiments consists of two groups of measurements using four to eight extracellular electrodes. The first group is a

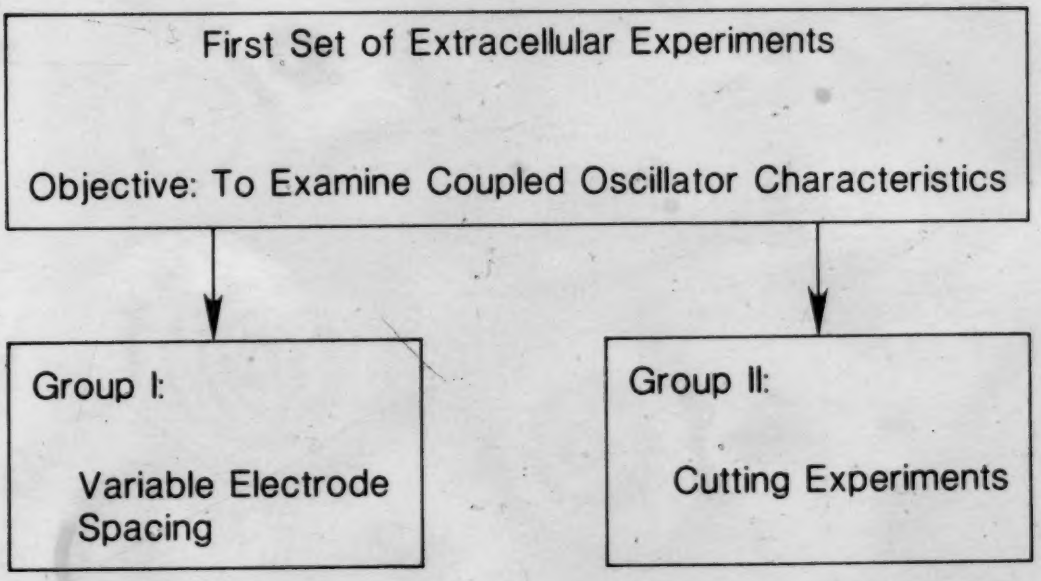

Figure 4.3 Multisite electrode experiments designed to examine coupled oscillator characteristics.

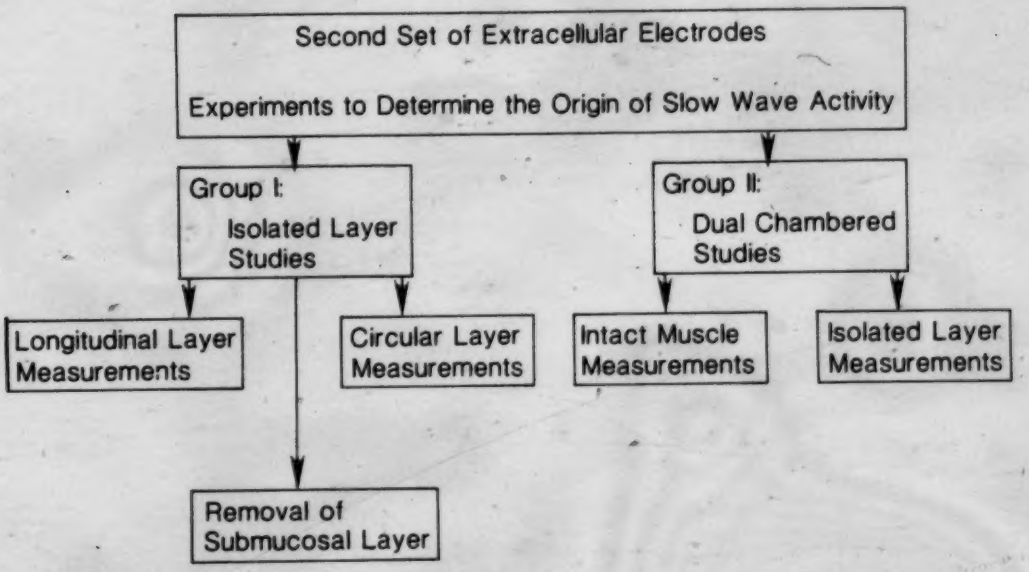

Figure 4.4 Experiments designed to determine the origin of the slow wave signal.

study of the relative phase angles in the longitudinal and circular directions as the inter-electrode spacing is varied from 2.5 mm to 7.5 mm. The second group is a study of signal frequencies and relative phase angles before and after the tissue has been cut between recording sites.

The first objective of this set of experiments was the generation of a data base of frequencies at and relative phase angles and between recording sites on the transverse and proximal colon. This data would be used to determine the size of groups of cells which oscillate together, to determine if a frequency gradient exists, and to determine differences in coupling between the longitudinal and circular directions. The second objective was to determine if the region of the mesentery has a role with respect to slow wave generation.

4.3.2 Phase Angles as a Function of Electrode Spacing

Six experiments were conducted to study the relative phase angle as a function of the spacing between recording sites. Strips of intact colonic muscle wall were prepared as described in Section 4.1 and placed in a constant temperature bath as shown in Figure 4.5 with the mucosal side facing up. The strips were cut either in a circular or longitudinal orientation. The specimen was superfused with oxygenated Krebs-Ringer solution at a rate of 6 ml/minute and the temperature maintained at $37.5^{o}C$.

The combined electrode holder and force transducer shown in Figure 4.5 was used to apply from two to four electrodes to the tissue with an average force of 0.059 newtons (6 grams) per electrode. The electrode spacing was set at 2.5 mm, 5.0 mm, or 7.5 mm.

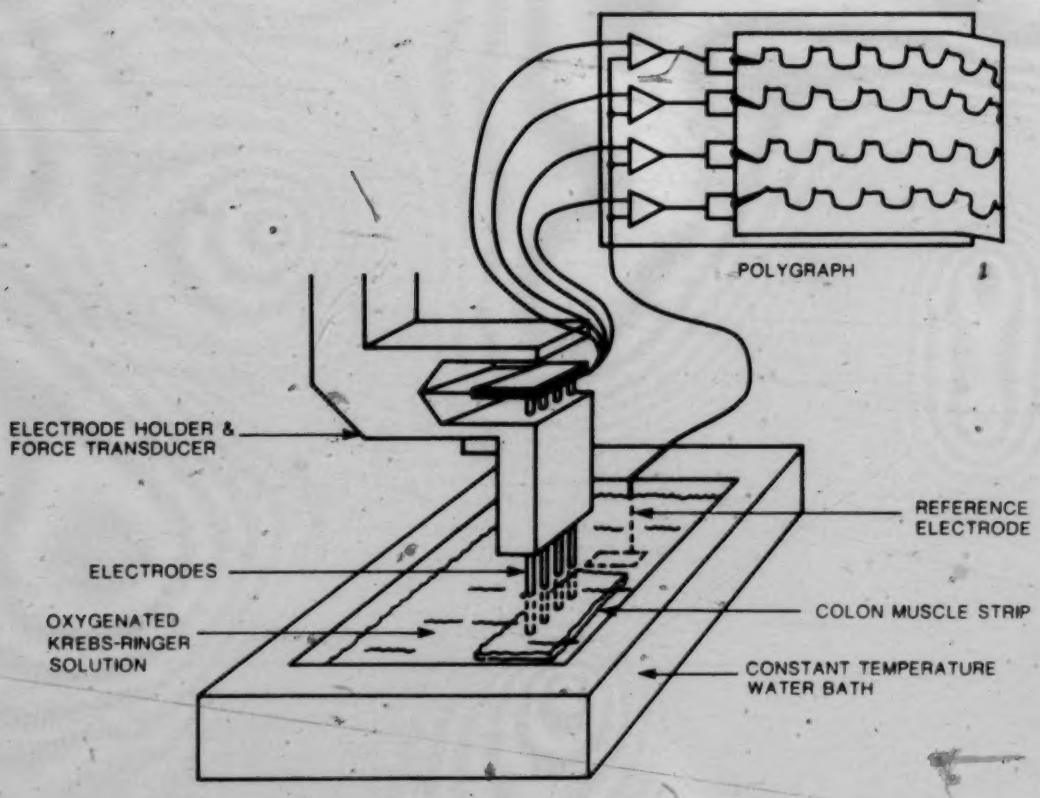

Figure 4.5 The constant temperature bath and extracellular measurement apparatus.

In these six experiments twelve sets of measurements were made in the circular direction and eighteen sets of measurements in the longitudinal direction.

In addition to these six experiments data was obtained from the basal recordings of seventeen experiments conducted for other purposes.

All of the data were recorded on a Type R Beckman polygraph as well as on an fm tape recorder for later computer processing as described in section 4.6.

4.3.3 The Cutting Experiments

In a system of poorly coupled oscillators as exists in the canine colon it is difficult to quantify the degree of coupling. Also it is difficult to determine if a gradient exists in the intrinsic frequencies of individual oscillators. In a tightly coupled system, as exists in the stomach, separation of oscillators by cutting has proven very effective in determining the frequency gradient as well as in providing insight into the type and degree of coupling (Sarna, 1971).

Twenty cutting experiments were conducted on intact muscle segments. Ten of these experiments were on muscle strips oriented in the longitudinal direction and ten were on strips oriented in the circular direction. For each experiment, circular and longitudinal strips were prepared as previously described in Section 4.1 and mounted in the constant temperature bath of Figure 4.5. After a period of 30 minutes, measurements from three to four sites were recorded on fm tape and on a polygraph recorder. These basal recordings were usually 15 to 30 minutes in duration. Upon completion of the basal recording the specimen was cut between two recording sites without moving either

the electrodes or the specimen. Of the ten experiments on circularly oriented strips, five utilized cuts on the mesenteric border and the remainder cuts 1 cm from the mesentery. Thirty minutes after the cutting procedure a second set of recordings was obtained.

The records from "before" and "after" cutting were analyzed visually and using the computer programs described in section 4.6. Also the computer was used to calculate the average coherence (Bendat and Piersol, 1966) for a band of descrete frequencies around the signal frequency. The coherence function is defined as the Fourier Transform of the cross-correlation of two signals divided by the product of the auto-correlation Fourier Transforms. The average coherence is a measure of the correlation and coupling between adjacent channels. For completely coupled signals the coherence value is unity, and for completely independent signals it is zero.

4.3.4 Studies of Isolated Muscle Layers

To determine the role played by each of the smooth muscle layers in the generation of the slow wave signal, it was necessary to determine the electrical activity of each of the isolated muscle layers. To do this, a dissection technique was developed for separating the longitudinal and circular muscle layers. In developing this technique it was discovered that a very thin layer of submucosa could be easily removed from the mucosal side of the circular muscle layer. Consequently, the electrical activities of the intact muscle and isolated circular layer were recorded with and without this submucosal layer.

4.3.5 Separation and Study of Longitudinal and Circular Muscle Layers

To separate the circular and longitudinal muscle layers a strip of intact colon wall was mounted with its serosal side facing down in a constant temperature bath of oxygenated Krebs-Ringer solution. The mucosa was removed using sharp dissection and the tissue was trimmed to form a 1 cm by 2 cm rectangle with edges parallel to the circular and longitudinal directions. The tissue was turned over and at an edge parallel to the circular muscle direction the two layers were teased apart using iris scissors. When an edge of longitudinal muscle (sufficiently large to be gripped with forceps) was developed, small strips of longitudinal muscle 2 to 4 mm in width were gently peeled back leaving behind the circular muscle layer. This procedure was continued until all of the longitudinal layer had been removed. Then strips of isolated circular muscle or longitudinal muscle were pinned to the bottom of the constant temperature bath for study with extracellular electrodes as illustrated in Figure 4.5.

Seven experiments using ten different specimens were conducted on isolated longitudinal and circular muscle. From each experiment histology specimens were prepared to confirm that the separation was in the plane between the circular and longitudinal layers. For this purpose portions of the intact wall and isolated layers were placed immediately into glucoaldehyde and later mounted and stained using hematoxylin-eosin or trichrome stains. Figure 4.6 shows three slides typical of the results obtained using hematoxylin-eosin stain. Figure 4.6a shows the intact muscle wall with the longitudinal layer near the left margin of the slide. The longitudinal muscle cells lie approximately parallel to the plane of the picture. Figures 4.6b

(a)

(b)

(c)

Figure 4.6 Histology slides showing (a) the intact muscle wall, (b) the isolated lonitudinal layer, and (c) the isolated circular layer. Magnification: x62.5.

COLOURED PICTURES
Images en couleur

and 4.6c show the longitudinal and circular layers respectively after separation. For the majority of histology specimens the separation occurred in the plane between the two layers.

4.3.6 Dual Chamber Studies

The dual chamber studies were conducted to further investigate the role of each of the muscle layers in the generation of slow wave activity. These experiments were based on the simultaneous recording of the amplitude and phase relationships of the slow wave signals on both sides of the intact muscle wall and isolated layers.

The dual chamber constant temperature bath shown in Figure 4.7 was designed to facilitate this set of experiments. This bath consisted of two electrically isolated chambers, each separately supplied with oxygenated Krebs-Ringer solution. Both chambers were maintained at the same constant temperature by a surrounding electrically insulated water bath.

A two centimeter square section of colonic muscle was prepared in the manner previously described in section 4.1 and mounted between the two chambers. A 1 cm diameter window permitted contact of opposite sides of the tissue with the Krebs-Ringer solution of the chambers. Petroleum jelly was used to insure good electrical insulation in all areas except for the 1 cm windows. Before each experiment the impedance between the chambers was checked to ensure the absence of leaks creating a short circuit condition.

A total of twelve experiments were conducted. Six of these experiments were conducted on specimens of intact muscle wall containing both circular and longitudinal

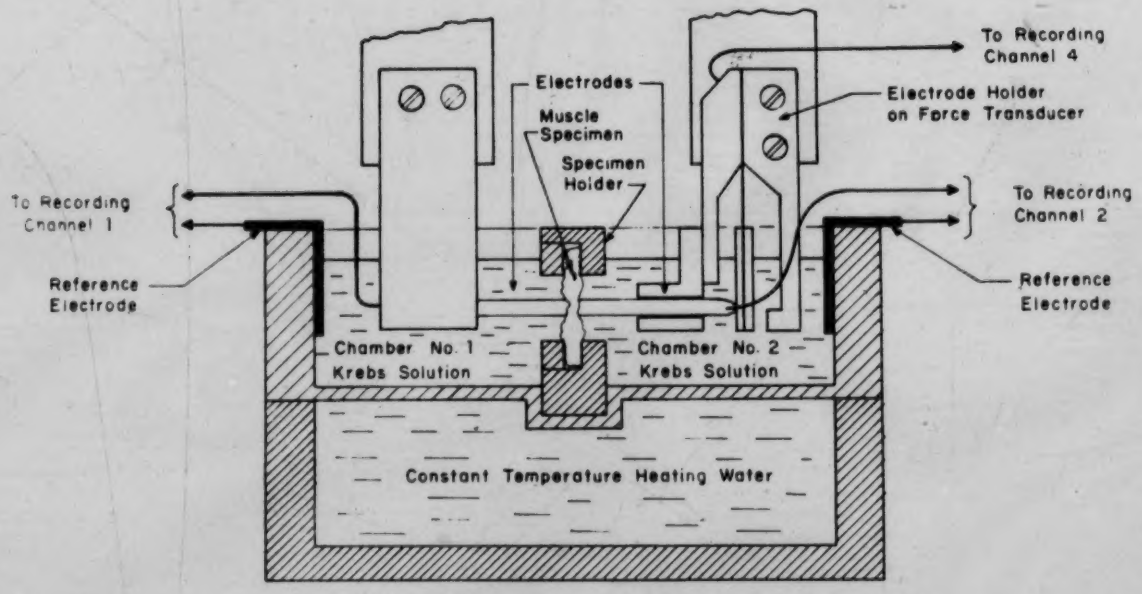

Figure 4.7 The dual chambered measurement system.

muscle layers. The other six experiments were conducted on isolated longitudinal and circular muscle.

4.4 INTRACELLULAR STUDIES

4.4.1 Introduction

Extracellular slow wave measurements would be of maximum benefit if they could be directly related to variations in intracellular potentials. This relationship was uncertain because information was not available on the intracellular potentials of canine colonic smooth muscle. Therefore it was necessary to conduct a number of microelectrode intracellular studies. These studies were also required to investigate the transduction mechanism responsible for the generation of the extracellular signal.

Microelectrode measurements on smooth muscle are difficult to perform because of the small size of smooth muscle cells and because the muscle is continually active. For successful penetration of this type of cell the microelectrode must be less than one micron in diameter. Such electrodes are very fragile and are easily broken by muscle movement or system vibration.

A measurement system was designed which minimized system vibration and electrode breakage. Twenty-four intracellular experiments were conducted on thirty-eight different specimens from the transverse and proximal colon. Eight of these studies included measurements on the intact muscle wall, five included studies of isolated longitudinal and circular muscle layers, eight were studies of the intracellular-to-extracellular transduction mechanism, and three recorded extracellular

and intracellular signals simultaneously. Basal measurements of intracellular potentials from the mucosal side of the intact muscle wall were obtained for all but five of the experiments.

4.4.2 The Measurement System

The intracellular measurement system is shown in Figure 4.8. It consisted of a vibration free table, the constant temperature tissue bath originally used for extracellular studies, a microelectrode manipulator and holder, a hydraulic manipulation system for precise control of electrode movement, and a battery powered electrometer-input amplifier. The output from the amplifier was simultaneously recorded on a storage oscilloscope, on an fm tape recorder, and on a paper chart recorder. The complete system with the exception of the recording devices and the hydraulic control micrometer was housed inside a Faraday cage.

The vibration-free bench consisted of a horizontal concrete platform (4 ft x 6 ft x 4 inches) supported by two legs made from concrete blocks. The Faraday cage was placed on this platform. Inside the cage and of slightly smaller dimensions was a second concrete platform supported by four air-filled rubber tennis balls and two balls of steel-wool. The rubber balls provided decoupling from building vibrations and the steel-wool balls were adjusted to provide suitable damping.

The microelectrode manipulator and holder was of the standard type designed for microelectrode measurements but a hydraulic control system was added to isolate the experimenter from the measurement system and to improve the precision of the microelectrode manipulation system. The details of the measurement system are shown in Figure 4.9. The

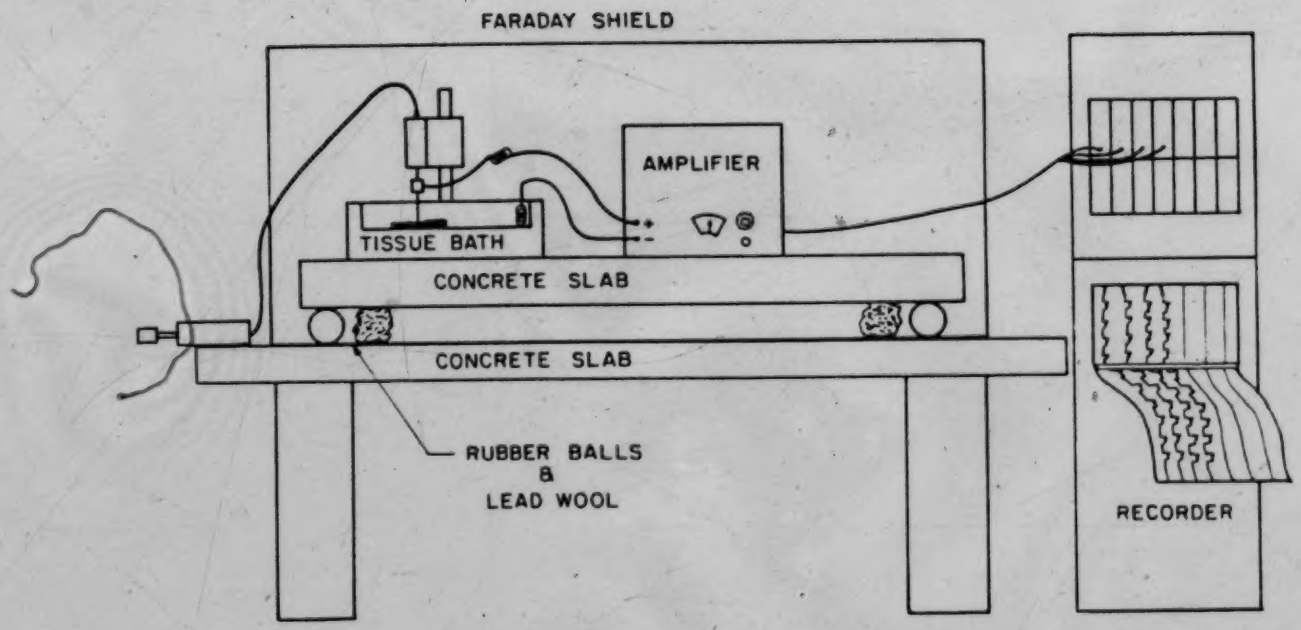

Figure 4.8 The intracellular measurement system.

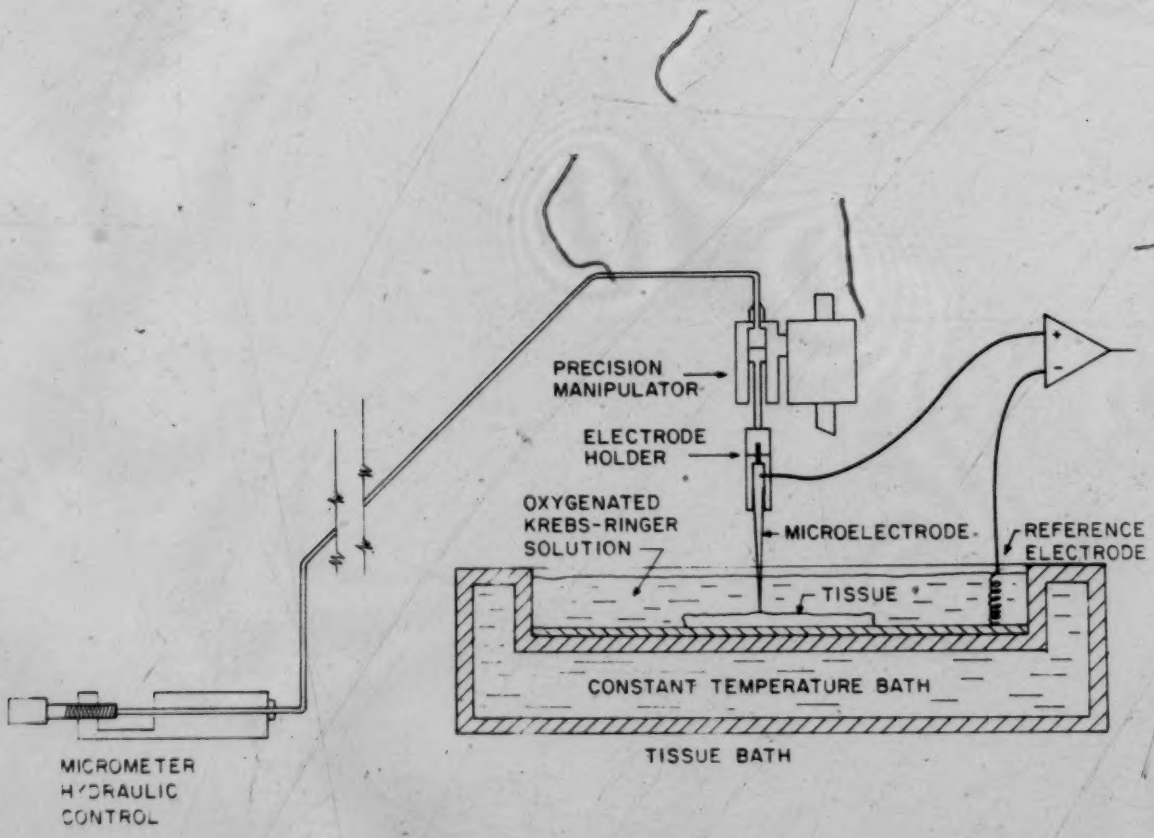

Figure 4.9 Details of the intracellular measurement system.

hydraulic system consisted of two oil filled precision syringes coupled by means of an oil filled polyethylene tube. The ratio of diameters for the two syringes was 25. The smaller of the two syringes was driven by a micrometer system which lay outside the Faraday cage. The control micrometer permitted a slow precise movement of the microelectrode with one unit movement of the micrometer corresponding to an electrode movement of 0.1 micron.

The microelectrode amplifier was a Medistor Model A-35L electrometer-input amplifier with an input impedance of 5×10^9 ohms and an RMS noise output of 20 μV.

The electrodes were pulled from 1.2 mm borosilicate glass tubing and they were filled with 3 M KCl. It was determined that an electrode impedance of between 50 and 100 megohms was optimum for this work. As shown by Firth and Defilice (1971) the tip diameter of such an electrode is in the range from 0.1 to 0.5 microns.

4.4.3 Circular Muscle Measurements

Ten experiments were conducted on the mucosal side of intact muscle strips (with the mucosa removed) to determine the best procedures for obtaining intracellular measurements and to obtain statistically significant information on the basal potentials in the circular muscle layer.

The tissue was prepared as described in section 4.1. However the final specimen was trimmed to the much smaller size of 0.2 cm by 1.0 cm to minimize problems caused by muscle contraction. This was done such that the specimen sides were parallel to the circular and longitudinal directions. The way in which a specimen is mounted in the tissue bath

is of critical importance for the success of an experiment. The optimum mounting arrangement is shown in Figure 4.10(a). The tissue is pinned in four locations such that it is not under tension and so that a line joining the two closest pins is parallel to the short dimension of the specimen. The optimum measurement location is then at the midpoint between these two pins. Care must be taken to ensure that the tissue is not pinched or distorted from its normal shape by the pins.

In addition to the above ten experiments, basal recordings on the mucosal side of the intact muscle wall were obtained from thirteen other experiments.

4.4.4 Longitudinal Muscle Measurements

The measurement of intracellular potentials in the longitudinal layer proved to be a much more difficult task than the measurement of such potentials in the circular muscle layer. The submucosal layer provided easy access to the circular muscle cells without problems due to electrode breakage. However, the serosa, inspite of the fact that it is a very thin layer, proved to be a major obstacle preventing access to longitudinal cells. Unsuccessful attempts were made to remove the serosa without causing significant damage to the longitudinal muscle. The technique which proved most successful utilized very thin cross-sections of colon wall cut parallel to the longitudinal direction. These sections were approximately 0.1 cm thick and were mounted as shown in Figure 4.10(b).

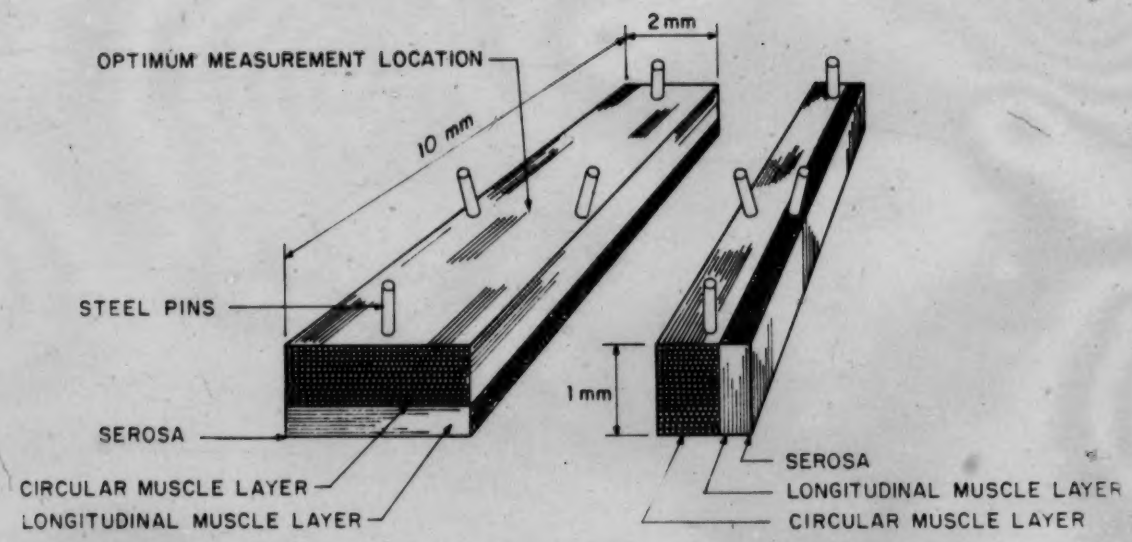

Figure 4.10 Tissue mounting configurations.

4.5 STUDIES OF THE INTRACELLULAR-TO-EXTRACELLULAR TRANSDUCTION PROCESS

4.5.1 Introduction

As reported in Chapter 3, the generation of an "injury potential" has been given as the reason for the existence of the the extracellular pressure electrode slow wave signals. However no research has been published which proves that this is correct. The work done by Gillespie (1962) produced evidence which led Bortoff (1967) and others to believe an "injury potential" was responsible for the extracellular signal. However, Gillespie's work related to large microelectrodes and individual smooth muscle cells. The pressure electrodes used in this present work are many times larger than the smooth muscle cells responsible for the signal generation. In fact, the 2 mm diameter electrode has of the order of five to ten million cells directly under it. One cannot assume the theory developed for individual cells applies in this situation. Consequently eleven experiments were conducted to investigate the relationship between the extracellular signals and the intracellular potentials of cells directly under the pressure electrodes.

The objective of this set of experiments was twofold: firstly, to demonstrate that the extracellular slow wave signal is a function of intracellular variations of the same shape and frequency; and secondly, to show that an injury potential of the type described by Gillespie (1962) exists in cells under pressure electrodes.

4.5.2 A Comparison of Intracellular and Extracellular Electrode Potentials

Three experiments were conducted to simultaneously record and

compare extracellular and intracellular potentials. This was difficult to accomplish because the extracellular electrode, in deforming the tissue, created an increased contractile activity around the extracellular measurement site. This tissue movement greatly reduced the number of successful penetrations. Also the smaller tissue specimens required by the intracellular measurements were not sufficiently large, to completely surround the extracellular electrode, as in the extracellular measurements of section 4.3. Consequently the extracellular signals obtained were smaller in amplitude, and the waveform not as constant from cycle to cycle. The extracellular and intracellular electrode holders prevented the two measurement sites from being closer than 5 mm.

4.5.3 Injury Potential Measurement

Eight experiments were conducted to determine if an "injury potential" was associated with the pressure electrode recordings. The apparatus shown in Figure 4.11 was designed to simulate the pressure electrode. It was constructed from the 2 mm diameter glass used to construct the extracellular electrodes. The glass was cemented to a metal holder to which a force was applied. This simulated electrode was first applied to the mucosal side of the tissue as shown in Figure 4.11 with a known force of 1 to 5 grams (.01 to .05 newtons). Then the microelectrode was positioned in the center of the cylinder and gradually advanced until cell penetration was obtained.

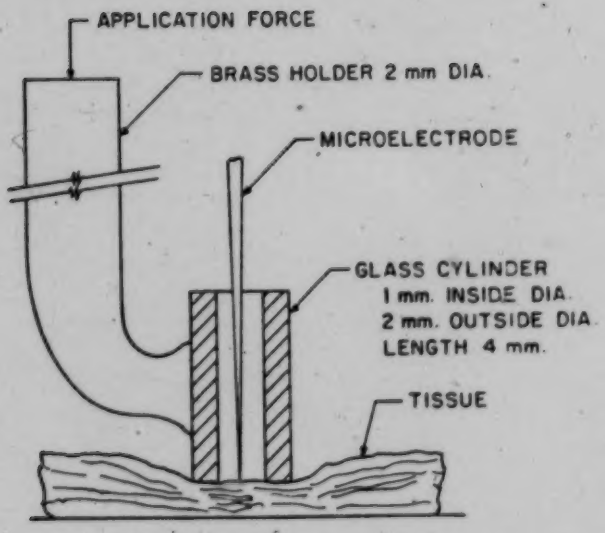

Figure 4.11 Apparatus simulating the application of the pressure electrode to an intact muscle specimen.

4.6 COMPUTER ANALYSIS

The data from all experiments were digitized and processed on a Hewlett-Packard 21 MX/E computer system. This system shown in Figure 4.12 consisted of the 21 MX/E computer, a 5 megabyte disc drive, an IBM compatible digital magnetic tape unit, an eight channel analog-to-digital converter, a three channel digital-to-analog converter connected to a CRT display, a high speed paper tape reader, and a high speed printer terminal. Programs were available for high speed analog-to-digital conversion and descrete Fast Fourier Transformation (Cooley & Tookey, 1969)*. Additional programs were written to perform the following functions:

1. To transfer data files to and from the computer and its storage and input/output devices.
2. To create and apply digital filters.
3. To do auto and cross-correlations of selected data channels.
4. To determine the statistical parameters of cycle-to-cycle frequencies and phase angles.
5. To determine the coherence function for selected channels.
6. To display and plot selected data files.

The programs, descriptions, and examples of typical inputs and outputs are contained in Appendix A.

---

*Both programs written by Dr. Z. Koles, University of Alberta.

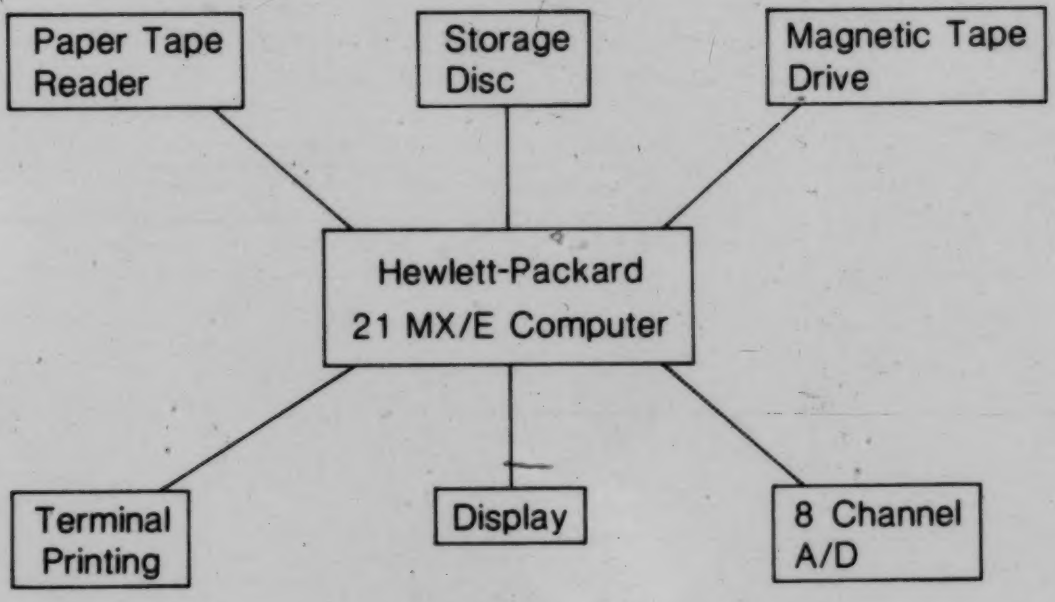

Figure 4.12 The Hewlett-Packard 21 MX/E computer system.

CHAPTER 5

EXPERIMENTAL RESULTS

5.1 INTRODUCTION

In this chapter the results obtained from the extracellular and intracellular experiments described in Chapter 4 are presented. The organization of this chapter parallels that of Chapter 4. The results from the electrode studies are presented first. Following this are the outcomes of the extracellular pressure electrode experiments. These results are divided into two parts, the results providing information on coupled oscillator characteristics and the results which provide evidence relating to the origin of the slow wave and the role played by the individual muscle layers in the generation of this activity. The reader is referred again to Figures 4.3 and 4.4 to see how the extracellular experiments and results have been organized. The extracellular information is followed by the intracellular results and then by the results of experiments investigating the relationship between extracellular and intracellular signals.

5.2 ELECTRODE CHARACTERISTICS

From the impedance versus frequency measurements on the silver-silverchloride pressure electrodes it was found that the impedance magnitude increases inversely with decreasing frequency down to 0.01 Hz. The resistance and reactance both vary as an inverse power of frequency and are close to being equal at all frequencies. The real

component of the impedance consists of two parts, a constant component and a component which varies with frequency. Figure 5.1 is a plot of the real and reactive components of a typical electrode. The equations describing the electrode resistance and reactance are:

$$R = 400 + 1820\ f^{-0.36}\ \text{ohms} \qquad 5.1$$

$$X = 1200\ f^{-0.36}\ \text{ohms} \qquad 5.2$$

The impedance characteristics of the electrodes changed continually from the time of chloriding. During the first 24 hours after chloriding the impedance characteristics were not measured. However, after this period the electrode impedance increased daily and changed such that it no longer varied as a constant power of frequency. A plot of the real and reactive components of the impedance of a twelve-day-old electrode is shown in Figure 5.2.

The amplitude of noise produced by these electrodes was very small. Using a high gain amplifier and a Beckman polygraph recorder, the noise amplitude was found to be of the order of 0.2 μV peak-to-peak. Figure 5.3 is a recording of typical electrode noise compared to the noise of an unchlorided silver electrode.

5.2.1 An Electrode Model

The electrode impedance may be modelled using a modification of the model proposed by Warburg (1899). The model is shown in Figure 5.4. This modification is necessary in order that the model better represent an electrode characteristic as demonstrated by our experiments, that is the bulk resistance of the electrode consists of two components.

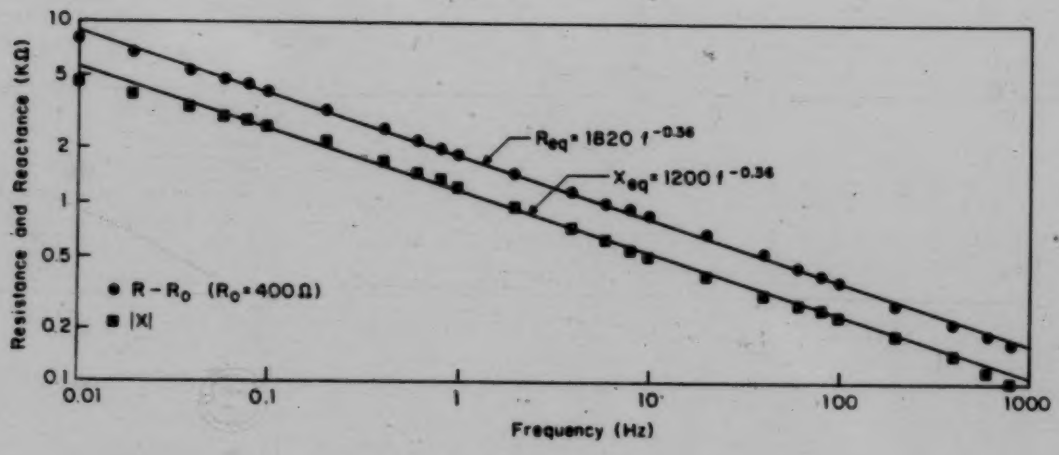

Figure 5.1 The real and reactive components of the impedance of a typical electrode plotted as a function of frequency.

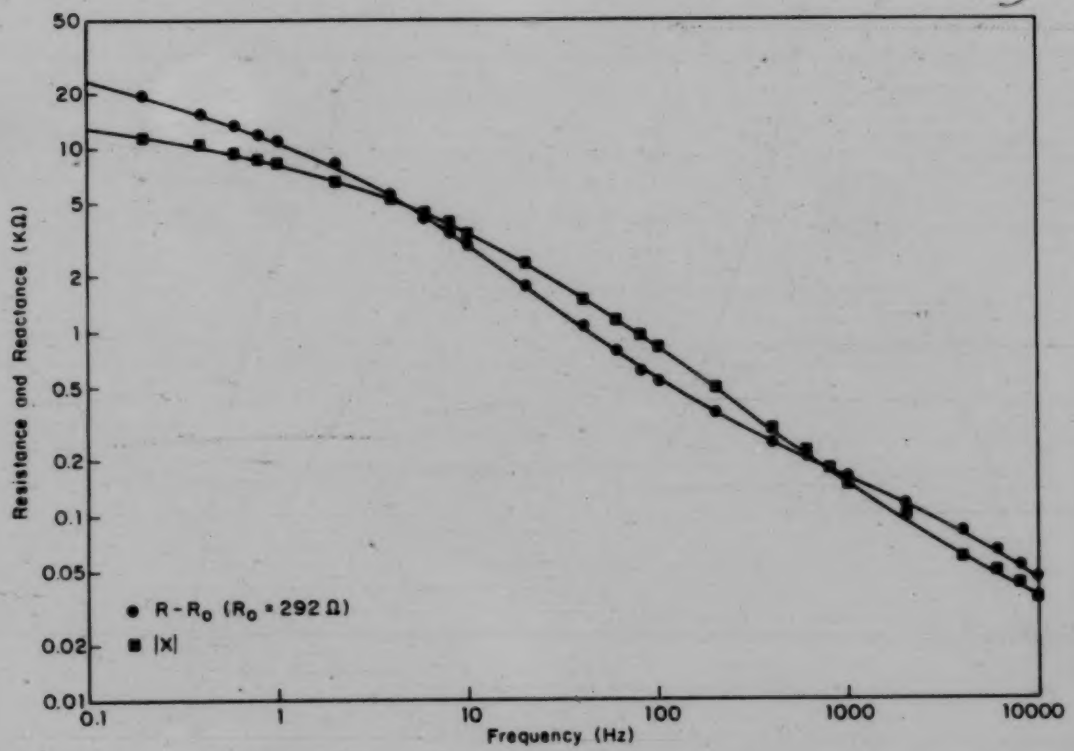

Figure 5.2 Real and reactive components of the impedance of a twelve-day-old electrode.

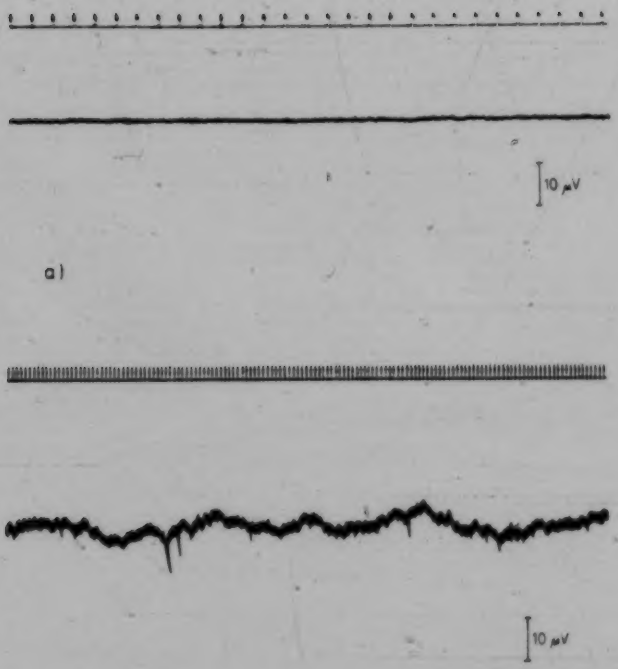

Figure 5.3 Electrode Noise
(a) Normal Electrode
(b) Unchlorided Electrode

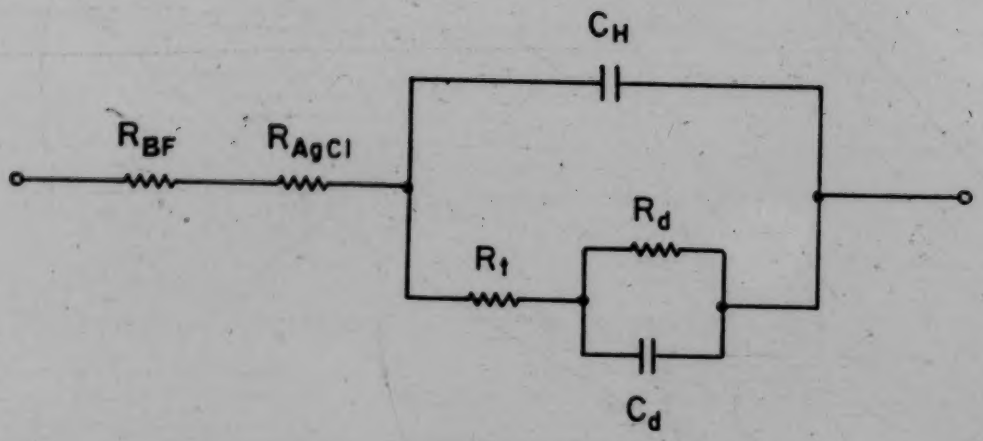

$R_{BF} = 300\,\Omega$

$R_{AgCl} = 100\,\Omega$

$C_H = 15 \times 10^{-9}$ farads

$R_f = 0.72\,\Omega$

$R_d = 1029\, f^{-0.36}$

$C_d = 102.1 \times 10^{-6} f^{-0.64}$

Figure 5.4 Electrode impedance model.

One component R_{BF} is the bulk resistance of the fluid surrounding the electrode tip, and the other R_{AgCl} is the bulk resistance of the silver-chloride layer. Measurement of the electrode impedance at high frequency before and after chloriding has yielded average values of R_{BF} and R_{AgCl} of 300 and 100 ohms respectively. Also from high frequency measurements the double layer incremental capacitance C_H has an average value of 15×10^{-3} microfarads. The charge transfer resistance of the electrode can be calculated. From Cobbold (1974), R_t is defined as follows:

$$R_t = \frac{RT}{zFI_o} \qquad 5.3$$

where R is the gas constant, T is the temperature in °K, z is the valence, F is Faraday's constant, and I_o is the exchange current of the electrode

If T = 300°K and the exchange current is the same as reported for Ag/Ag+ in 0.1 Normal saline (Cobbold, 1974); the calculated value of R_t is 0.72 ohms.

From plots such as Figure 5.1, R_d and C_d can be calculated. For the electrode of Figure 5.1

$$R_d = 1029\ f^{-0.36} \text{ ohms} \qquad 5.4$$

and $$C_d = 102.1 \times 10^{-6}\ f^{-0.64} \text{ farads.} \qquad 5.5$$

5.2.2 Consideration of Signal Distortion Due to Electrode Characteristics

One reason for studying the electrode impedance was the concern that the electrode might create signal distortion due to the very low frequency components of the signal and because silver-silverchloride electrode impedances greatly increase with decreasing frequency. To

determine the significance of signal distortion caused by the electrode, the electrode model is considered in the slow wave measurement circuit of Figure 5.5. The equivalent source resistance R_{eg} of the slow wave was measured and found to be in the range from 20 KΩ to 40 KΩ. In the circuit a mean value of 30 KΩ is used. Using the values for R_d and C_d given in the previous section, the equivalent impedance Z_{eg} of the electrode is defined by the following equation:

$$Z_{eg} = \frac{400.72 + 1029f + j(0.48 + 27.1 \times 10^{-6} f + 38.8 \times 10^{-3} f^{0.64})}{1 - 45.2 \times 10^{-9} f + j(67.9 \times 10^{-9} f + 97.0 \times 10^{-6} f^{0.64})} \quad 5.6$$

The slow wave signal will have no significant frequency components above 100 Hz. Thus, when considering the effect of the electrode impedance on the slow wave signal, Z_{eg} may be approximated by the following equation:

$$Z_{eg} \simeq \frac{400.72 + 1029f + j(0.48 + 38.3 \times 10^{-3} f^{0.64})}{1 + j0} \quad 5.7$$

From the circuit of Figure 5.5, the potential v at the input to the amplifier is given by

$$v = \frac{2 \times 10^6}{2.03 \times 10^6 + Z_{eg}} \cdot v_{sw} \quad 5.8$$

where the input impedance R_i of the amplifier is 2 MΩ. Substituting the approximate value of Z_{eg} from equation 5.7 into equation 5.8 gives

$$v \simeq \frac{2.0 \times 10^6}{2.03 \times 10^6 + 400 + 1029f + j(0.48 + 38.3 \times 10^{-3} f^{0.64})} \quad 5.9$$

For frequencies below 100 Hz the imaginary component of this expression is not significant and the phase shift produced by the electrode is

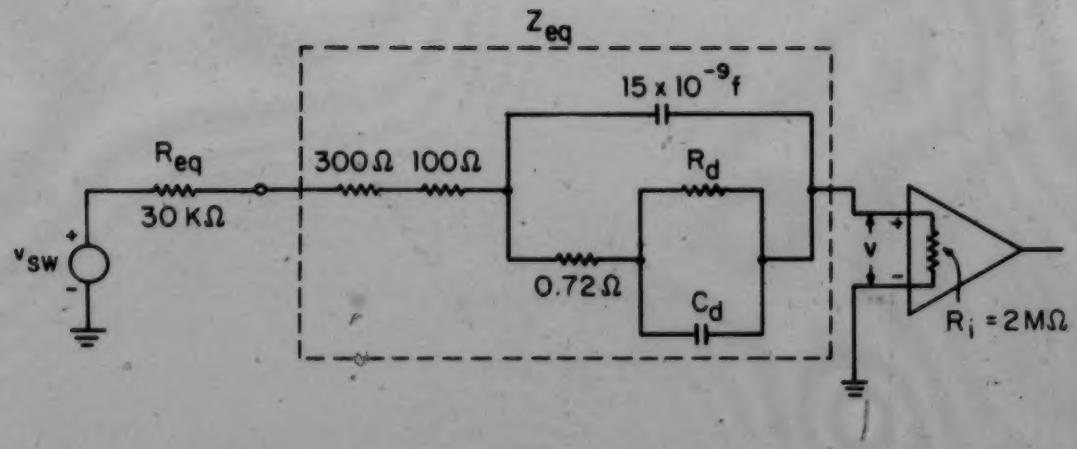

Figure 5.5 Slow wave measurement circuit.

very close to zero degrees. Therefore, for frequency components from zero to 100 Hz, the measured voltage v ranges from 0.94 v_{sw} to 0.99 v_{sw} with no significant distortion due to phase shift. Thus, if the pressure electrode theory described in Chapter 3 is correct, the intracellular slow wave will be faithfully reproduced with only amplitude scaling.

5.3 EXTRACELLULAR RESULTS

5.3.1 Phase Angles as a Function of Electrode Spacing

As described in Chapter 4, section 4.3.2, six experiments were conducted with from two to four electrodes applied to one side of the intact muscle wall with the objective of studying the frequency and phase relationships of the oscillating regions of the colon. In addition, multisite recordings were obtained from seventeen experiments conducted for other purposes. Figure 5.6 shows a typical recording from four electrodes applied to the mucosal side of the intact muscle wall. The electrodes were oriented in the circular direction with a spacing of 2.5 mm. Similar recordings were obtained from the serosal side of the intact wall.

The data from the above twenty-three experiments were digitized and processed using fast fourier transform, zero crossing, and cross-correlation programs. For the recordings of Figure 5.6 the output of the fast fourier transform program "PSPT" is shown in Figure 5.7. Normalized signal power is plotted versus frequency in cycles/minute. Figure 5.8 is the print-out of the program "PHSE" which utilizes zero

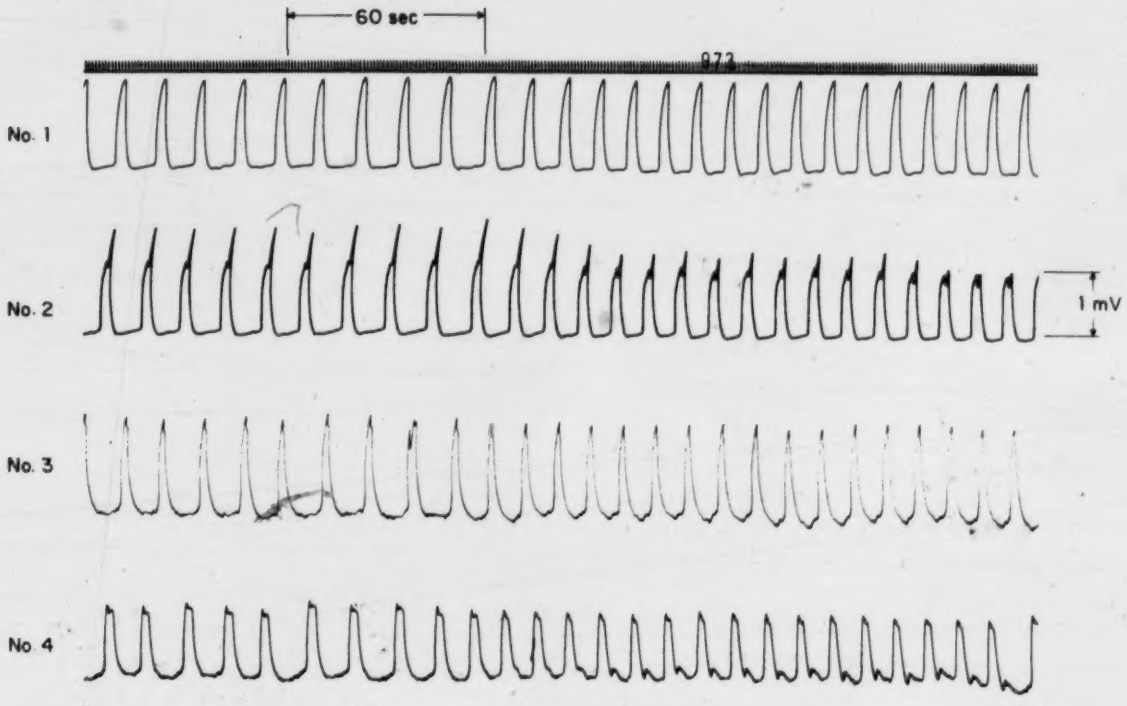

Figure 5.6 A recording from four pressure electrodes applied to the mucosal side of the intact muscle wall. The electrodes are oriented in the circular direction with a spacing of 2.5 mm.

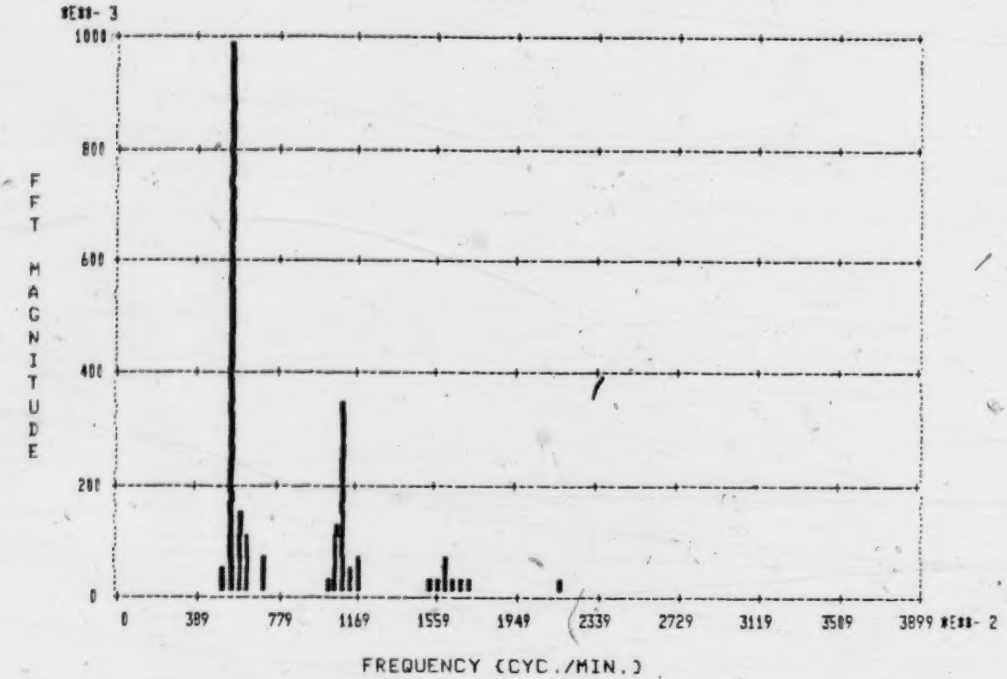

Figure 5.7 Output from the fourier transform program "PSPT".

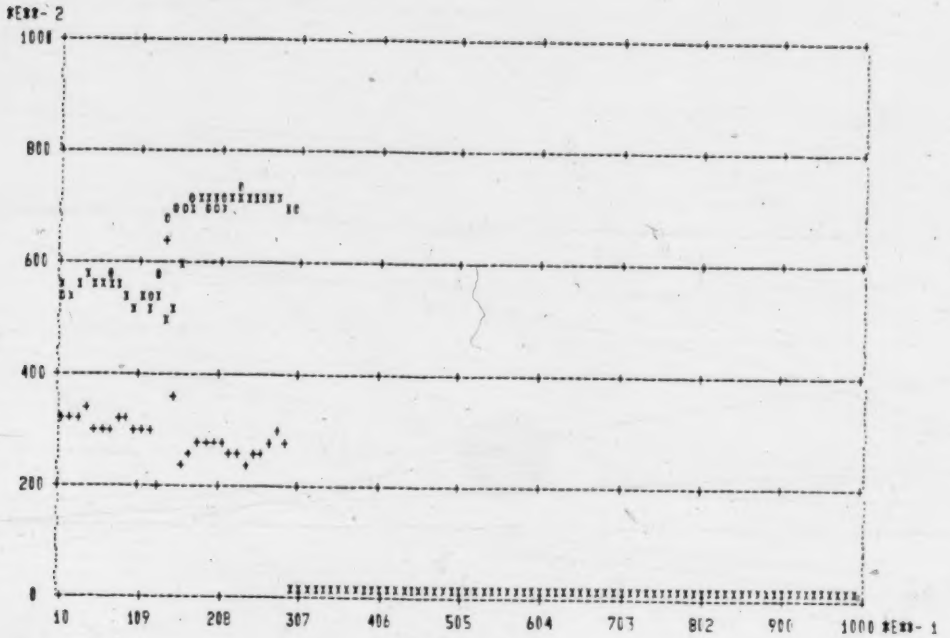

EX3706,SPEC. B2,LONGITUDINAL MESENTERY
CH. NO.1 xxxx, GPH MAX. = 10.0 CYC./MIN. AVG. FREQ. = 6.14± .85 CYC./MI
CH. NO.2 oooo, GPH MAX. = 10.0 CYC./MIN. AVG. FREQ. = 6.34± .81 CYC./MI
PH. ANG.(2 wrt 1) ++++, GPH MAX. =360.0 DEG. AVG. ANGLE = 104.2±25.6 DEG.
CORRECTED AVG. ANGLE = 104.2±25.6 DEG.

f1 = 4.904 + .082*X
f2 = 5.123 + .079*X
PH = 116.827 + -.843*X

Figure 5.8 Output from the zero-crossing program "PHSE".

crossing techniques to compute cycle-by-cycle frequencies and relative phase angles of two selected channels. The frequency of each channel and the relative phase angle in degrees is plotted versus the cycle number. Figure 5.9 is the output of the cross correlation program "XCORR" when applied to the recordings of Figure 5.6. The plot gives the normalized cross-correlation function versus the delay time in seconds. Program listings, flow charts, and typical input/output data for each of these programs is given in Appendix A.

As indicated in section 4.3.2 of Chapter 4, only six of the nine experiments produced useful data.

The data from the above experiments are summarized in Table 5.1. Each entry in the table is an average based on a cycle-by-cycle analysis of a ten to fifteen minute recording analyzed visually as well as with the zero-crossing program "PHSE" and the cross-correlation program "XCORR".

5.3.2 Interpretation of Results

The following two observations can be deducted from Table 5.1:

1. There is great variability of phase angles for each of the electrode spacings.
2. The average phase angle in the circular direction is less than that in the longitudinal direction.

These two points require further clarification. In Chapter 3 it was postulated that the extracellular slow wave signal is produced by the distortion of cells under and around the periphery of the pressure electrode. The area encompassed by these cells is not known

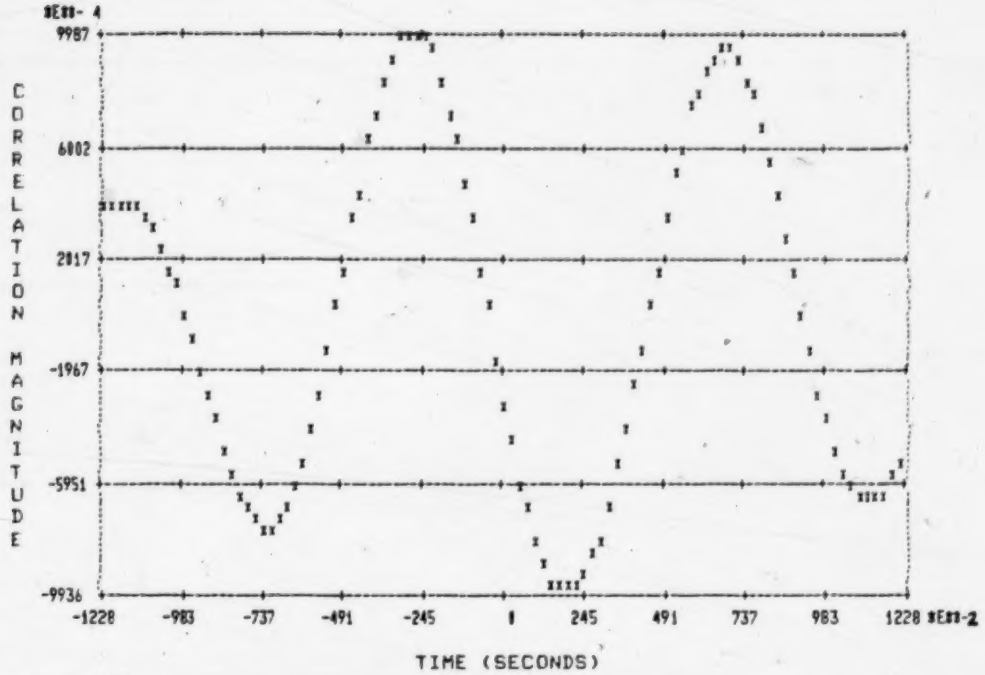

CH. 1 RELATIVE TO CH. 2 EX3706,SPEC. B2,LONGITUDINAL MESENTERY
% SHIFT = 4.17 FREQ. = 6.31 CYCLES/MIN. PHASE =-101.73 DEGREES
MAXIMUM CORRELATION AMPLITUDE IS .371480E+12

Figure 5.9 Output from the x-correlation program "XCORR".

Table 5.1 Phase angle between recording sites as a function of electrode spacing.

EXPERIMENT	CIRCULAR				LONGITUDINAL			
	FREQ.	PHASE ANGLE (DEGREES)/ ELECTRODE SPACING			FREQ.	PHASE ANGLE (DEGREES)/ ELECTRODE SPACING		
		2.5 mm	5.0 mm	7.5 mm		2.5 mm	5.0 mm	7.5 mm
EXP. 3	5.8, 5.8, 5.8, 5.6, 5.5, 5.5, 5.5, 5.5, 5.5, 5.5 5.5	69 4 20	124 32 -49	60 155 255	6.4, 6.3, 6.3, 6.2, 5.4, 5.5, 5.4, 5.4, 5.6, 5.7, 5.7, 5.5, 6.0, 5.8, 5.9, 5.8, 5.6, 5.6, 5.6	122 103	128 120 255 142 209 242 95 94 103	146 94
EXP. 5		20 5 -0.75				10 150 109		
EXP. 6	4.7, 5.1, 4.7, 5.1, 4.2, 4.2, 4.5, 4.5	-21.7 17 -44	278 162 182	61	5.1, 5.1, 4.7, 4.3, 4.3, 4.7, 4.7, 4.7, 4.3, 5.1	34 69	165 158 166 177 142	132

Table 5.1 Phase angle between recording sites as a function of electrode spacing (cont.).

EXPERIMENT	CIRCULAR				LONGITUDINAL			
	FREQ.	PHASE ANGLE (DEGREES)/ ELECTRODE SPACING			FREQ.	PHASE ANGLE (DEGREES)/ ELECTRODE SPACING		
		2.5 mm	5.0 mm	7.5 mm		2.5 mm	5.0 mm	7.5 mm
EXP. 7						59 121 118		
EXP. 8	7.8, 7.8, 7.8, 7.2, 7.3, 7.3, 7.2	-63 0.1 59	76 17 242		8.9, 8.9, 8.9, 8.9, 7.2, 7.4, 7.3, 7.3	185 223 143	339 14 182	125
EXP. 9	6.0, 6.0, 6.3, 6.6	-28 35 -49			7.4, 7.4, 7.4, 6.9, 6.5, 6.5, 6.8	141 210 127		6 154
AVG.±SDEV.	5.87±1.10	29.0±23.2 n=15	93.1±56.4 n=9			117.3±51.0 n=17	168±79.4 n=19	
AVG. from Experiments Conducted for other Purposes			66.4±47.3 n=120					
AVG. from all Experiments			68.3±48.0 n=129					

and will be a function of a particular tissue and of the force with which the electrode is applied. Because of this fact, the distance between regions from which different slow waves originate is unknown. For the 2 mm diameter electrodes with center-to-center spacing of 2.5 mm, the spacing between oscillating regions could range from less than 0.5 mm to more than 4.5 mm. Also, more than two oscillating regions could exist between the electrodes.

The above situation, plus the fact that the visual analysis and the zero-crossing program measure angles with a modulus of 360 degrees, make it impossible to be certain about the phase angles existing between oscillating regions.

However some insight may be gained from these measurements regarding the probable order of magnitude of both the relative phase angle and the spacing between regions. If the spacing of oscillating regions in any particular direction is much smaller than the effective electrode spacing, more than two regions exist between the electrodes. The resulting phase angle will be a product of the average phase angle between regions and the number of regions less one. If this product is 180 degrees or greater, doubling the electrode spacing will not necessarily result in a doubling of the measured angle, because the angle is determined with respect to the modulus 360 degrees. However, if the spacing between regions is of the same size as the effective electrode spacing, the phase angle would increase in proportion to the increase in electrode spacing.

In the circular direction the average phase angles for 2.5 mm and 5.0 mm electrode spacings are 29.0 ± 23.2 and 68.3 ± 48.0 degrees respectively. A doubling of the electrode spacing results in the average

phase angle changing by a factor of 2.36. This is evidence that the average phase angle per millimeter is of the order to 11.60 degrees in the circular direction. However, in the longitudinal direction, doubling the electrode spacing results in the mean phase angle changing from 117.3 ± 51.0 to 168.0 ± 79.4 degrees. This increase of only 43 percent indicates either (1) a very large phase lag between oscillating regions, (2) a spacing between oscillating regions much smaller than the electrode spacing, or (3) a combination of both these factors.

5.3.3 The Results from the Cutting Experiments

The results from the twenty cutting experiments may be divided into two parts (1) the results from longitudinally oriented muscle specimens and (2) the results from the circularly oriented specimens. The results from the longitudinally oriented muscle strips are summarized in Table 5.2. The following facts can be obtained from this table:

1. The average frequency of the slow waves before cutting was 5.6 ± 1.2 cycles/minute and there was no significant change in frequencies at recording sites on either side of the cut. (Paired Student t test, $p < .06$.)
2. For an electrode spacing of 2.5 mm the average phase angles between the sites to be decoupled was 121.7 ± 49.8 degrees. After cutting the phase angle continually varied and neither visual analysis nor program "PHSE" could determine a meaningful average phase angle in 80 percent of the results. In these cases "NC" meaning "not coupled" is shown in the table.
3. The average coherence before cutting is 0.60 ± 0.24, and the average after cutting is 0.23 ± 0.21. There is a significant drop of 61

Table 5.2 Cutting experiment results for longitudinally oriented strips, NC is defined as Not Coupled.

EXPERIMENT NO.	BEFORE CUTTING				AFTER CUTTING			
	FREQUENCY		PHASE	COHERANCE	FREQUENCY		PHASE	COHERANCE
	$\bar{f}_1$	$\bar{f}_2$	$\bar{\theta}$	MAGNITUDE	$\bar{f}_1$	$\bar{f}_2$	$\bar{\theta}$	MAGNITUDE
1	5.6	5.6	173.5±7.0	.95	6.0	6.9	211.4±31	.23
2	7.5	7.5	NC	.53	7.0	6.4	-	.73
3	7.6	7.6	99±32	-	4.9	4.9	NC	-
4	5.4	5.4	143±46	-	5.1	5.1	NC	-
5	4.8	4.8	NC	.76	4.5	2.8	NC	.12
6	4.9	5.0	163±65	.64	4.5	4.9	NC	.24
7	5.7	5.7	137±30	.25	5.0	6.4	NC	.06
8	5.6	5.6	26±27	.62	5.0	5.9	NC	.08
9	4.9	4.9	NC	.27	6.6	5.0	NC	.15
10	4.0	4.0	110.3±47	.76	4.5	5.1	NC	.25
AVERAGE	5.6±1.2	5.6±1.1	121.7±49.8	0.60±.24	5.3±.90	5.3±1.2	80% NC	0.23±.21

percent in the coherance figure as a result of the decoupling caused by cutting.

The results may be interpeted as follows:

1. There is no frequency gradient in the longitudinal direction since the frequencies are not changed by the cutting.
2. The average phase angle is 121.7 ± 49.8 degrees. This supports the figure of 117.3 ± 51.0 degrees computed previously. Prior to these experiments it was considered a possibility that a phase angle might exist because of measurement technique and not due to coupling between regions. This hypothesis is rejected by virtue of the fact that an average phase angle could not be computed in 80 percent of the observations after cutting.
3. The results show that the average coherence may be used as a gross indicator of the degree of coupling. They do not indicate a means of relating coherence magnitude directly to the degree of coupling. However, Table 5.2 shows that the amount by which this factor is less than one is an indicator of the statistical variation which will exist in the relative phase angle.

The data from strips oriented in the circular direction are summarized in Table 5.3. These results are divided into two sections, for experiments involving cuts on the mesenteric border and for experiments involving cuts 1 cm from the mesentery.

The results are summarized as follows:

1. The mean frequency before cutting was 7.75 ± 1.2 cycles/minute and the mean phase angle was 70.2 ± 52.4 degrees. After cutting either on or off the mesentery no meaningful average angle could be computed. This situation is indicated as "NC" in the table.

Table 5.3 Cutting experiment results for circularly oriented strips. NC is defined as Not Coupled.

EXPERIMENT NO.	BEFORE CUTTING				AFTER CUTTING			
	FREQUENCY		PHASE	COHERANCE	FREQUENCY		PHASE	COHERANCE
	$\bar{f}_1$	$\bar{f}_2$	$\bar{\theta}$	MAGNITUDE	$\bar{f}_1$	$\bar{f}_2$	$\bar{\theta}$	MAGNITUDE
ON MESENTERY								
1	6.0	6.0	14±3.9	.97	4.0	4.4	NC	.45
2	8.3	8.3	18.1±4.1	.98	4.2	4.5	NC	.32
3	6.9	6.9	21±66	.40	6.2	6.3	NC	.34
4	9.4	9.4	127±18	.74	5.8	4.9	NC	.11
5	7.5	7.5	102±27	.96	6.1	5.5	NC	.05
AVERAGE	7.6±1.3	7.6±1.3	56.4±53.8	.81±.25	6.1±1.6	5.1±.8	NC	.25±.17
OFF MESENTERY								
1	7.8	7.8	45±20	.98	7.0	3.9	NC	.25
2	9.5	9.5	143±5.7	.99	4.0	4.3	NC	.66
3	6.7	6.7	NC	.29	6.4	4.3	NC	.17
4	8.1	8.1	38±67	.89	7.3	5.3	NC	.88
5	7.6	7.6	110±9.4	.93	6.1	3.1	NC	.29
AVERAGE	7.9±1.0	7.9±1.0	84±51.0	.82±.3	6.2±1.3	4.2±.8	NC	.45±.3

2. After cutting on the mesentary there is a drop in frequency at all recording sites but not a significant difference in frequency between sites.
3. After cutting 1 cm from the mesentery there is a drop in frequency at all recording sites, but the drop at sites decoupled from the mesentery because of the cut is much greater.
4. In all cases the coherence value dropped significantly as a result of cutting.

These results may be interpreted as follows:

1. Coupling is again shown to be better in the circular direction than in the longitudinal direction, as indicated by the much smaller average phase angle.
2. There is a frequency gradient in the circular direction in both directions away from the mesentery. This is indicated by the drop in frequency of regions decoupled by cutting on either side of the mesentery.
3. The mesenteric border plays a role in determining slow wave frequency. This is indicated by the above as well as by the fact that cutting on the mesentery resulted in a drop in frequency at all recording sites.
4. Again it is apparent that the coherence figure is a good indicator of the statistical variation in relative phase angle, and consequently an indicator of the degree of coupling.

5.3.4 Results from the Studies of Isolated Muscle Layers

With the development of a suitable dissection procedure it was possible to study isolated longitudinal and isolated circular muscle.

The electrical activity from isolated longitudinal muscle was recorded in four experiments. Slow wave activity was not observed in any of these experiments. Figure 5.10 is a typical record from four extracellular electrodes applied to the serosal side of the isolated longitudinal layer.

Seven extracellular experiments were conducted on the isolated circular muscle layer. In five out of seven experiments slow wave activity was present on both sides of the isolated circular muscle layer. In two of the seven, when the dissection had been particularly difficult, no slow wave was observed. In each experiment the signal obtained from the longitudinal side of the circular muscle was lower in amplitude and more irregular in shape from cycle to cycle. It is presumed that this was due to cell damage caused by the dissection process. Figure 5.11(a) is a typical record obtained from four electrodes applied to the mucosal side of the isolated circular muscle layer while Figure 5.11(b) is a record obtained from the serosal side of that same specimen.

5.3.5 The Submucosal Layer

As described in Chapter 4, in preparation for the in vitro measurements the mucosa and muscularis mucosa are removed. Upon the removal of these two layers a thin layer of submucosa remains attached to the intact muscle wall. It was discovered that this thin layer of submucosa could be easily and uniformly peeled from the circular muscle layer. In fact, the removal of this layer is accomplished much more easily than the separation of longitudinal and circular muscle layers. However, what was most unexpected was that slow wave activity in the intact wall and in isolated circular muscle ceased when this layer

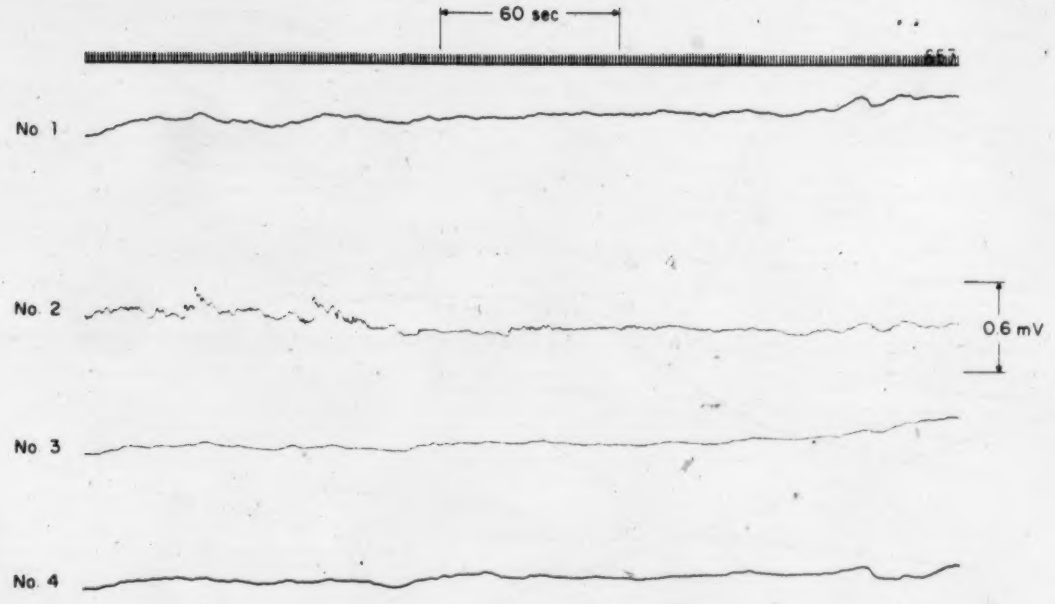

Figure 5.10 Four pressure electrode signals from the serosal side of isolated longitudinal muscle.

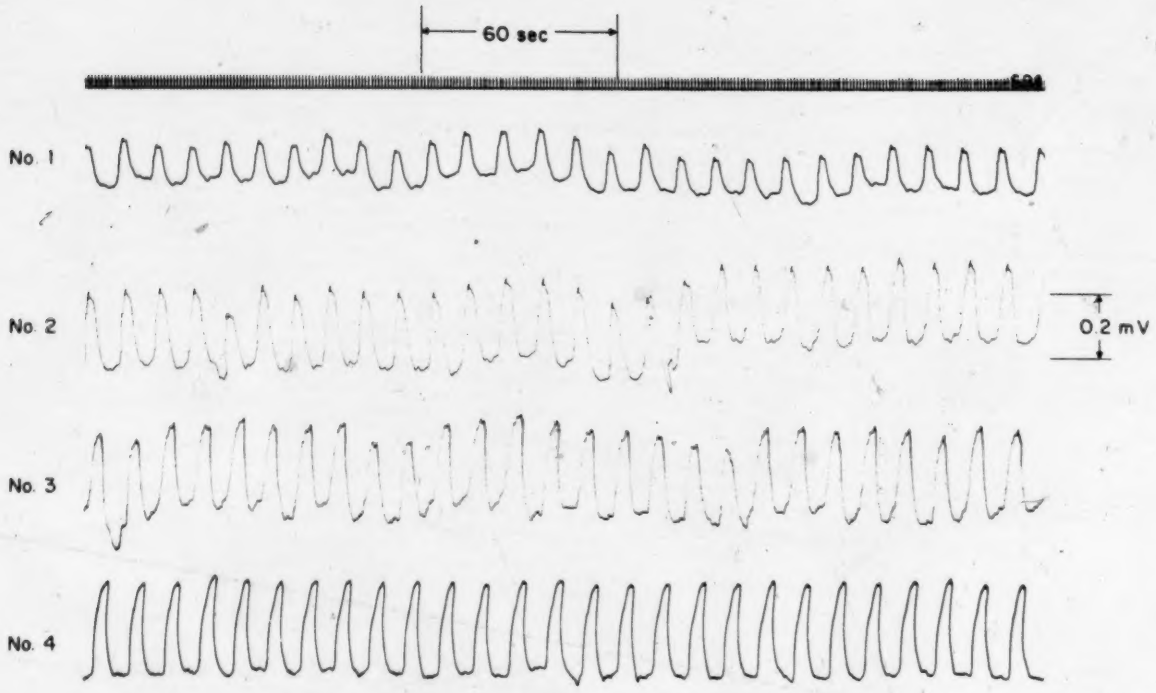

Figure 5.11(a) Slow waves from the mucosal side of isolated circular muscle.

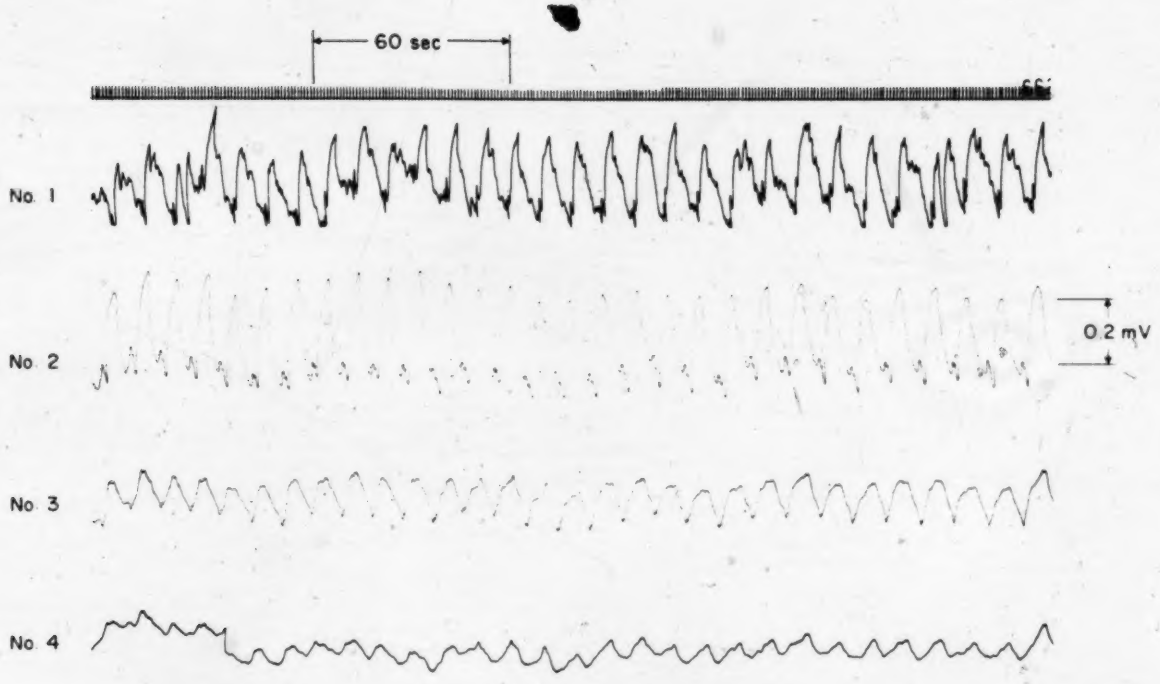

Figure 5.11(b) Slow waves from the longitudinal side of isolated circular muscle.

was removed.

In five experiments using twelve different specimens the normal slow wave was abolished in all cases by complete removal of the submucosal layer. For only two of the specimens was there anything which could be interpreted as cyclic electrical activity.

Histology specimens were prepared for all of these experiments. Figure 5.12 is typical of the histology results showing the circular muscle layer before and after the removal of the submucosal layer and also showing the isolated submucosal layer. All three slides have been treated with Trichrome stain. As can be seen the submucosal layer consists mainly of colagen, appearing as a green color on the slides. Also a small layer of cells which look similar to circular muscle cells is present in the submucosal layer. All attempts to differentiate these cells using different histology stains have been unsuccessful.

In the above five experiments normal slow wave activity was first recorded on the intact specimen. Then the submucosal layer was removed from half of the circular muscle. Recordings were made from the intact half of the tissue as well as from the area where the submucosa had been removed. Normal slow wave activity was recorded from the intact half. However, slow wave activity was found in the other half as well but with amplitude diminishing as a function of distance from the intact portion of the tissue. Figure 5.13 shows a typical recording from four electrodes before and after the removal of half of the submucosal layer. Electrode four is closest to the intact tissue and electrode one is furthest away.

Finally the remaining half of the submucosal layer was removed and as shown by Figure 5.14, all slow wave activity was abolished.

(a)

(b)

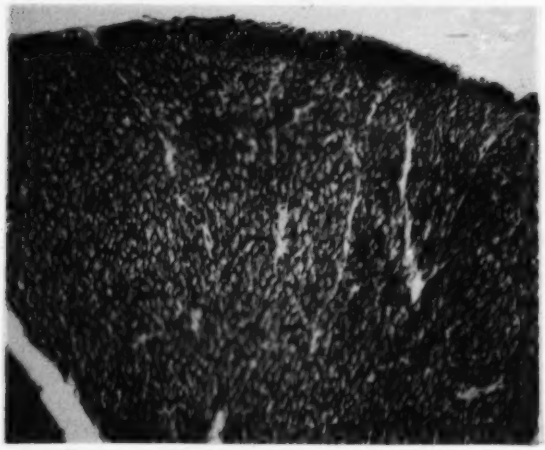

(c)

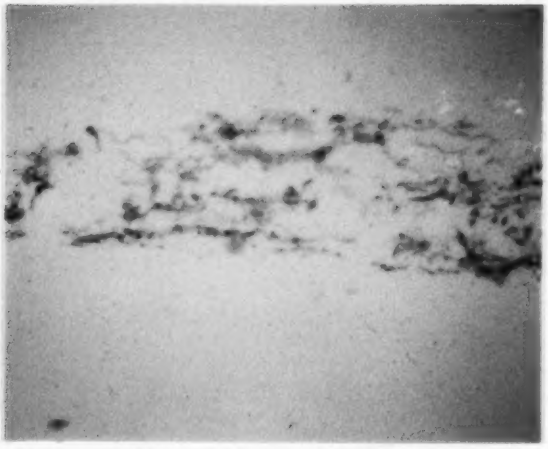

Figure 5.12 Histology slides showing (a) the circular muscle before the removal of the submucosal layer, (b) the circular muscle after the removal of the submucosal layer, and (c) the submucosal layer. Magnification: x62.5.

COLOURED PICTURES
Images en couleur

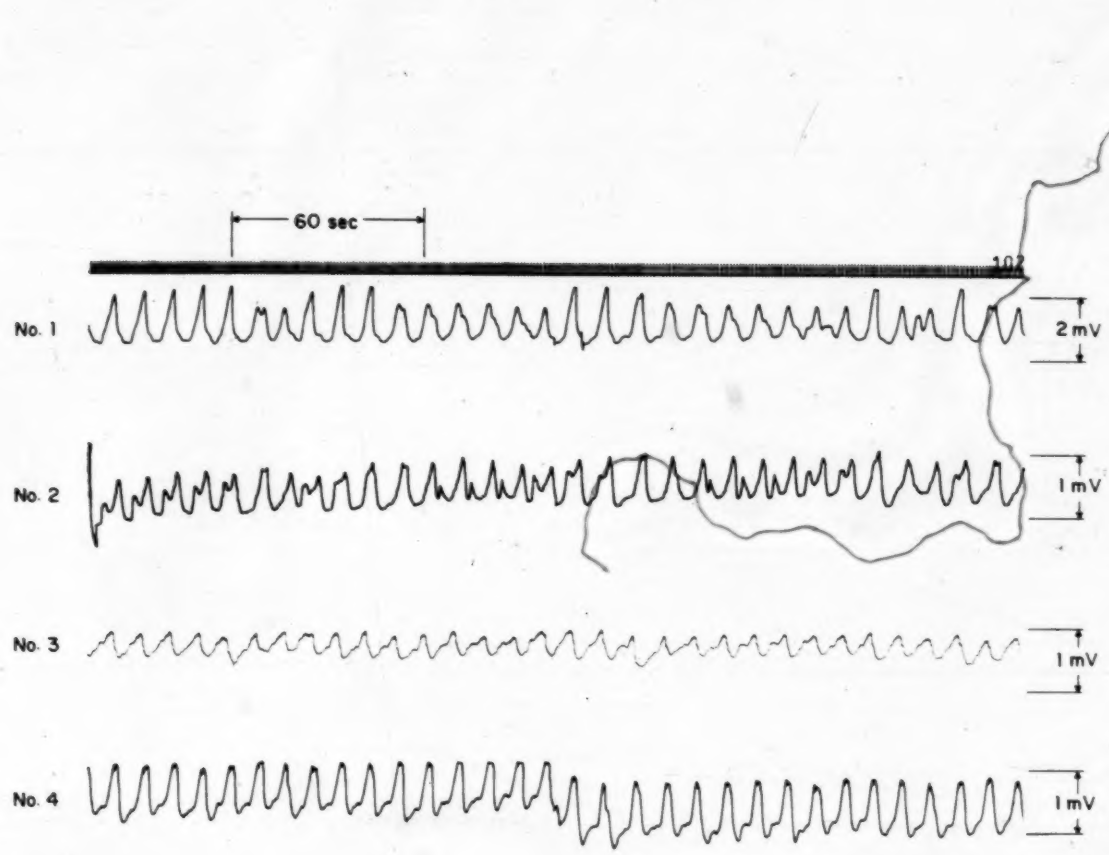

Figure 5.13(a) Slow waves recorded from the mucosal side of the intact muscle wall before removal of the submucosa.

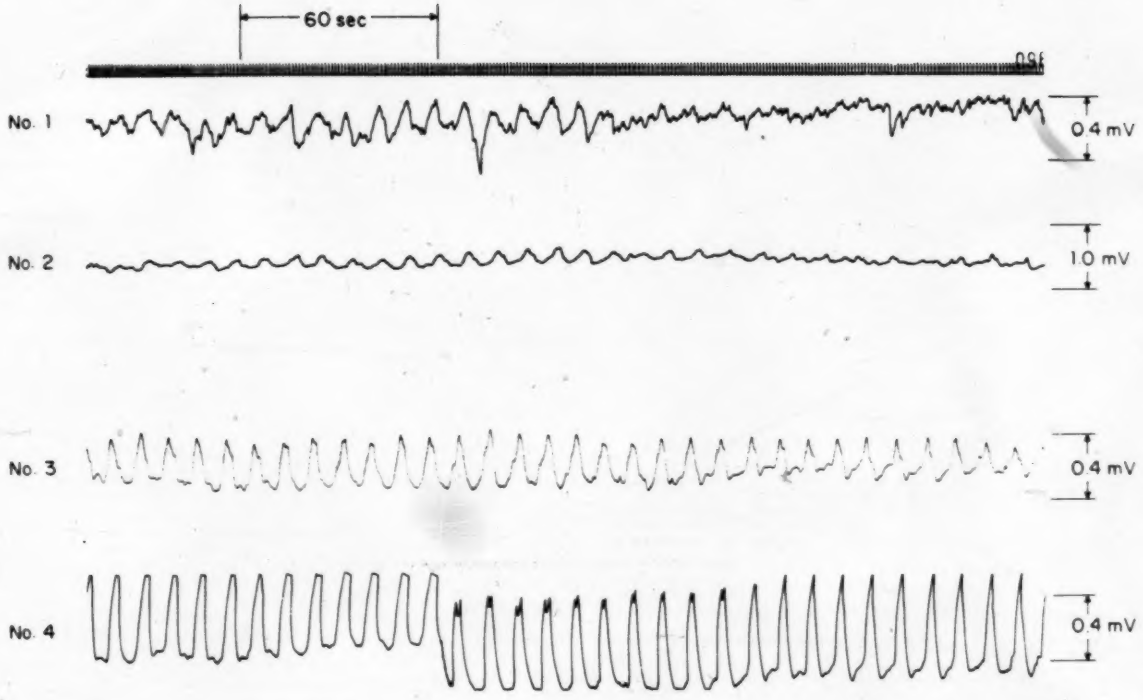

Figure 5.13(b) Slow waves recorded from the mucosal side of the intact muscle wall after removal of the submucosa from half of the specimen.

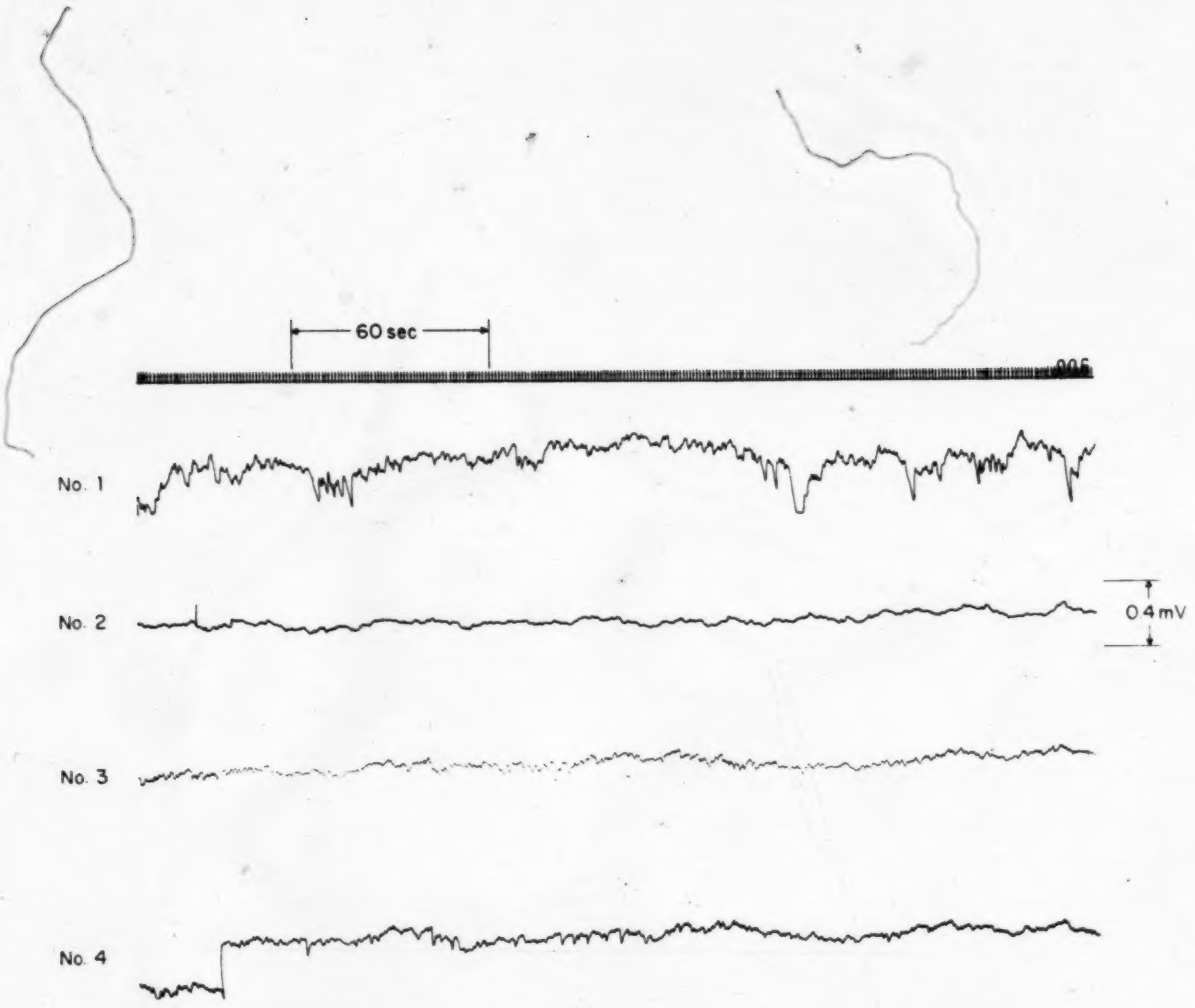

Figure 5.14 A recording from the mucosal side of the intact muscle wall after complete removal of the submucosal layer.

No electrical activity was found in the isolated submucosal layer. Also, upon removal of the submucosa it was impossible to produce any cyclic activity similar to slow waves through external electrical stimulation of the circular muscle.

5.3.6 Results from the Dual Chamber Studies

Twelve dual chamber studies were conducted as described in Chapter 4, section 4.3.6. Six of these experiments were conducted on the intact muscle wall and six were conducted on isolated longitudinal and isolated circular muscle. For the intact muscle segments the signals recorded on the mucosal side were always 3 to 5 times larger in amplitude than those on the serosal side. A typical recording is shown in Figure 5.15. Channel 1 is the signal recorded from the serosal side of the tissue, channel 2 is the signal from the mucosal side, and channel 3 is the difference of channels 1 and 2. These signals were recorded on an fm magnetic tape. They were later studied at fifteen times normal speed using a storage oscilloscope to measure the relative phase angles of the serosal signal versus the mucosal signal. With the time scale expanded fifteen times, the relative phase angle of channel 1 versus channel 2 was too small to be measured.

It has been shown by Bortoff (1965) that an increased concentration of 30 m M KCl causes depolarization of small intestine smooth muscle and abolishes slow waves in that organ. In a set of four experiments, an increased concentration of 30 m M KCl applied to the chamber in contact with the mucosal side significantly reduced the amplitude of the slow wave on both sides. This occurred in four out of four experiments

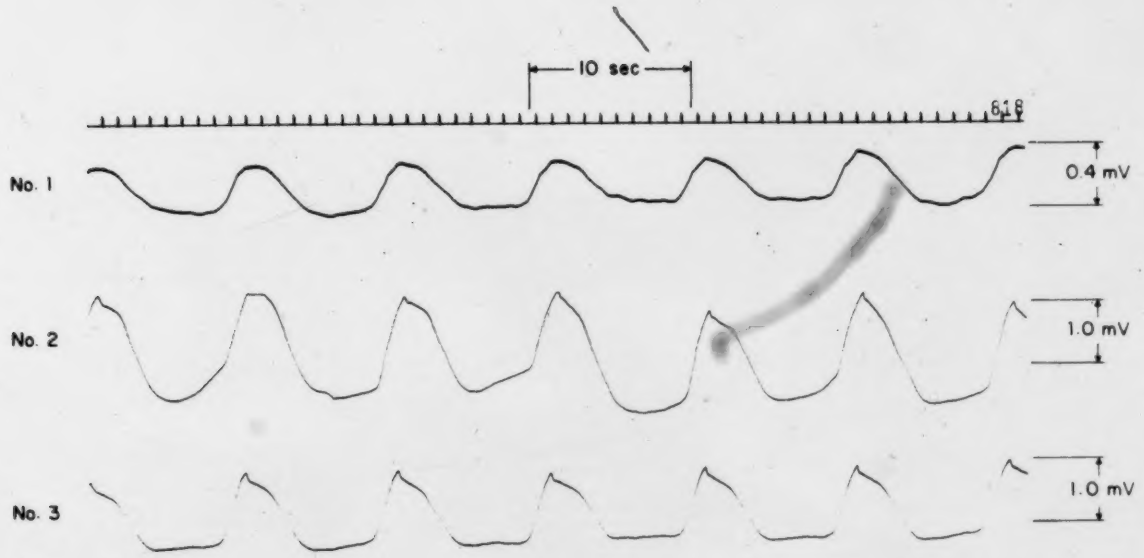

Figure 5.15 Typical signals from an intact muscle specimen in the dual chambered bath.
No. 1 is the serosal signal, No. 2 is the mucosal signal, and No. 3 is the difference of Nos. 1 and 2.

and a representative recording is shown in Figures 5.16 (a) and (b). Washing with normal Krebs-Ringer solution reversed the effect, and slow waves returned as shown in Figure 5.16(c). As shown by Figure 5.16(d) an increased concentration of 30 m M KCl on the longitudinal side had no measurable effect.

In six experiments the circular and longitudinal layers were separated and studied independently. Normal slow waves were recorded from both sides of the isolated circular muscle layer. The amplitude of the signal recorded on the serosal side was of the same order of magnitude as that recorded on the mucosal side. Again the average phase angle of one side with respect to the other was too small to be measured. A typical recording is shown in Figure 5.17.

Increasing the KCl concentration to 30 m M on the mucosal side greatly reduced the slow wave amplitudes measured on both sides of the circular muscle layer. Again the effect was reversed by washing with normal Krebs-Ringer solution. Increasing the KCl concentration on the serosal side of the circular muscle layer produced no immediate effect, but abolished slow waves after a twenty to thirty minute delay.

The isolated longitudinal muscle layer produced no slow wave activity. However, another type of signal was observed. This signal, shown in Figure 5.18, consisted of bursts of activity with a mean frequency of 23.5 cycles/minute and an average of 19.25 cycles/burst. The bursts occurred 1.82 times/minute and were not always present. Their occurrence appeared to be a function of the tension with which the specimen was mounted, since it could be abolished by reducing tissue tension.

Neither this activity nor the normal slow wave was affected by

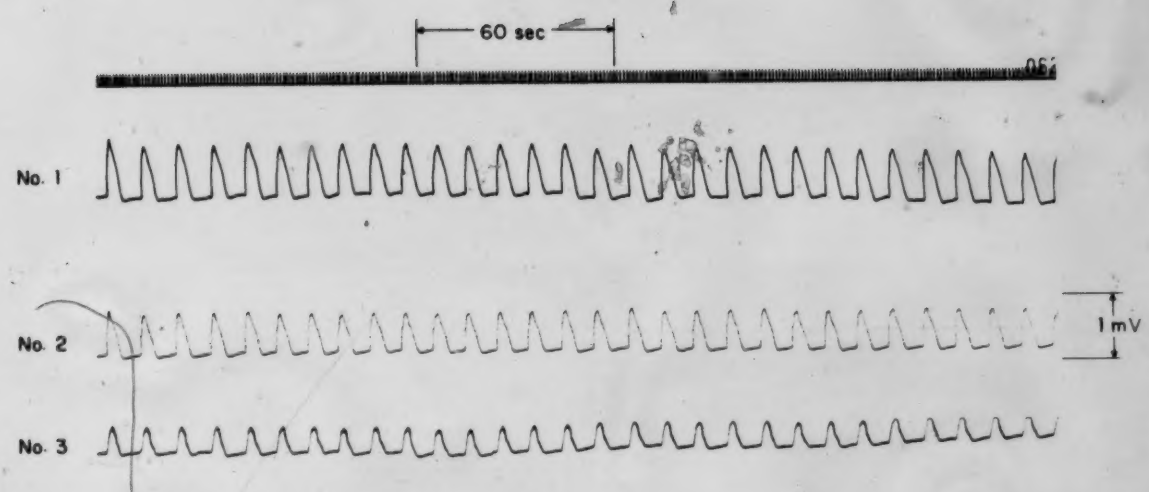

Figure 5.16(a) Dual chamber recording with normal Krebs-Ringer solution. Channels 1, 2, and 3 are as in Fig. 5.15.

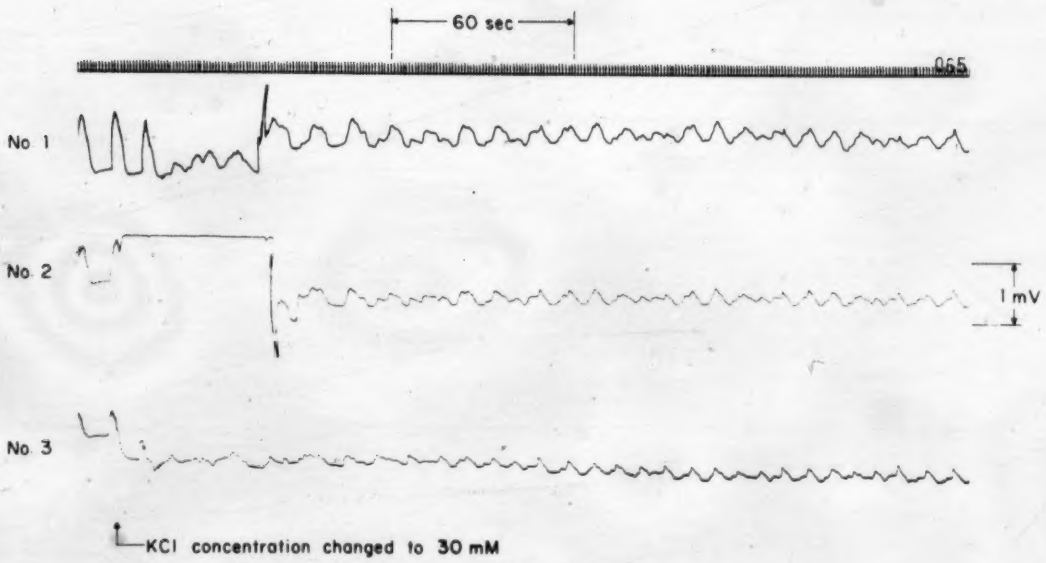

Figure 5.16(b) KCl concentration changed to 30 mM on the mucosal side of the bath.
Channels 1, 2, and 3 are as in Fig. 5.15.

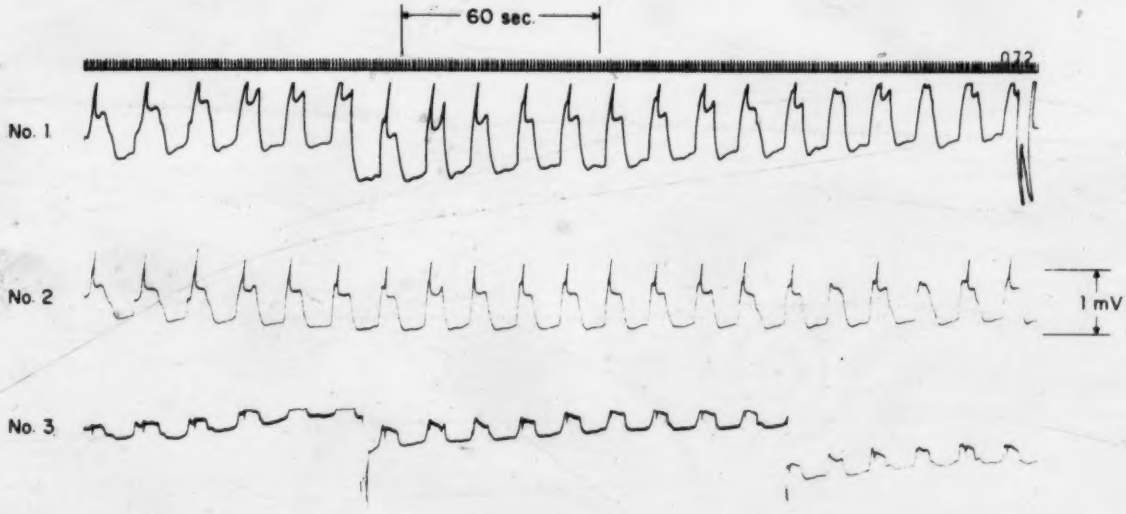

Figure 5.16(c) Tissue washed with noraml Krebs-Ringer solution. Channels 1, 2, and 3 are as in Fig. 5.15.

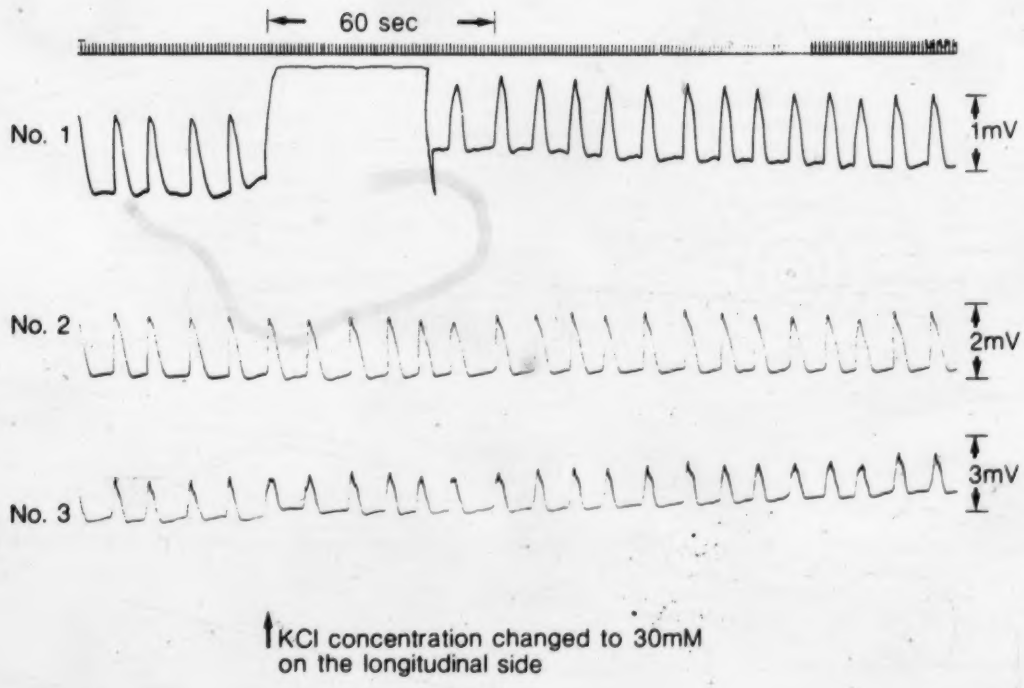

Figure 5.16(d) KCl concentration changed to 30 mM on the longitudinal side of the bath.
Channels 1, 2, and 3 are as in Fig. 5.15.

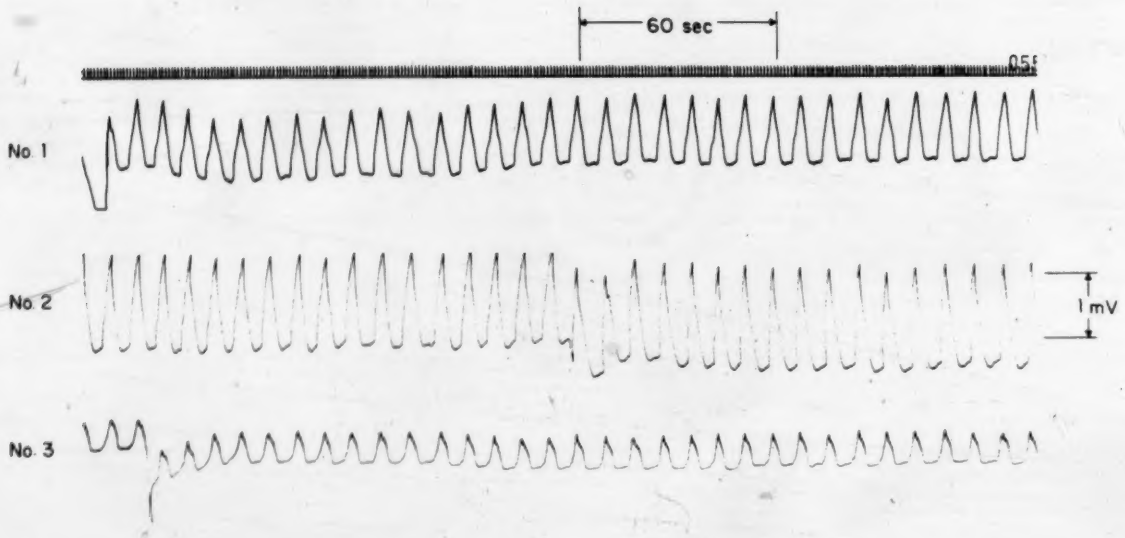

Figure 5.17 Dual chamber study of isolated circular muscle.
Channel 1 is from the longitudinal side,
Channel 2 is from the mucosal side, and
Channel 3 is the difference.

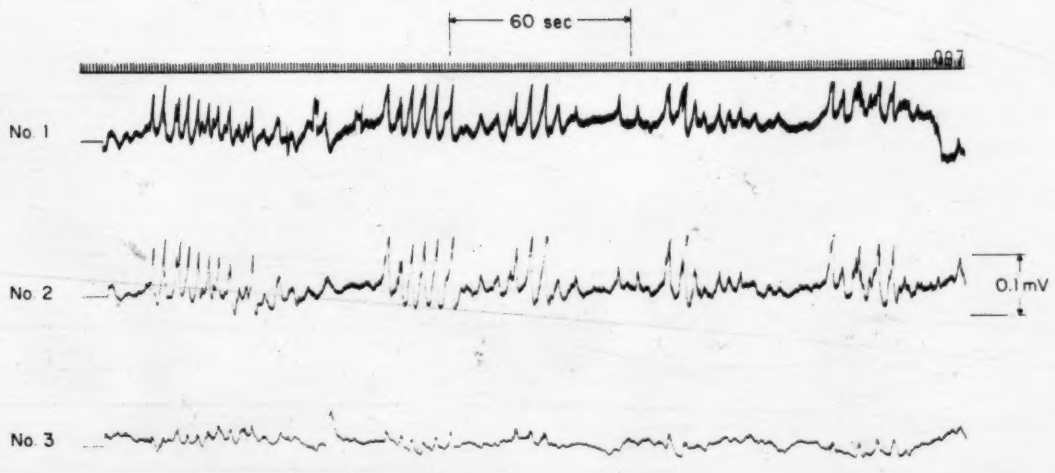

Figure 5.18 Burst activity recorded from isolated longitudinal muscle. Channels 1, 2, and 3 are as in Fig. 5.17.

the administration of 10^{-7} and 10^{-6} M tetrodotoxin to either chamber of the bath.

Another measurement of interest was that of the potential of the reference electrode in the chamber adjacent to the circular muscle with respect to the reference electrode in the other chamber. Records of two such measurements are shown in Figure 5.19. Trace 5.19(a) was recorded in the presence of an intact muscle specimen while trace 5.19(b) was recorded in the presence of an isolated circular muscle specimen. The signals associated with both types of specimens were cyclic with the same repetition frequency as the slow wave. However, the signals associated with isolated circular specimens were much smaller in amplitude than those associated with intact muscle specimens.

5.4 INTRACELLULAR RESULTS

5.4.1 Circular Muscle Measurements on the Intact Muscle

As described in Chapter 4, section 4.4.3, ten intracellular experiments were conducted on the mucosal side of intact muscle strips. In eight of these experiments successful cell penetrations were achieved and maintained for up to twenty minutes. Two experiments were not successful in achieving cell penetrations of sufficient duration to be included in the results. A typical intracellular recording is shown in Figure 5.20. Both channels 1 and 2 represent the same intracellular potential. However, channel 1 is calibrated to permit measurement of the dc intracellular resting potential while channel 2 has the dc offset removed to permit a higher amplifier gain and a more exact display of the slow wave itself.

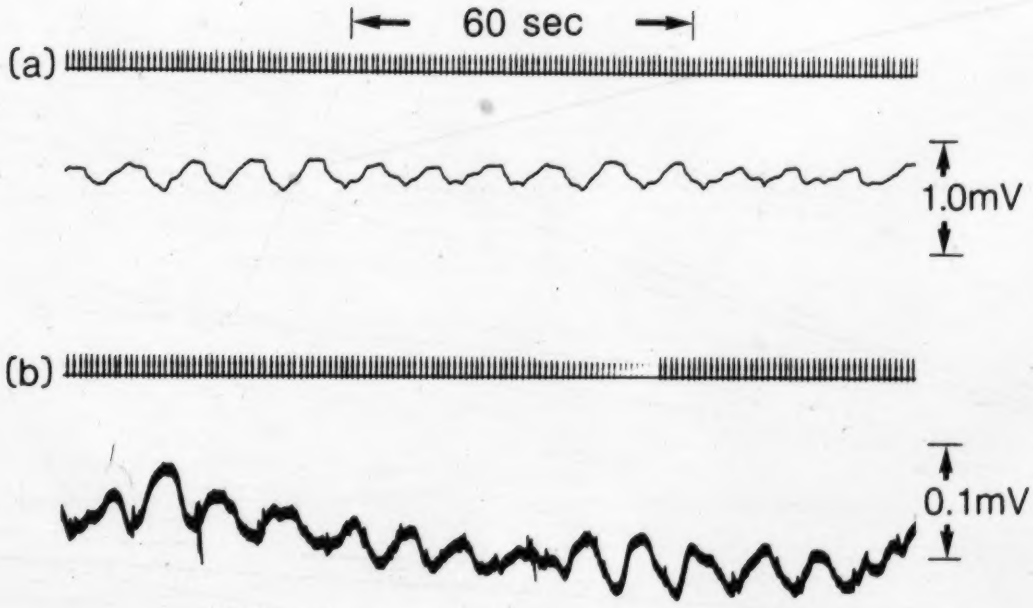

Figure 5.19 Recordings of the potential of the circular reference electrode with respect to the longitudinal reference electrode in the presence of (a) an intact muscle specimen, and (b) an isolated circular muscle specimen.

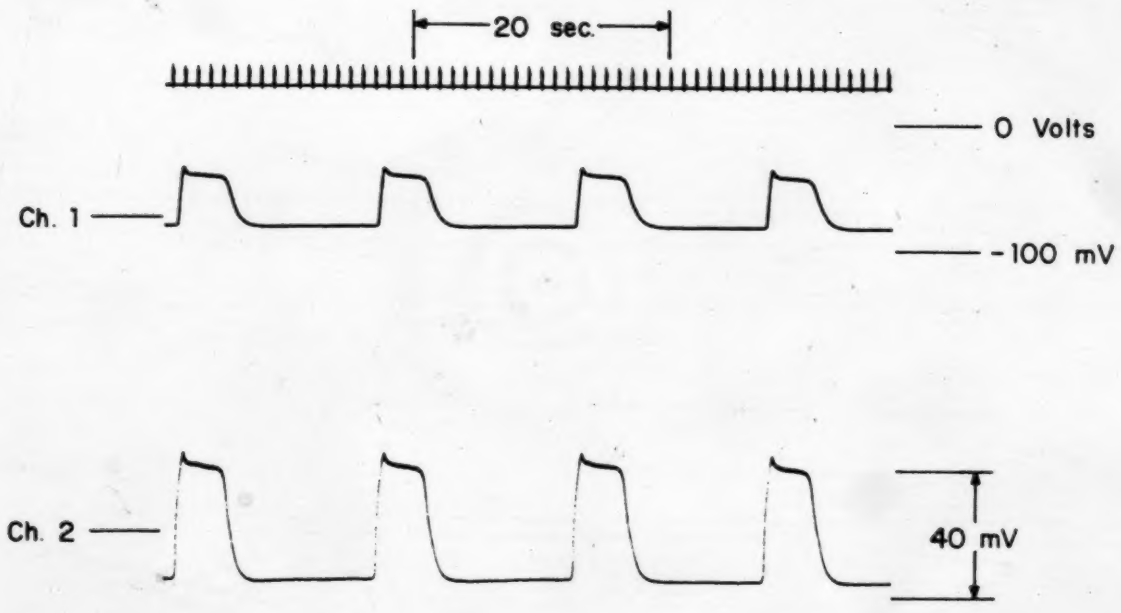

Figure 5.20 A typical intracellular recording from a circular muscle cell. Channel 1 is calibrated to show the resting potential and Channel 2 is calibrated to better show the slow wave amplitude.

In addition to the above eight experiments, intracellular recordings from the mucosal side of the intact muscle wall were obtained from thirteen other experiments.

As shown in Table 5.4, 233 successful penetrations were obtained in the circular muscle cells of 38 specimens. The mean values of the resting potential and the slow wave in the circular muscle layer of proximal and transverse canine colon were calculated to be -77.8 ± 6.8 mV and 28.9 ± 5.5 mV respectively.

5.4.2 Measurements on Isolated Circular Muscle

Five experiments were conducted on isolated muscle layers. These layers were prepared as described in Chapter 4 and were mounted in the same manner as the intact muscle specimens. Table 5.5 is a summary of the results from these experiments. The mean resting potential and the slow wave amplitude on the mucosal side of the isolated circular muscle layer were -73.9 ± 5.9 mV and 30.7 ± 4.9 mV respectively. These values are not statistically different from those obtained for intact muscle strips (Student's t Test $p < .05$). However, on the longitudinal side of the isolated circular muscle layer the resting potential and slow wave amplitude were very different. From twenty-eight measurements the mean resting potential and slow wave amplitude were computed to be -54.3 ± 5.3 mV and 6.6 mV ± 2.0 respectively. The explanation for this difference may be due to cell damage caused by the dissection process.

In two experiments intracellular measurements were obtained from the circular muscle layer after the removal of the submucosa. These measurements confirmed the absence of the slow wave and verified the extracellular results of section 5.3.5. The mean resting potential

Table 5.4 Intracellular Results on the Intact Muscle.

EXPERIMENT NO.	NO. OF SPECIMENS	CIRCULAR MUSCLE			LONGITUDINAL MUSCLE	
		NO. OF MEASUREMENTS	RESTING POTENTIAL (mV)	SLOW WAVE AMPLITUDE (mV)	NO. OF MEASUREMENTS	RESTING POTENTIAL (mV)
55	1	8	-68.5±6.0	25.1±8.0		
56	1	29	-81.0±9.0	29.4±6.2		
57	2	18	-82.8±4.5	30.1±5.0	3	-51.0±1.0
58	2	3	-80.0±8.7	25.7±6.7		
59	3	12	-87.4±3.5	25.0±4.0	1	-50.0
60	2	21	-76.9±10.4	26.3±3.8		
61	3	18	-73.8±7.6	27.7±7.3		
62	1	2	-85.0±7.1	23.0±1.4		
63	2	12	-75.8±5.8	24.8±3.2		
64	2				3	-51.3±8.1
65	2	19	-76.3±6.8	28.0±4.4	6	-52.5±9.9
66	2	12	-77.8±2.9	32.3±4.1	8	-60.9±7.1
67	2	9	-76.5±2.3	35.1±5.7	7	-44.7±5.1
68	1	8	-78.8±4.2	31.6±3.6		
69	2	8	-79.1±9.9	31.9±8.4		
70	1	2	-80.0±4.2	31.0±1.4		
71	2	2	-80.0±7.1	31.5±12	2	-45.0±7.1
72	2	13	-74.6±3.8	29.2±4.4		
73	1	14	-78.9±5.9	26.7±5.4		
74	1	10	-76.5±7.5	33.7±4.3		
75	3	13	-71.3±4.2	31.2±5.2		
MEAN	38	233	-77.8±6.8	28.9±5.5	28	-52.6±7.0

Table 5.5 A summary of intracellular results from isolated longitudinal and circular layers.

EXP. NO.	CIRCULAR MUSCLE							LONGITUDINAL MUSCLE	
		n	MUCOSAL SIDE	n	LONGITUDINAL SIDE	n	WITHOUT SUBMUCOSA	n	CIRCULAR SIDE
59	V_{max} V_{min} S.W.Amp.					4	-77.3±24.2 NO SLOW WAVE		
64	V_{max} V_{min} S.W.Amp.	5	-56.6±5.5 -80.0±6.1 27.0±7.2	7	-49.7±6.1 -53.6±8.0 4.0±1.5			4	-52.5±6.8 No slow wave
65	V_{max} V_{min} S.W.Amp.	5	-35.8±4.1 -67.2±4.5 31.8±2.2	5	-44.8±3.6 -57.0±6.7 +12.2±4.1			6	-51.7±5.8 No slow wave Burst activity
66	V_{max} V_{min} S.W.Amp.	4	-42.5±7.6 -74.5±7.1 34.0±3.7	16	-47.8±2.7 -53.8±2.5 6.0±1.0			5	-59.0±7.4 No slow wave Burst activity
71						2	-62.5±3.5		
Average	V_{max} V_{min} S.W.Amp.	14	-45.1±5.8 -73.9±5.9 30.7±4.9	28	-47.7±4.0 -54.3±5.3 6.6±2.0	6	-72.4±19.9	15	-54.3±6.6

of the circular muscle cells after the removal of the submucosal layer was found to be -72.4 ± 19.9 mV.

5.4.3 Longitudinal Muscle Measurements

A total of thirty successful penetrations in the longitudinal muscle cells of six different specimens were obtained. In none of these measurements was slow wave activity observed. A typical recording from a longitudinal cell penetration is shown in Figure 5.21. The data from these measurements are summarized in Table 5.4. The mean resting potential for longitudinal muscle cells was -52.6 ± 7.0 millivolts.

The results from the five experiments on isolated muscle layers also confirmed the absence of slow waves in isolated longitudinal muscle. Fifteen measurements from three different specimens of isolated longitudinal muscle produced a mean resting potential of -54.3 ± 6.6 millivolts. This is not statistically different from the value computed for longitudinal cells of the intact muscle wall.

Figure 5.22 presents another interesting result obtained from two specimens of isolated longitudinal muscle. This recording shows a high frequency burst of activity not unlike that previously observed in the extracellular experiments (section 5.3.6). This activity was not present in all specimens. The mean resting potential during this activity was -52.5 ± 9.9 mV. The mean frequency of the activity was 16.81 ± 2.6 cycles/minute. The repetition rate of the bursts was not always regular, but when it was, the mean duration of each burst was 23.6 seconds and the mean repetition rate was 0.71 cycles/minute.

The interesting aspect of this data is that it can be thought of

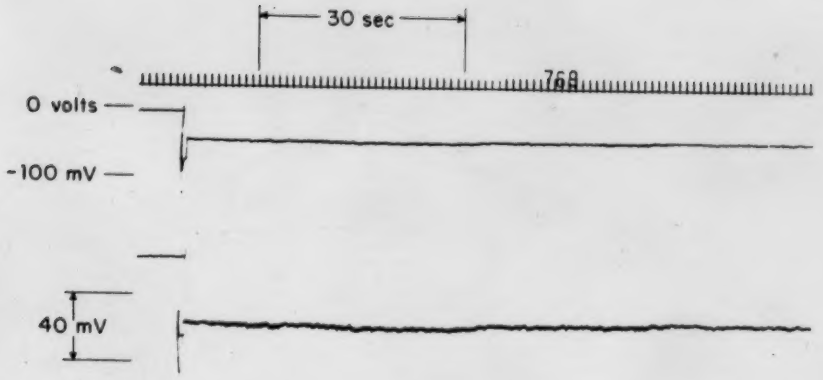

Figure 5.21 A typical intracellular recording from a longitudinal cell. Channels 1 and 2 are as in Fig. 5.20.

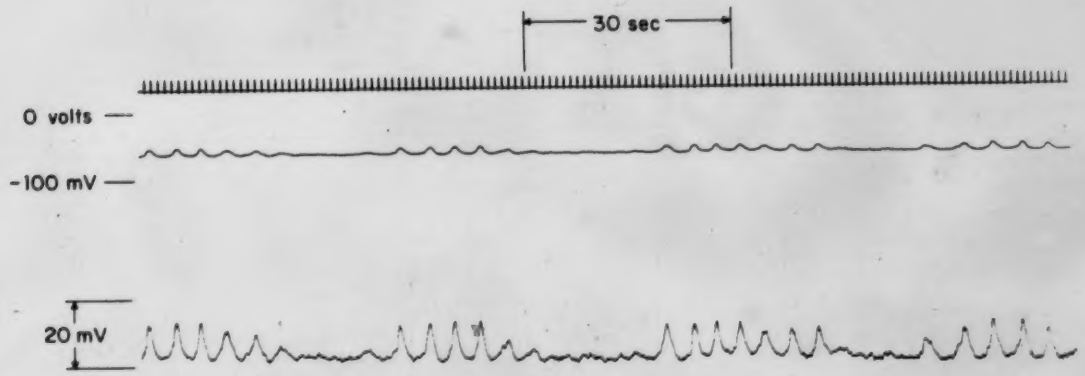

Figure 5.22 Burst activity recorded intracellularly from a longitudinal cell penetration.

as the mixing (interaction) of two intracellular signals. Frequently, extracellularly recorded slow waves produced signals similar to that shown in Figure 5.22. However, this extracellular phenomena had been assumed to be the result of the beating of oscillator cell groups of slightly different frequency (Kingma et. al., 1979). The observations from this experiment create the possibility that the waxing and waning of extracellularly recorded slow waves could be occurring at the cellular level.

5.5 RESULTS FROM STUDIES OF THE INTRACELLULAR-TO-EXTRACELLULAR TRANSDUCTION PROCESS

5.5.1 A Comparison of Simultaneous Intracellular and Extracellular Measurements

As was described in Chapter 4 section 4.5.2, three experiments were conducted to simultaneously record and compare extracellular and intracellular potentials.

A typical recording from this set of experiments is shown in Figure 5.23. Channels 1 and 2 show the intracellular signal and Channel 3 the extracellular signal.

A study of the results from these three experiments showed clearly that the extracellular waveform is a function of the intracellular variations in cells up to 5 mm away from the extracellular recording site. The phase angle between the two sites ranged from zero to fifteen degrees but the variation in extracellular waveform shape made it difficult to obtain a mean value for the phase angle. In addition, the limited number and short duration of these measurements

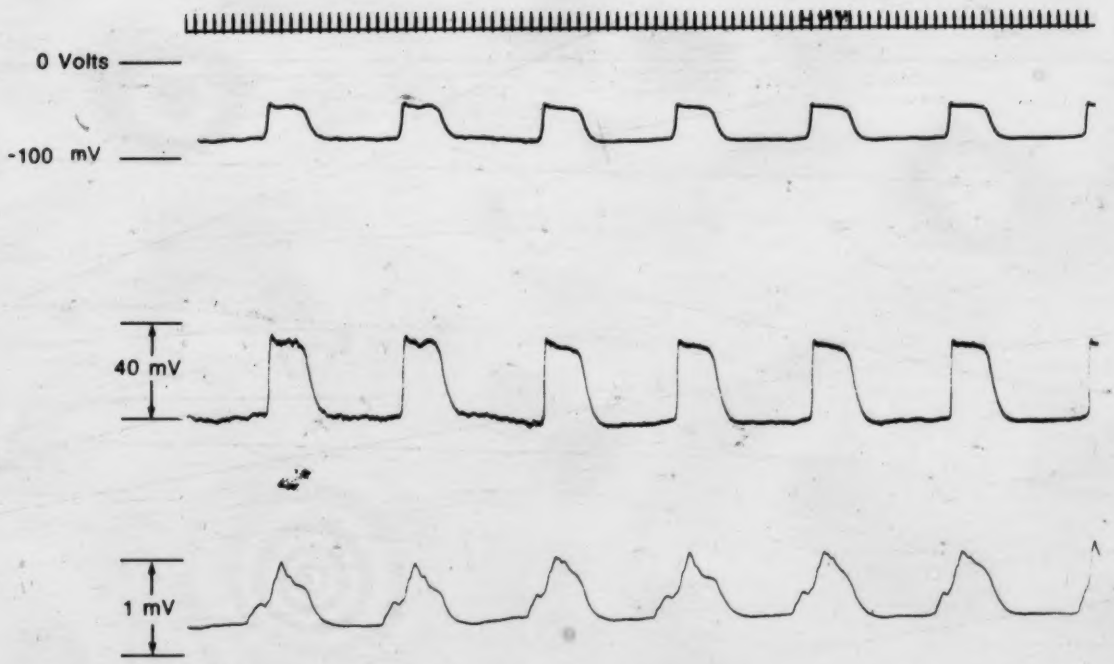

Figure 5.23 Simultaneous recording of intracellular and extracellular signals.

preclude the computation of a statistically significant value for the phase angle.

5.5.2 Injury Potential Measurement

Eight experiments were described in Chapter 4 section 4.5.3 which were conducted to determine if an "injury potential" is responsible for the extracellular pressure electrode signal. Figure 5.24 is a typical recording from one of these eight experiments. The top two tracings show the intracellular potential recorded from a circular muscle cell under the simulated pressure electrode when no force was applied. The bottom two tracings show the intracellular potential under the same pressure electrode at the same location but with a one gram force applied.

The results of the eight experiments are given in Table 5.6. V_{max} and V_{min} indicate values of the maximum and minimum intracellular potentials which occur at the slow wave plateau and trough respectively.

To investigate the relationship between the intracellular potentials and the applied force of the extracellular electrode, the mean potentials associated with each application force are given in Table 5.7. One of the eight experiments showed only a small change in slow wave amplitude as a result of the pressure electrode. The remaining seven experiments showed a significant reduction in slow wave amplitude from a mean value of 28.9 ± 4.0 mV to a mean value of 14.43 ± 4.3 mV with the application of forces ranging from 0.5 to 1 gram. As the force of the pressure electrode increased the slow wave trough (or resting potential) increased from a mean of -76.4 ± 6.8 mV to a mean of -59.7 ± 7.0 mV. However, the level of the slow wave plateau

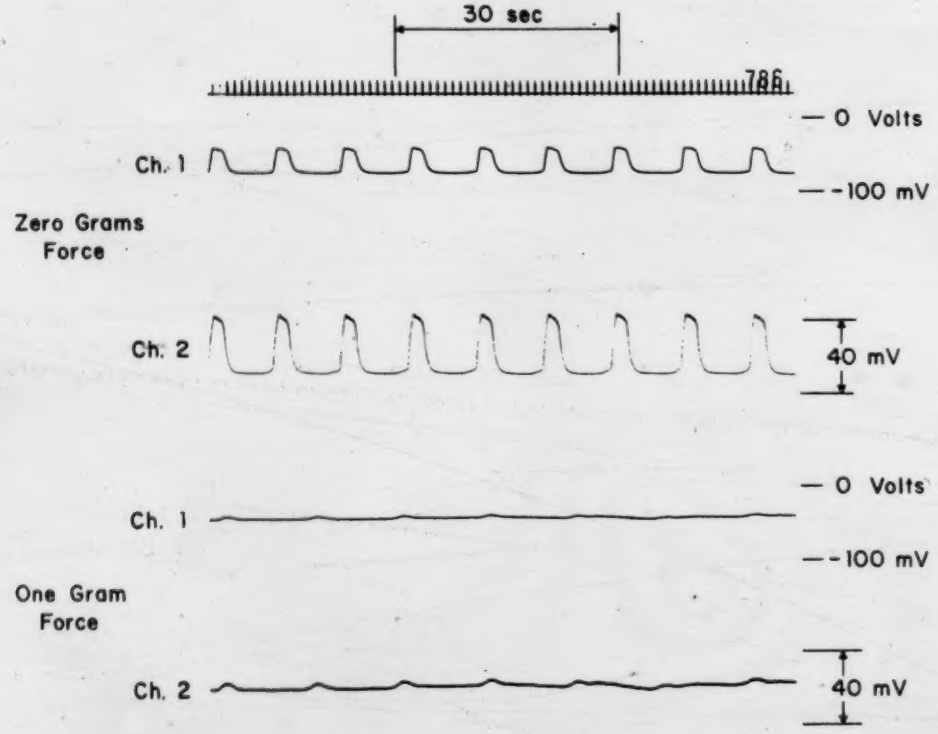

Figure 5.24 Intracellular potentials in the presence of an extracellular pressure electrode.
Channel 1 is calibrated for dc potentials and
Channel 2 has the dc component removed.

Table 5.6 Results from experiments to determine the affect of extracellular electrode force on intracellular potential.

EXP. NO.	FORCE(GMS)	N	V_{max} (mV)	V_{min} (mV)	SLOW WAVE AMPLITUDE (mV)
60	0	21	-52.4±10.9	-76.9±10.4	26.3±3.8
	1	1	-70.0	-70.0	0.0
61	0	18	-43.0±6.3	-73.8±7.6	27.7±7.3
	1	4	-45.0±4.4	-70.0±7.1	25.3±8.1
	2	5	-54.0±15.2	-79.8±8.7	25.8±7.3
	3	2	-43.5±.71	-65.0±7.1	21.5±6.4
63	0	9	-51.1±4.6	-74.0±3.5	23.3±3.7
	1	3	-47.0±0	-63.3±2.9	14.7±2.1
	2	5	-44.4±4.0	-54.0±6.5	13.3±2.2
	3	3	-47.5±4.1	-54.0±1.7	9.3±1.2
	4	3	-47.3±2.5	-58.5±4.9	10.0±0.0
	5	2	-40.0±0.0	-50.0±0.0	10.0±0.0
68	0	5	-45.0±1.4	-81.0±3.8	33.2±3.3
	1	2	-41.0±1.4	-51.0±5.7	10.5±4.9
	0	3	-44.7±4.0	-75.0±0.0	30.3±4.0
	1	2	-42.0±2.8	-48.0±5.7	6.0±2.8
69	0	3	-40.3±6.4	-82.3±2.5	40.0±6.1
SPEC.1	0.5	1	-60.0	-75.0	15.0
	0	3	-43.3±14.4	-71.3±9.3	28.0±5.3
SPEC.2	0	1	-39.0	-76.0	34.0
	0.5	2	-42.5±3.5	-57.0±0	13.5±0.71
	1	2	-45.0±0.0	-50.0±0	5.5±0.7
	0	1	-71.0	-96.0	24.0
73	0	13	-53.1±8.3	-79.6±5.6	26.7±5.6
	1	2	-47.5±3.5	-65.0±0.0	19.0±1.4
	2	3	-50.0±0	-64.7±0.6	14.7±0.6
	4	2	-47.5±3.5	-60.0±7.1	12.5±3.5
	0	1	-43.0	-70.0	27.0
74	0	6	-43.3±10.0	-78.7±9.2	36.3±1.6
	0.5	3	-35.7±9.0	-45.0±26.0	13.3±16.2
	0	4	-44.3±3.0	-73.3±2.4	29.8±4.2
75	0	1	-35.0	-80.0	45.0
SPEC.1	0.5	3	-55.7±4.0	-74.0±1.7	19.0±4.0
	1	5	-42.8±7.0	-59.0±5.5	15.0±3.1
	0	4	-36.3±4.8	-70.5±6.4	35.5±3.7
SPEC.2	0	1	-35.0	-70.0	35.0
	0.5	1	-35.0	-70.0	34.0

Table 5.6 Results from experiments to determine the affect of extracellular electrode force on intracellular potential (cont.).

EXP. NO.	FORCE(GMS)	N	V_{max} (mV)	V_{min} (mV)	SLOW WAVE AMPLITUDE (mv)
	1	1	-47.0	-65.0	18.0
	2	1	-45.0	-65.0	20.0
	3	1	-43.0	-68.0	25.0
SPEC.3	0	3	-44.3±1.2	-70.7±1.2	26.7±2.9
	0.5	2	-41.5±2.1	-73.5±4.9	31.0±1.4
	1	2	-45.0±0.0	-62.0±0.0	17.0±0
	2	1	-45.0	-70.0	25.0
	2.5	1	-50.0	-65.0	15.0
	3	1	-45.0	-60.0	15.0
	4	2	-49.9±1.4	-63.5±4.9	14.5±3.5
	5	2	-47.5±3.5	-57.5±3.5	10.0±0
	0	4	-45.3±2.1	-70.8±1.5	26.5±2.6

Table 5.7 Summary of the results of Table 5.6 arranged in order of increasing electrode force.

FORCE(GM)	NO. OF PENETRATIONS	V_{max} (mV)	V_{min} (mV)	S.W. AMPLITUDE (mV)
0	83	-47.9±7.9	-76.4±6.8	28.9±4.0
.5	12	-44.8±5.2	-63.6±13.1	19.6±8.4
1	20	-45.7±3.8	-58.6±3.9	12.7±2.5
2	10	-46.2±2.8	-59.9±4.6	15.6±1.6
3	5	-46.1±3.2	-58.0±1.3	13.5±.9
4	7	-47.8±2.6	-60.4±5.6	12.0±2.6
5	4	-43.8±2.5	-53.8±2.5	10.0±0.0

increased only a very small amount from -47.9 ± 7.9 mV to -45.8 ± 3.8 mV for the full range of pressure electrode forces. In some experiments the plateau level remained unchanged. Figure 5.25 is a plot of slow wave amplitudes (normalized with respect to basal values) versus pressure electrode application force in grams. These graphs show that the relationship between applied force and slow wave amplitude is nonlinear. However, for a force of 1 gm or greater the mean slow wave amplitude is reduced to 60 percent or less of its basal value.

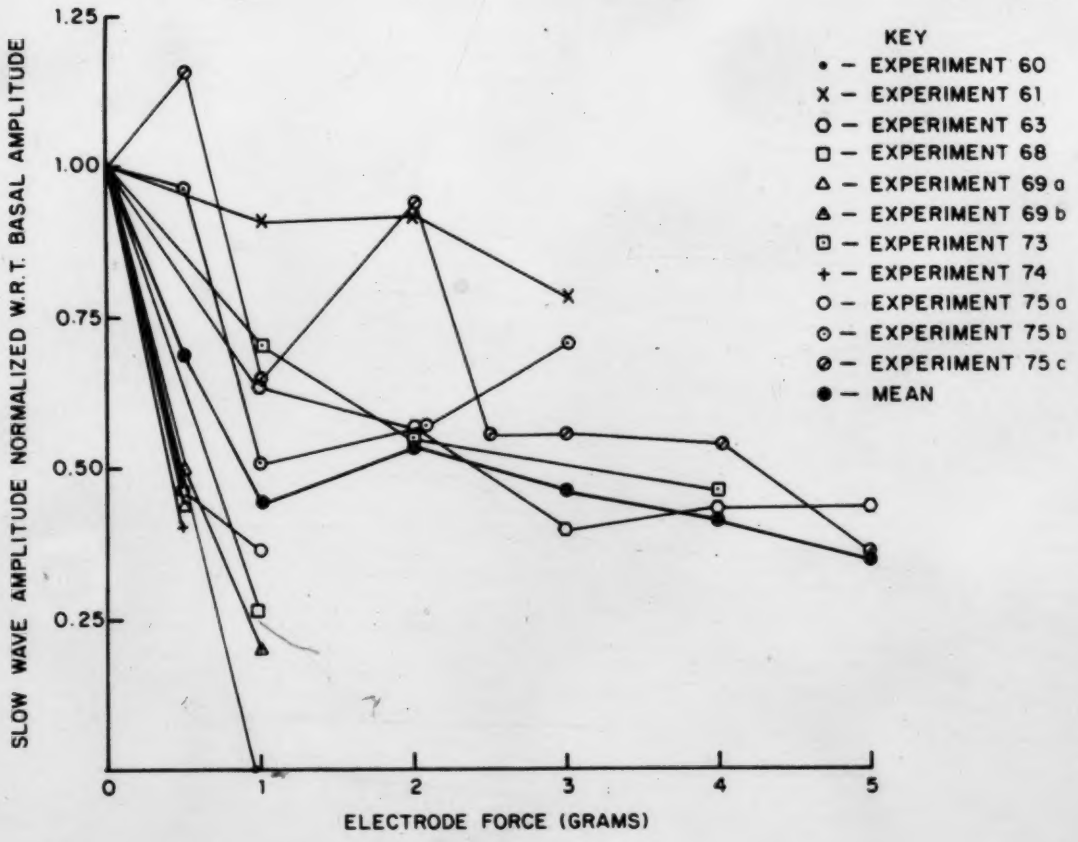

Figure 5.25 Normalized slow wave amplitude versus extracellular electrode application force.

CHAPTER 6

CONCLUSIONS

6.1 INTRODUCTION

The results of Chapter 5 give a better understanding of the origin, intracellular characteristics, and coupling of canine colon electrical activity. The results also give some insight into the role played by each of the muscle layers in the generation of this activity and into the mechanism for intracellular-to-extracellular transduction of slow wave signals. In this chapter each of these areas is examined and conclusions from the results of the previous chapter are given. Intracellular results, single-sided extracellular recordings, and double-sided extracellular recordings are compared to present information in support of each of the conclusions.

Following this, electrical models are presented of slow wave generation at the cellular level and of the intracellular-to-extracellular transduction mechanism. A model is also presented to show the roles played by each of the muscle layers in the generation and coupling of slow wave activity.

The chapter concludes with an indication of the direction of further work.

6.2 SLOW WAVE ORIGIN

The following conclusions may be drawn concerning the origin of slow wave activity:

1. The slow wave originates in a layer of cells at the boundary of the circular muscle layer and the submucosa.
2. This layer is essential for the generation of slow wave activity in the circular muscle layer.
3. Slow waves are not generated in the cells of the longitudinal muscle layer.

These conclusions are supported by the results of the single-sided and double-sided studies of the intact muscle wall and isolated muscle layers as well as by intracellular measurements.

The isolated layer studies of Chapter 5, section 5.3.4 provide information relating to the origin of the slow wave activity. In five of seven experiments, slow waves were recorded extracellularly from both sides of the isolated circular muscle layer. However, in none of four experiments were slow waves recorded extracellularly on either side of the isolated longitudinal muscle layer. This led to the suspicion that the slow wave origin was either in the circular muscle layer or its associated submucosal layer.

As was described in Chapter 5, section 5.3.5, the submucosal layer could easily be removed from the circular muscle layer. In five experiments using twelve different specimens the normal slow wave in the circular muscle layer was abolished by the complete removal of the submucosal layer. However, when the submucosal layer was removed from only part of the specimen, the slow wave was abolished only in the region from which the submucosa had been removed. As seen in Figure 5.13, the amplitude of the slow wave in the region devoid of the submucosa was a function of the distance from the intact portion of the tissue. The circular muscle layer thus requires the presence

of the submucosal layer to produce slow wave activity.

The dual chamber studies provided additional information about the slow wave origin. The pertinent results are as follows:

1. Slow waves recorded simultaneously on both sides of the intact muscle wall had, in every experiment, larger amplitudes on the mucosal side of the specimen.
2. An increased concentration of 30 m M KCl applied to the mucosal side of an intact muscle specimen in all cases significantly reduced slow wave activity as recorded on both sides of the specimen. However, the same increased concentration applied to the serosal side produced no effect. Thus the mucosal side of the circular muscle layer is of particular significance with regard to the generation of the slow wave.
3. Slow waves were recorded on both sides of isolated circular muscle and were always of approximately the same amplitude.
4. Slow waves were never recorded on either side of isolated longitudinal muscle.

The most convincing evidence relating to the origin of the slow wave are the results of the intracellular experiments present in Chapter 5, section 5.4. Slow waves were recorded from 233 penetrations of cells located throughout the circular muscle layers of 37 intact specimens. Slow waves were also recorded throughout the isolated circular muscle layer when its submucosa was intact. However, slow waves were not recorded from the circular muscle layer after the submucosa had been removed. In 28 penetrations of longitudinal muscle cells in the intact wall, slow wave activity was never recorded. This was also observed for isolated longitudinal muscle.

To recapitulate, slow waves do not exist inside longitudinal muscle cells, but they originate in the circular muscle layer at the boundary with the submucosa. Cells within the submucosa or special cells near the inner surface of the circular muscle layer interact with the cells of the circular muscle layer to generate slow waves.

Two of the more likely explanations of this interaction are:

(1) That pacemaker cells within the submucosal layer or in the immediately adjacent circular muscle layer provide an electrical stimulus to the circular muscle layer.

or (2) That cells in the submucosal layer provide a chemical input to the circular layer changing the resting potential to cause slow wave generation within the inner circular layer.

Slow waves recorded extracellularly on the longitudinal side of the intact muscle wall are the result of passive current flow from the circular muscle layer through the longitudinal muscle. This is confirmed by the lower amplitude slow wave recorded on the longitudinal side of the specimen in the dual chamber experiments. The potentials generated by the circular muscle layer are attenuated by the resistance of the longitudinal layer. This is also supported by results from the measurement of the potential of the longitudinal reference electrode with respect to the circular reference electrode as described in Chapter 5, section 5.3.6. In the presence of an intact muscle specimen this potential varied at the same frequency as the slow wave. However, these variations were an order of magnitude smaller with isolated circular muscle in the tissue bath. Slow wave currents flowing from the circular layer through the longitudinal layer cause the potential of the circular side to vary with respect to the serosal side. However,

in the case of isolated circular muscle the slow wave currents from the circular muscle cells flow directly to each reference electrode passing through only the low resistance of the tissue bath on both sides of the tissue.

6.3 INTRACELLULAR SLOW WAVE CHARACTERISTICS

Prior to this work, intracellular recordings from the canine colon have not been reported in the literature. Consequently, this work has produced the first comprehensive intracellular study of canine slow wave characteristics.

As reported in Chapter 5, section 5.4, 233 successful penetrations were obtained from the circular muscle layers of 37 different specimens of intact muscle wall from the proximal and transverse colon. There was no variation in cellular resting potential or slow wave amplitude throughout the circular muscle layer or over the regions of the colon studied. The mean resting potential and slow wave amplitude were -77.8 ± 6.8 mV and 28.9 ± 5.5 mV respectively. From the results of five experiments (described in Chapter 5, section 5.4.2) conducted on the isolated circular muscle layer, the mean resting potential and slow wave amplitude on the mucosal side of this layer were found to be -73.9 ± 5.9 mV and 30.7 ± 4.9 mV respectively. This is not signifigantly different (Student's t test, $p < .05$) from the corresponding results from the intact muscle wall. Therefore, the separation of the layers does not affect slow wave generation. However, the intracellular results confirmed that the removal of the submucosal layer abolished the slow wave in the circular muscle layer (Chapter 5, section 5.4.2).

The intracellular results from the circular muscle layer also confirmed that the extracellularly recorded slow wave signal is an accurate representation of the intracellular potential variations of the cells surrounding the electrode.

Intracellular measurements were also obtained from the longitudinal muscle cells in both the intact muscle wall and the isolated longitudinal layer. Because the longitudinal layer is much thinner than the circular layer and because the serosa was an impediment to electrode penetration, the number of successful penetrations in the longitudinal layer were less than that in the circular layer. Nevertheless, 28 successful penetrations were obtained in six different specimens of intact muscle wall and 15 successful penetrations were obtained in three different specimens of isolated longitudinal muscle. Slow waves were not observed in any of these recordings. The mean resting potentials for intact and isolated longitudinal muscle were -52.6 ± 7.0 mV and -54.3 ± 6.6 mV. Again, the process of muscle separation has not affected the intracellular potentials.

Another interesting result obtained from the intracellular experiments was the recording of a higher frequency burst activity observed intracellularly in longitudinal muscle cells (Chapter 5, section 5.4.3 and Figure 5.21). This activity was also observed extracellularly as reported in the results of the dual chamber studies (Chapter 5, section 5.3.6) and has been reported by El-Sharkawy (1979). The intracellular results of section 5.4.3 indicate that this burst activity is an intracellular phenomena and not the result of the mixing of signals from different cell groups.

6.4 ELECTRICAL COUPLING WITHIN THE COLON

The data from 23 single-sided extracellular experiments was processed on the HP 21MX/E computer (as described in Chapter 5, section 5.3.1) to determine the relative phase lag between recording sites. The results from this processing confirmed that electrical coupling between oscillating regions in the colon is very poor. There was great variability in the relative phase angles of slow waves recorded from sites separated by as little as 2.5 mm. However, from the large amount of data processed it was determined that the mean phase angle between recording sites separated by 2.5 mm was 29.0 ± 32.2 degrees in the circular direction and 117.3 ± 51.0 in the longitudinal direction. A conclusion to be deduced from this data is that coupling is much better in the circular direction than in the longitudinal direction.

The results from the cutting experiments (described in Chapter 5, section 5.3.3) also support the hypothesis that coupling between regions is better in the circular direction than in the longitudinal direction. In addition to this, these results show that no gradient of natural frequencies exists in the longitudinal direction but that such a gradient exists in the circular direction with respect to the mesentery. This indicates (as stated in section 5.3.3) that the mesentery plays a role in determining slow wave frequency.

6.5 PRESSURE ELECTRODE SIGNAL TRANSDUCTION

The currently accepted theory for the generation of the pressure electrode slow wave signal is that it results from an injury potential

caused by cell distortion. This theory was reviewed in Chapter 3 and extended to explain the situation when many cells are electrically coupled. However, descrepancies exist between the theory described in Chapter 3 and the results of the transduction experiments described in Chapter 5, section 5.5.2.

The extension of Gillespie's model (Gillespie, 1962) as described in Chapter 3 proposes that cell distortion causes membrane depolarization resulting from a drop in membrane resistance. This drop in membrane resistance was represented in the model of Figure 3.6 by the variable resistor R_L. However, this drop in resistance would result in the reduction of both the dc and the ac components of the intracellular potential. Both ac and dc components of the intracellular potential of the cells of the rabbit large intestine were reduced by the same factor when these cells were injured by large microelectrodes (Gillespie, 1962). The results of Chapter 5 include only the data from what were considered to be successful cellular penetrations. However, on many occasions in all intracellular experiments, signals were obtained from what were recognized as "unsuccessful penetrations". These unsuccessful penetrations were identified by the fact that the resting potential and slow wave amplitude were not maintained constant during the penetration. Immediately after the penetration the resting potential increased slowly towards zero potential. In these cases the slow wave amplitude was reduced in proportion to the reduction in the magnitude of the resting potential. The value of the plateau potential of the slow wave was also changed by the same factor. These "unsuccessful" penetrations produced results consistant with Gillespie's injury potential theory. However, the results from the study of the

pressure electrode mechanism (Chapter 5, section 5.5.2) do not support the injury potential hypothesis.

In seven of eight experiments the application of a pressure electrode with a force of 0.5 to 1 gm caused a significant reduction in slow wave amplitude from 28.9 ± 4.0 mV to 14.4 ± 4.3 mV. However, this reduction occurred without a change in the slow wave plateau potential. The mean plateau potentials before and after the pressure electrode application are -47.9 ± 7.9 mV and -45.8 ± 3.8 mV respectively.

The reduction in slow wave amplitude results almost entirely from an increase in the cellular resting potential. The "injury potential" theory requires a proportional reduction of both resting and slow wave plateau potentials.

This leads to the following conclusions: First, if an "injury potential" is created by the pressure electrode, it is not the result of a total reduction in membrane resistance. Second, the results imply the existence of separate mechanisms for the maintenance of the cellular resting potential and for the initiation of the slow wave plateau phase. Third, the distortion caused a reduction in the cellular resting potential but did not interfere with the ionic mechanism responsible for the initiation of the slow wave plateau. The latter two of these conclusions require further clarification.

6.6 A PROPOSED THEORY FOR SLOW WAVE GENERATION AND PRESSURE ELECTRODE SIGNAL GENERATION

Since it was not one of the objectives of this thesis to examine

the ionic mechanisms responsible for the slow wave, the above conclusions are implied by the results but are not proven. The two generally accepted theories with respect to slow wave generation involve either modulation of the Na-K pump or modulation of the membrane impedance associated with such a pump. In either case if the slow wave were the result of a relaxation oscillator involving a membrane voltage threshold, it would be expected that a change in resting potential would result in a change in slow wave frequency. This did not happen when the membrane resting potential was altered by the application of the simulated pressure electrode. This is an indication that the start of the slow wave was not the result of a threshold phenomena involving either of the ions associated with the Na-K pump. The time of the slow wave upswing and the slope of the intracellular potential prior to the upswing were unchanged with the change in resting potential. The indication is that some other ion (which has little effect on the membrane potential) is responsible for the slow wave. The concentration of such an ion would move towards a threshold value while the cellular potential is at the resting value. When the threshold concentration is attained, this ion could initiate the slow wave plateau phase by either a direct effect on the membrane impedance or by inhibition of the Na-K pump. During the plateau phase the concentration of this ion would return to a subthreshold level. El-Sharkaway and Daniel (1975 b) and Connor (1979) postulated that the Ca^{++} ion might fulfill such a role in the stomach and small intestine.

The plateau level of the slow wave is not significantly changed by the pressure electrode application. This indicates that the ions and membrane conductances associated with the plateau are not altered by cell distortion. This work provides no evidence regarding the identity

of such ions or why such conductances remain unchanged.

However the results provide support for the hypothesis that slow waves are the result of a modulation of the membrane impedance. The results are consistent with the idea that the membrane impedance consists of two parallel components, a constant impedance which is primarily responsible for the resting potential and another variable impedance which causes the membrane potential variations called slow waves. Distortion due to the pressure electrode reduces the constant component of the membrane impedance but does not affect the variable component and consequently does not affect the level of the slow wave plateau.

The generation of the cellular resting potential and the slow wave potential variations can be modelled as shown in Figure 6.1. This model is not designed to include action potential generation. R_m represents the normal membrane resistance in the absence of an action potential. I_m is a constant current source representing the total current produced by the electrochemical gradients and the Na-K pump. A time varying current source i_{sw} models the slow wave potential varation.

The pressure electrode causes cell distortion which results in an increase in the resting potential. The intracellular potential rises to a resting value corresponding to the level of the slow wave plateau. This is illustrated in Figure 5.24. Similarly, damage due to the dissection process produces the same results. This was verified by the data from the intracellular measurements on isolated circular muscle presented in section 5.4.2. These results show that on the longitudinal side of the isolated circular muscle layer, the plateau potential of the slow wave is -47.7 mV, corresponding to that found in

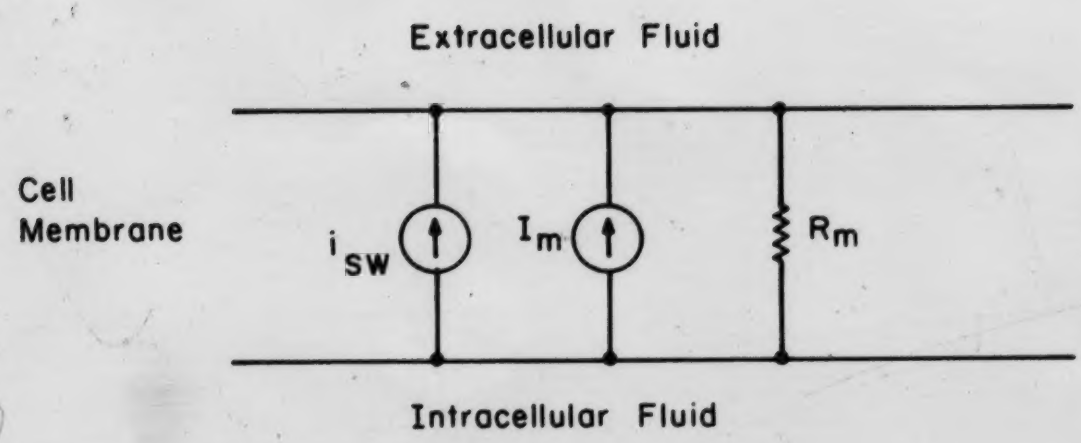

Figure 6.1 Model of the smooth muscle membrane.

the circular layer of the intact muscle wall. However, the slow wave amplitude was reduced to a mean of 6.6 mV indicating a reduction in i_{sw}.

The generation of the extracellular pressure electrode signal may be explained using Figure 6.2. The current source i'_{sw} represents the equivalent slow wave generator of all cells distorted by the pressure electrode. R_s is the shunt resistance between the active surface of the pressure electrode and the reference electrode in the tissue bath. R_i and R_c are the equivalent internal and coupling resistances of the cells from which the recording is obtained. Assuming an infinite input impedance for the amplifier, the recorded voltage v(t) as determined from the circuit of Figure 6.2(b) will be

$$v(t) = \frac{[i'_{sw}(t) - i_{sw}(t)]R_m R_s}{2R_m + 2R_i + R_c} \qquad 6.1$$

If in the limit i'_{sw} (t) is reduced to zero as indicated by the abolition of slow waves under the pressure electrode, then

$$v(t) = \frac{-i_{sw}(t)\, R_m R_s}{2R_m + 2R_i + R_c} \qquad 6.2$$

However for the normal cell, the slow wave component $v_{sw}(t)$ of the intracellular potential is given by

$$v_{sw}(t) = -i_{sw}(t)\, R_m \qquad 6.3$$

Substituting this into equation 6.1 gives

$$v(t) = \frac{R_s}{2R_m + 2R_i + R_c} \cdot v_{sw}(t) = K \cdot v_{sw}(t) \qquad 6.4$$

where K is a constant.

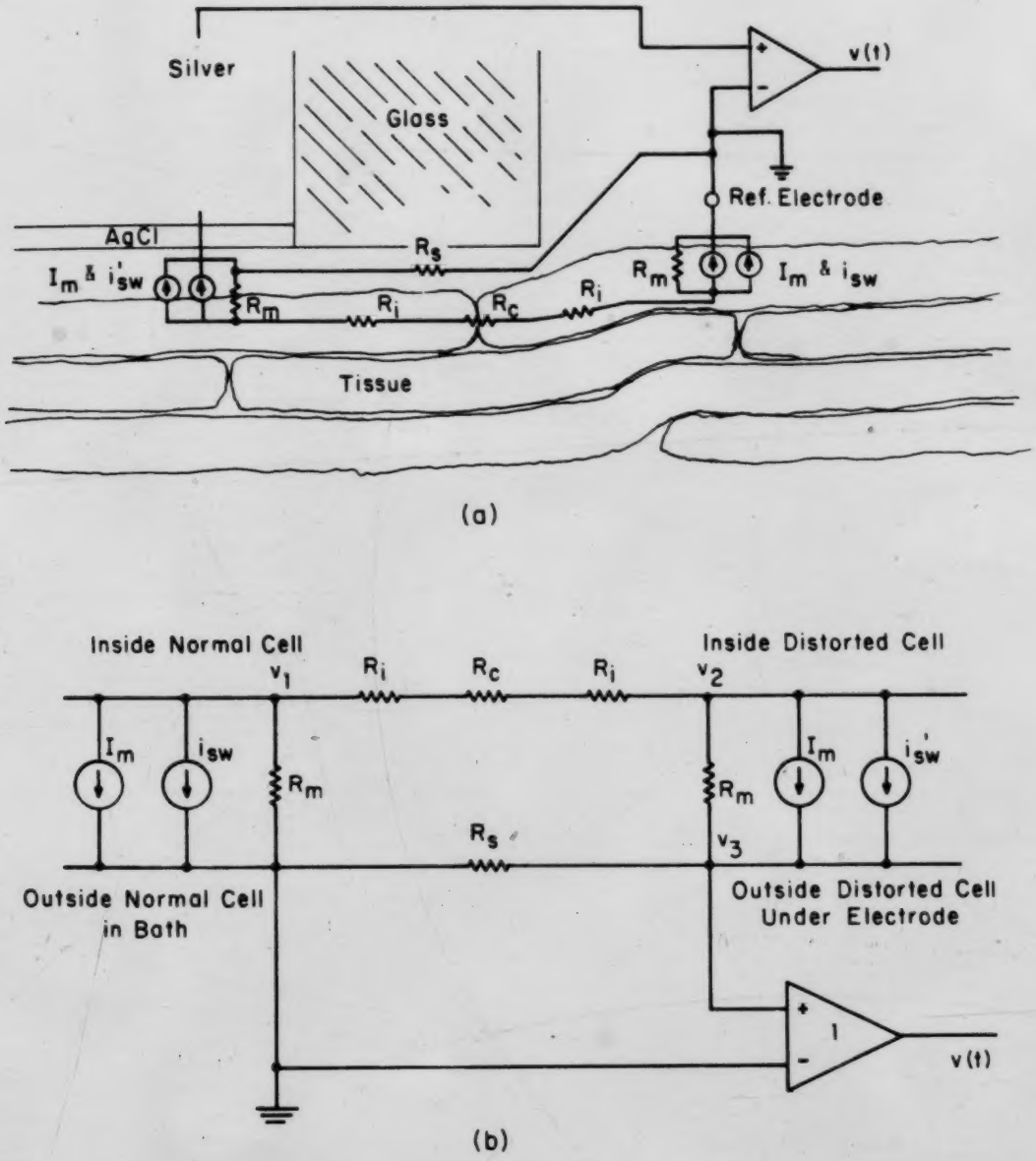

Figure 6.2 Extracellular pressure electrode slow wave generation.

Therefore the extracellular slow wave signal is proportional to the intracellular potential variation $v_{sw}(t)$. If the amplifier input impedance R_{in} is finite, then R_s in the above expression must be replaced by the value of the parallel combination of R_s and R_{in}.

6.7 AN EXAMINATION OF THE ROLES PLAYED BY THE INDIVIDUAL MUSCLE LAYERS IN THE GENERATION OF SLOW WAVE ACTIVITY

6.7.1 The Circular Layer

Evidence presented in this work indicates that a special layer of cells at the boundary of the submucosa and the circular muscle layer is essential for the existence of slow waves in the circular muscle layer. In the absence of the special layer the circular muscle cells have intracellular potentials which remain constant at approximately -72 mV. Therefore the biological oscillators of the circular muscle layer are either a monostable type requiring an input trigger signal from the special layer or they require a chemical or hormonal input to change oscillator parameters to cause oscillations. If the oscillators are of the monostable type, the trigger signal from the special layer must be generated by astable oscillators within that layer or within the circular layer of the boundary with the submucosa. A model showing a possible arrangement of these oscillators is shown in Figure 6.3. The physiological units represented by the astable oscillators could be individual cells or groups of tightly coupled cells oscillating in unison.

The results from the cutting experiments (Chapter 5, section 5.3.3) show that the oscillators of the colon have a frequency gradient

with respect to the mesentery. The frequency of slow wave oscillations is reduced significantly when the tissue is separated from the mesentery.

The model of Figure 6.3 shows coupling to exist between the oscillators of the circular muscle layer. This was shown to be correct because partial removal of the special layer did not result in total abolition of the slow wave in the regions devoid of the special layer. The amplitudes of slow waves recorded in these regions diminished with distance from the portion of the tissue with the special layer intact.

6.7.2 The Longitudinal Layer

The cells of the longitudinal layer do not actively participate in slow wave generation. The evidence obtained from the work described in this thesis indicates that this layer acts as a passive conductor for electrical activity generated in the circular muscle layer. The lack of a measurable phase lag across this layer indicates that the layer is almost purely resistive.

In the model of Figure 6.3 the longitudinal muscle layer is represented by the resistors R_{CL} and R_L. The resistance R_{CL} represents the coupling which exists between the circular and longitudinal muscle layers. R_L represents the distributed resistance of the longitudinal layer. Although R_{CL} is shown connected to a separate output of the monostable oscillator, it is possible that it could be connected to the normal output coupling the oscillator to an adjacent oscillator. In either case, R_{CL} and R_L are factors which influence electrical coupling in both the longitudinal and circular directions.

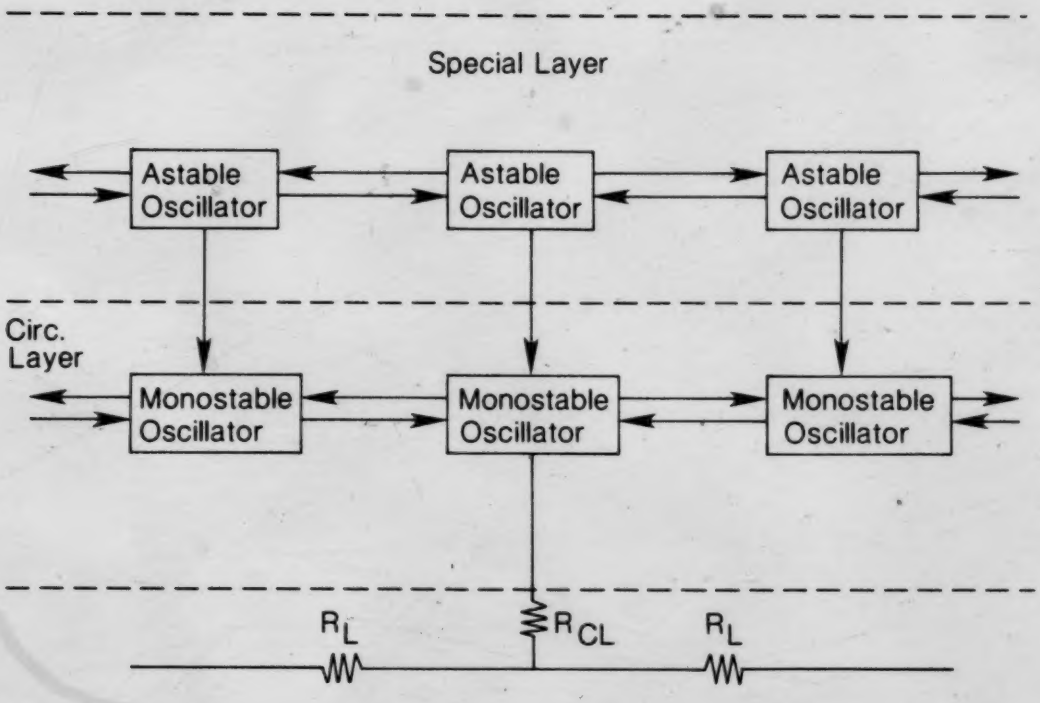

Figure 6.3 A model showing a possible arrangement of oscillators in the colon wall.

6.8 FUTURE WORK

The quest for knowledge is an unending search. As a consequence of this it is expected that the research described in this thesis will present a number of questions to be dealt with in future work. The more interesting of these questions pertain to the metabolic mechanisms responsible for slow wave generation. The hypothesis presented in Section 6.6 should be tested. This can be accomplished by conducting intracellular measurements using voltage clamp or chemical clamp techniques.

The knowledge gained from the canine colon studies has significance only if it can be related to the electrical activity of the human colon. At present, intracellular studies of human colon specimens have not been very successful. Using the procedures and equipment developed for the canine studies, future measurements on human colon tissue should be more successful. Procedures should be developed to insure the viability of human specimens. With such procedures the small number of human specimens will be optimally used and procedures for successful cellular penetrations will be developed. Then the knowledge gained from the canine studies can be applied to the study of normal and abnormal human tissue with the final objective being the treatment of disease.

REFERENCES

Alverez, W.C. & Mahoney, L.J. (1922). Action current in the stomach and intestine. Am. J. Physiol., 58:476-493.

Bass, P. (1968). Invivo electrical activity of the small bowel. In: Handbook of Physiology: Alimentary Canal. Sect. 6, Vol. IV. Motility (ed. C.F. Code), pp. 2051-2074. American Physiological Society, Washington, D.C.

Bendat, J.S. & Piersol, A.G. (1966). Measurement and analysis of random data, Wiley, New York.

Bennett, M.R. (1967). The effect of intracellular current pulses in smooth muscle cells of guinea-pig vas-deferens at rest and during transmission. J. Gen. Physiol., 50:2459-2475.

Bennett, M.R. (1972). Autonomic neuromuscular transmission. Cambridge University Press.

Bennett, M.R. & Rogers, D.C. (1967). A study of the innervation of the taenia coli. J. of Cell. Biology, 33:573-596.

Bennett, M.R. & Merrillees, N.C.R. (1966). An analysis of the transmission of excitation from autonomic nerves to smooth muscle. J. Physiol., 185:520-535.

Bortoff, A. (1965). Electrical transmission of slow waves from longitudinal to circular intestinal muscle. Am. J. Physiol., 209(6): 1254-1260.

Bortoff, A. (1967). Configuration of intestinal slow waves obtained by monopolar recording techniques. Am. J. Physiol., 213(1):157-162.

Bortoff, A. (1975). Recording of extracellular electrical activity, In: Methods in Pharmacology, vol. 3, Smooth Muscle, eds. E.E. Daniel and D.M. Paton, pp. 185-199, Plenum Press, New York.

Bowes, K.L., Shearin, N.L., Kingma, Y.J., & Koles, Z.J. (1977). Frequency analysis of electrical activity in dog colon. In: Proceedings of the 6th International Symposium on Gastrointestinal Motility, edited by H.L. Duthie, pp. 251-269, MTP Press, Lancaster, England.

Brading, A.F. (1979). Maintenance of ionic composition. Br. Med. Bull., 35:227-234.

Brightman, M.V. & Reese, T.S. (1969). Junctions between intimately opposed cell membranes in the vertebrate brain. J. Cell. Biology, 40:648-677.

Cajal, S. (1933). Histology. Bailliere, Tindall, & Co., London.

Cannon, W.B. (1902). The movements of the intestine studied by means of roentgen rays. Am. J. Physiol., 6:251-277.

Casteels, R. (1969). Calculation of the membrane potential in smooth muscle cells of the guinea pig's taenia coli by the Goldman equation. J. Physiol. London, 205:193-208.

Casteels, R. (1970). The relation between the membrane potential and the ion distribution in smooth muscle cells. In: Smooth Muscle, edited by E. Bulbring, A.F. Brading, A.W. Jones, & T. Tomita, pp. 70-99, Williams & Wilkins, Baltimore.

Casteels, R. & Van Breeman, C. (1975). Active and passive Ca++ fluxes across cell membranes of guinea pig taenia coli. Pfluegers Arch., 359:197-207.

Chambers, M.M., Bowes, K.L., Kingma, Y.J., Bannister, C., and Cote, K.R. (1981). In vitro electrical activity in human colon. Gastroenterology, 81:502-508.

Christensen, J. (1975). Myoelectric control of the colon. Gastroenterology, 68:601-609.

Christensen, J., Anuras, S., & Hauser, R.L. (1974). Migrating spike bursts and electrical slow waves in the cat colon: effects of sectioning. Gastroenterology, 66:240-247.

Christensen, J., Caprilli, R., & Lund, G.F. (1969). Electric slow waves in circular muscle of cat colon. Am. J. Physiol., 217: 771-776.

Christensen, J. & Hauser, R.L. (1971 a). Longitudinal axial coupling of slow waves in proximal cat colon. Am. J. Physiol., 221:246-250.

Christensen, J. & Hauser, R.L. (1971 b). Circumferential coupling of electric slow waves in circular muscle of cat colon. Am. J. Physiol., 221:1033-1037.

Christensen, J. & Rasmus, S.C. (1972). Colon slow waves: size of oscillators and rates of speed. Am. J. Physiol., 223:1330-1333.

Cobbold, R.S.C. (1974). Transducers for Biomedical Measurements. John Wiley & Sons, New York.

Code, C.F., Szurszewski, J.H., Kelly, K.A., & Smith, I.B. (1968). A concept of control of gastrointestinal motility. In Handbook of Physiology: Alimentary Canal, Sect. 6, Vol. V (ed. C.F. Code), pp. 2881-2896, American Physiological Society, Washington, D.C.

Connor, J.A. (1979). On exploring the basis for slow potential oscillations in the mamalian stomach and intestine. J. Exp. Biol., 81:153-173.

Connor, J.A. & Prosser, C.L. (1974). Comparison of ionic effects on longitudinal and circular muscle of cat jejunum. Am. J. Physiol., 226:1212-1218.

Connor, J.A., Prosser, C.L., & Weems, W.A. (1974). A study of pacemaker activity in intestinal smooth muscle. J. Physiol. London, 240:671-701.

Connor, J.A., Kreulen, D., Prosser, C.L., & Weigel, R. (1977). Interaction between longitudinal and circular muscle in intestine of cat. J. Physiol. London, 273:665-689.

Cooley, J.W. & Tookey, J.W. (1965). An algorithm for the machine calculation of complex fourier series. Math. Comp., 19:297-301.

Daniel, E.E. & Chapman, K.M. (1963). Electrical activity of the gastrointestinal tract as an indication of mechanical activity. Am. J. Digest. Diseases, 8:54-102.

Daniel, E.E., Honour, A.J. & Bogoch, A. (1960). Electrical activity of the longitudinal muscle of dog small intestine studied in vivo using microelectrodes. Am. J. Physiol., 198:113-118.

Daniel, E.E. & Irwin, J. (1968). Electrical activity of gastric musculature. In Handbook of Physiology: Alimentary Canal, Sect. 6, Vol. IV. Motility (ed. C.F. Code), pp. 1969-1984, American Physiological Society, Washington, D.C.

Daniel, E.E. & Sarna, S. (1978). The generation and conduction of activity in smooth muscle. Am. J. Physiol., 216:301-307.

Daniel, E.E., Wachter, B.T., Honour, A.J., & Bogoch, A. (1960). The relationship between electrical and mechanical activity of the small intestine of dog and man. Can. J. Biochem. Physiol., 38:777-801.

Dewey, M.M. & Barr, L. (1962). Intercellular connection between smooth muscle cells: the nexus. Science, 137:670-672.

Diamant, N.E., Rose, P.K. & Davison, E.J. (1970). Computer simulation of intestinal slow wave frequency gradient. Am. J. Physiol., 219(6):1684-1690.

Duthie, H.L. (1975). Colonic motility in man. Mayo Clinic Proc., 59:519-522.

El-Sharkawy, T.Y. (1978). Electrophysiological control of motility in canine colon. In: Gastrointestinal Motility in Health and Disease. Proc. 6th Int'l. Symposium on Gastrointestinal Motility, ed. H.L. Duthie, pp. 387-398, MTP Press, Lancaster, England.

El-Sharkawy, T.Y., Bardakjian, B.L. & MacDonald, W.M. (1982). Origins of multiple patterns of electrical control activity in the colon. In: Motility of the Digestive Tract, ed. M. Wienbeck, Raven Press, New York.

El-Sharkawy, T.Y. & Daniel, E.E. (1974). The ionic basis of electrical control potentials (slow waves). Proc. 4th Int. Symp. on Gastrointestinal Motility, Banff, Alberta, Canada, pp. 39-52, Mitchell Press, Vancouver, B.C.

El-Sharkawy, T.Y. & Daniel, E.E. (1975 a). Electrical activity of small intestinal smooth muscle and its temperature dependence. Am. J. Physiol., 229:1268-1276.

El-Sharkawy, T.Y. & Daniel, E.E. (1975 b). Ionic mechanisms of intestinal electrical control activity. Am. J. Physiol., 229:1287-1298.

El-Sharkawy, T.Y. & Daniel, E.E. (1975 c). Electrogenic sodium pumping in rabbit small intestinal smooth muscle. Am. J. Physiol., 1277-1286.

El-Sharkawy, T.Y., Morgan, K.G. & Szurszewski, J.H. (1978). Intracellular electrical activity of canine and human gastric smooth muscle. J. Physiol. Lond., 279:291-307.

Firth, D.R. & Defilice, L.J. (1971). Electrical resistance and volume flow in glass microelectrodes. Can. J. Physiol. Pharmacol., 49:436-447.

Fitzhugh, R. (1961). Impulses and physiological states in theoretical models of nerve membrane. Biophysical Journal., 1:445-466.

Geddes, L.A. (1972). Electrodes and the Measurement of Bioelectric Events. Wiley-Interscience, New York.

Geddes, L.A. & Baker, L.E. (1968). Principles of Applied Biomedical Instrumentation. John Wiley & Sons, Inc., New York.

Gillespie, J.S. (1962). Spontaneous mechanical and electrical activity of stretched and unstretched intestinal smooth muscle cells and their response to sympathetic nerve stimulation. J. Physiol., 162:54-92.

Graham, J. & Gerrard, R.W. (1946). Membrane potentials and excitation of impared single muscle fibres. J. Cell. & Comp. Physiol., 28:99-116.

Goldman, D.E. (1943). Potential, impedance and rectification in membrane. J. Gen. Physiol., 27:37-60.

Hodgkin, A.L. & Huxley, A.F. (1952). A quantitative description of membrane current and its application to conduction and excitation in nerve. J. Physiol. Lond., 117:500-544.

Kobayashi, M., Nagai, T. & Prosser, C.L. (1966). Electrical interaction between muscle layers of cat intestine. Am. J. Physiol., 21(6):1281-1291.

Kuriyama, H. & Tomita, T. (1965). The response of single smooth muscle cells of the guinea-pig taenia coli to intracellular applied currents, and their effect on the spontaneous electrical activity. J. Physiol., 178:270-289.

Kelly, K.A., Code, C.F. & Elveback, L.R. (1969). Patterns of canine gastric electrical activity. Am. J. Physiol., 217:461-470.

Kelly, K.A. & Code, C.F. (1971). Canine gastric pacemaker. Am. J. Physiol., 220:112-118.

Kingma, Y.J., Durdle, N.G., Lenhard, J.M. & Bowes, K.L. (1980). A small silver-silverchloride electrode for the measurements of low frequency biological signals. Digest of the 8th Can. Med. & Biol. Engineering Conf., Hamilton, Canada.

Kuriyama, H. & Tomita, T. (1965). The response of single smooth muscle cells of the guinea-pig taenia coli to intracellularly applied currents, and their effect on the spontaneous electrical activity. J. Physiol., 178:270-289.

McGeachie, T.K. (1975). Smooth muscle regeneration. Monographs in Developmental Biology, Vol. 9, ed. A. Wolsky, S. Karger Publications.

Mills, R.G. & Taylor, G.S. (1971). Studies of intestinal slow wave activity with double surcrose gap apparatus. Life Sci., 10: 347-353.

Nelsen, T.S. & Becker, J.C. (1968). Simulation of the electrical and mechanical gradient of the small intestine. Am. J. Physiol. 214:749-757.

Papasova, M.P., Nagai, T., Prosser, C.L. (1968). Two component slow waves in smooth muscle of cat stomach. Am. J. Physiol., 214(4): 695-702.

Prosser, C.L. (1974). Smooth muscle. Ann. Rev. Physiol., 36:503-537.

Prosser, C.L., Burnstock, G. & Kahn, J. (1960). Conduction in smooth muscle: Comparative structural properties. Am. J. Physiol., 199:545-552.

Porvenzale, L. & Pisano, M. (1971). Methods for recording electrical activity of the human colon in vivo. Dig. Dis. Sci., 16:712-722.

Roberge, F.A. & Nadeau, R.A. (1966). Simulation of sinus node activity by an electronic relaxation oscillator. Can. J. Physiol. Pharmacol., 44:301-305.

Sarna, S.K. (1971). Computer models of gastrointestinal electrical control activity. A thesis submitted to the Faculty of Graduate Studies, University of Alberta.

Sarna, S.K., Daniel, E.E. & Kingma, Y.J. (1971). Simulation of slow wave activity of the small intestine. Am. J. Physiol. 221(1): 166-175.

Sarna, S.K., Daniel, E.E. & Kingma, Y.J. (1972). Simulation of the electrical control activity of the stomach by an array of relaxation oscillators. Am. J. Digestive Diseases., 17(4):299-310.

Sarna, S.K., Bardakjian, B.J., Waterfall, W.E. & Lind, J.F. (1980). Human colonic electrical control activity (ECA). Gastroenterology., 78:1526-1536.

Schofield, G.C. (1968). Anatomy of muscular and neural tissues in the alimentary canal. pp. 1579-1628, Handbook of Physiology, ed. C.F. Code, Am. Physiological Society.

Shearin, N.L., Bowes, K.L. & Kingma, Y.J. (1979). In vitro electrical activity in canine colon. Gut., 20:780-786.

Snape, W.J., Carlson, G.M. & Cohen, S. (1976). Colonic myoelectrical activity in the irritable bowel syndrome. Gastroenterology., 70:326-330.

Staehelin, L.A. & Hull, B.E. (1978). Junctions between living cells. Sci. Am., 238(5):140-152.

Stoddard, C.J., Duthie, H.L., Smallwood, R.H. & Linkens, D.A. (1979). Colonic myoelectrical activity in man: comparison of recording techniques and methods of analysis. Gut., 20:476-483.

Szurszewski, J.H. (1981). Electrical basis for gastrointestinal motility. In Physiology of the GI Tract, ed. L.R. Johnson, Raven Press, N.Y., pp. 1435-1466.

Taxi, J. (1965). Contribution a l'etude des connexion des neurones motuer du systeme nerveux anatome. Annls. Sci. Nat. (Zool.) Ser. 12, 7:413-674.

Taylor, G.S., Daniel, E.E. & Tomita, T. (1975). Origin and mechanism of intestinal slow waves. In: Proc. of the 5th Int'l. Symp. on Gastrointestinal Motility, ed. G. Vantrappen, pp. 102-106. Typoff-Press, Herentals, Belgium.

Taylor, A.B., Kreulen, D.L. & Prosser, C.L. (1977). Electron microscopy of the connective tissues between longitudinal and circular muscle of small intestine of cat. Am. J. Anat., 150:427-442.

Tomita, T. (1967). Spike propagation in the smooth muscle of the guinea-pig taenia coli. J. Physiol., 191:517-527.

Vanasin, B., Vstach, T.J. & Schuster, M.M. (1974). Electrical and motor activity of human and dog colon in vitro. Hopkins Med. J., 134:201-210.

Van der Pol, B. & Van der Mark, J. (1928). The heart beat considered as a relaxation oscillator and an electrical model of the heart. Phil. Mag. Suppl., 6:763-775.

Van Merwyk, A.J. & Duthie, H.L. (1980). Characteristics of human colonic smooth muscle in vitro. In: Gastrointestinal Motility, ed. J. Christensen, Raven Press, New York, pp. 473-478.

Warburg, E. (1899). Über das Verhalten sogenannter unpolarisirbarer Elektroden gegen Wechselstrom. Ann. Phy. Chem., 67:493-499.

Woodbury, L.A., Hecht, H.H. & Christopherson, A.R. (1951). Membrane resting and action potentials of single cardiac fibres of frog ventricle. Am. J. Physiol., 164:307-318.

APPENDIX A

COMPUTER PROGRAMS		PAGE
Appendix A-1	Introduction	154
Appendix A-2	Program FLOCT	156
	Program DWRI	163
	Program STPT	165
	Program DREA	168
	Program RDPT	170
Appendix A-3	Program TDSPT	172
Appendix A-4	Subroutine PLOT	177
Appendix A-5	Program FILTR	186
	Program DCAC	190
Appendix A-6	Program PSPT	192
Appendix A-7	Program PHSE	201
Appendix A-8	Program XCORR	210
Appendix A-9	Program MAIN	216

APPENDIX A-1 INTRODUCTION

This appendix provides detailed information on each of the major programs developed specifically to process the data obtained from this research. These programs permit the transfer of data between various computer storage devices, display and plot graphical results, and process the data. The data processing is used to eliminate noise and to provide signal statistics, power spectra, and the correlation between data channels.

On many large computer systems, such as the Amdahl 370 system, packaged programs are usually available to perform the functions described above. Because of the difficulties in obtaining high speed analog-to-digital conversion on the university Amdahl 370 system, a Hewlett-Packard 21 MX/E minicomputer had been previously obtained to digitize the data from human and canine colon studies. It was more convenient and cheaper to use the minicomputer for the required data processing. Therefore the programs described in this appendix were developed.

Because of the high speed and random nature of data access from the computer disc, any data file requiring processing is initially transferred from magnetic tape to the disc.

This transfer is accomplished using program FLOCT described in Appendix A-2. All other programs obtain their input data from the disc and many place their processed results back on the disc. Programs TDSPT and PLOT, described in Appendices A-3 and A-4 respectively, are utility programs to display unprocessed or processed results in graphical form on the system CRT display or on the high speed teleprinter. Appendix A-5 describes programs FILTR and DCAC. Program FILTR applies

a band pass digital filter to the data file on disc and program DCAC removes the dc component of the data record. Appendices A-6 to A-8 describe programs PSPT, PHSE, and XCORR which determine data power spectra, phase and frequency statistics, and cross correlation data between channels. Program MAIN, described in Appendix A-9, is a master program which permits the researcher to select a menu of any or all of the above programs for application to a particular data file.

Each of the following appendices provides a brief description of each program, a list of input parameter and subroutine requirements, a flow chart of the more complex programs, and a complete listing of each program and its required subroutines.

APPENDIX A-2

PROGRAM FLOCT (File LOCate and Transfer)

Description

Program FLOCT is designed to transfer digital data files from magnetic tape to the HP 21 MX/E disc. The program provides the user with the options (1) of defining the record by tape location or file name, (2) of transferring all or any portion of a data file, and (3) of reducing the effective sampling rate by transferring on every n'th sample. Prior to the transfer the data is appropriately filtered to prevent aliasing errors. The filtering is accomplished with a fourth order recursive digital filter. Two forms of the data file are transferred to the disc using the subroutines DWRI and STPT. Both of these subroutines are also described later in this section. Subroutine DWRI writes the data file onto disc without change while STPT scales that data and changes it into a form suitable for output to the CRT display. A flow chart of program FLOCT is provided in Figure A-2-1 and the program is given in Program Listing A-2-1.

Subroutines Required:

1. DWRI (Disc WRIte)
2. STPT (STore PloT)

Required User Input:

1. File name or +N or -N
   a. The program examines the first six characters of a file name to locate a file.

b. A space followed by +N or -N will advance or rewind the tape N files. The space cannot be omitted.

c. If the record cannot be found the program will search to the end of the tape, rewind, and print "FILE NOT FOUND". The user may then input a new file name or tape location.

2. Following "OK TO PROCEED"

   a. Answer "YES" or "NO". Printing "NO" provides the option of selecting another file.

3. Number of channels in the data file.

4. The number of 256 word records to be skipped before data transfer begins.

   a. This permits transfer of any portion of the file.

5. The number of 256 word records to be transferred.

6. The data sampling rate.

7. The number of data samples to be skipped during the transfer. (Process every N'th sample.)

   a. "N" must be a power of 2. If it is not, it will be reduced to the nearest such power.

Program Output:

1. File name.

2. Actual data sampling rate.

3. Number of 256 word records transferred.

4. Error messages:

   i. File not found.

   ii. End of file (EOF) encountered.

   iii. Wrong number of channels.

   iv. Tape read error.

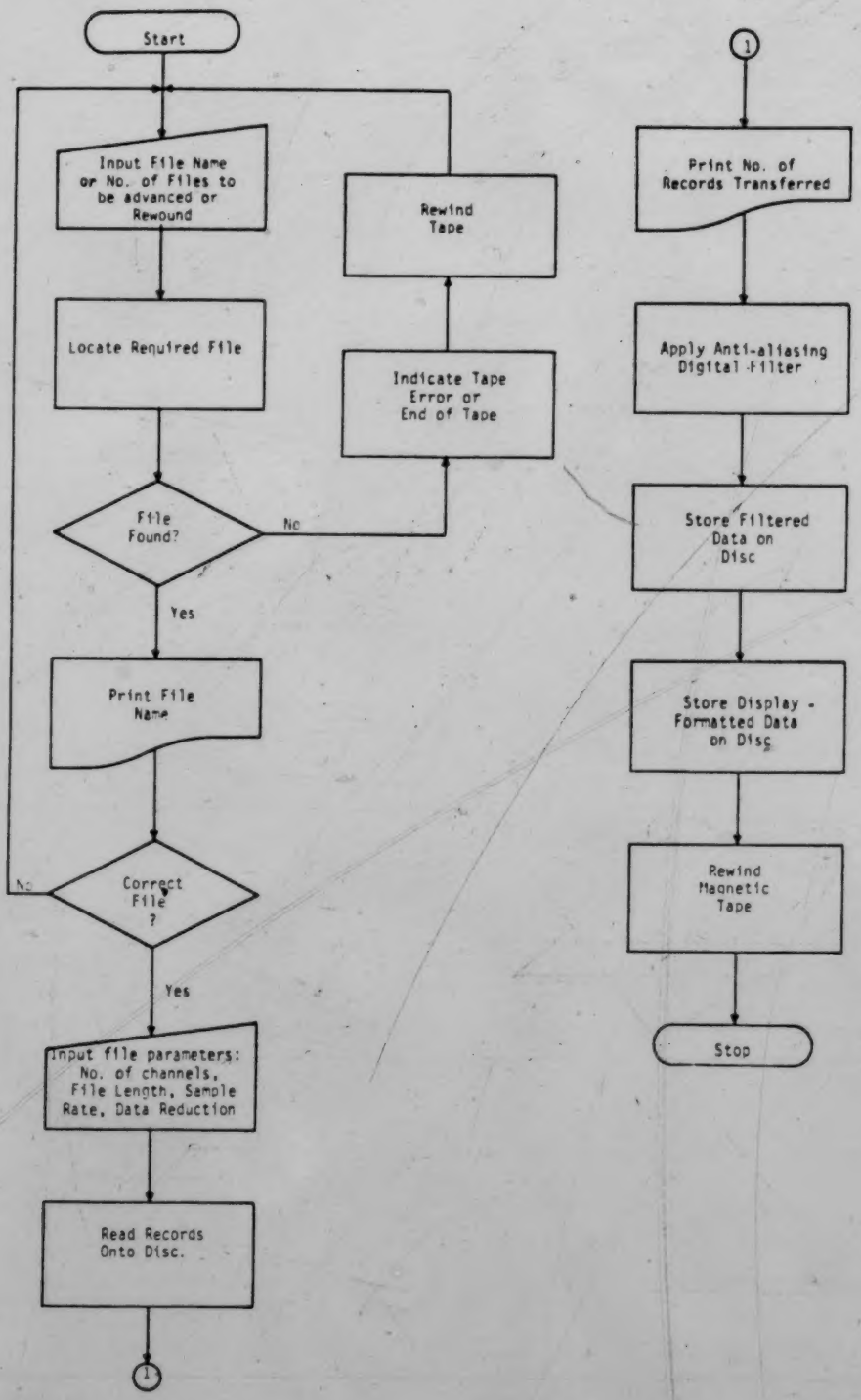

Figure A-2-1 Flow chart of FLOCT.

Program Listing A-2-1 FLOCT

```
PAGE  0001              (FTN4--RELEASE 24177B--JULY, 1971)

0001  FTN4,L
0002        PROGRAM FLOCT
0003        DIMENSION IRAY(2048),JRAY(8,256),KRAY(256),Y(256),Y1(8,4),
0004       1 A(5),B(5),INAM(3),LABF(135),X1(8,8),Y2(8),MAX(8,96)
0005        EQUIVALENCE (Y2(5),Y)
0006        CALL EXEC(17,IFTRK,ILTRK,ISIZE)
0007      5 WRITE(1,100)
0008    100 FORMAT(/"INPUT FILE NAME OR + N OK- N TO ADVANCE OR REWIND N FI
0009       1")
0010        READ(1,101)(INAM(I),I=1,3)
0011    101 FORMAT(3A2)
0012        IF(INAM(1).NE.2H+ )GO TO 7
0013        GO TO 6
0014      7 IF(INAM(1).NE.2H- )GO TO 15
0015      6 INH=INAM(2)/256
0016        INL=INAM(2)-INH*256
0017        IF(INL.EQ.40B)GO TO 21
0018        INH=(INH-60B)*10
0019        INL=INL-60B
0020        I=(INH+INL)*2
0021        GO TO 22
0022     21 I=(INH-60B)*2
0023     22 IF(INAM(1).EQ.2H+ )GO TO 23
0024        I=-I-1
0025     23 CALL PTAPE(12,I,0)
0026        CALL EXEC(1,114B,IRAY,2048)
0027        IF(IEOT(12).LT.0)GO TO 1004
0028     31 IF(IWRDS(12).EQ.36)GO TO 25
0029        CALL PTAPE(12,-1,-2)
0030        CALL EXEC(1,114B,IRAY,2048)
0031        IF(IWRDS(12).EQ.36)GO TO 25
0032        CALL PTAPE(12,2,0)
0033        GO TO 31
0034     24 CALL PTAPE(12,2,0)
0035     15 CALL EXEC(1,114B,IRAY,2048)
0036        IF(IEOT(12).LT.0)GO TO 1004
0037     10 IF(IWRDS(12).EQ.36)GO TO 11
0038        CALL PTAPE(12,-1,-2)
0039        CALL EXEC(1,114B,IRAY,2048)
0040        IF(IWRDS(12).EQ.36)GO TO 11
0041        CALL PTAPE(12,2,0)
0042        GO TO 10
0043     11 IF(IRAY(1).NE.INAM(1))GO TO 24
0044        IF(IRAY(2).NE.INAM(2))GO TO 24
0045        IF(IRAY(3).NE.INAM(3))GO TO 24
0046     25 DO 16 I=1,36
0047        LABF(I)=IRAY(I)
0048        IF(IRAY(I).EQ.0)GO TO 17
0049     16 CONTINUE
0050     17 WRITE(1,104)
0051    104 FORMAT(/"*FILENAME**"/)
0052        CALL EXEC(2,1,IRAY,I)
0053        WRITE(1,105)
0054    105 FORMAT(/"OK TO PROCEED?  _")
0055        READ(1,106)IANS
0056    106 FORMAT(A2)
```

216619

Program Listing A-2-1 FLOCT (cont.)

```
PAGE  0002  FLOCT     (FTN4--RELEASE 24177B--JULY, 1971)

0057          IF(IANS.EQ.2HYE)GO TO 18
0058          CALL PTAPE(12,-1,0)
0059          GO TO 5
0060       18 WRITE(1,107)
0061      107 FORMAT(/"NO. OF CHANNELS?  _")
0062          READ(1,108)NCHA
0063      108 FORMAT(I1)
0064          LABF(37)=NCHA
0065          WRITE(1,110)
0066      109 FORMAT(/"SKIP N RECORDS?  _")
0067          READ(1,*)NRECS
0068          IF(NRECS.GT.96)NRECS=96
0069          WRITE(1,109)
0070      110 FORMAT(/"NO. OF RECORDS?  _")
0071          READ(1,*)NSKP
0072          WRITE(1,111)
0073      111 FORMAT(/"DATA SAMPLING RATE PER MINUTE?  _")
0074          READ(1,*)SR
0075          WRITE(1,112)
0076      112 FORMAT(/"PROCESS EVERY N'TH SAMPLE?  _")
0077          READ(1,*)NTH
0078          IF(NTH.LT.64)GO TO 19
0079          NTH=64
0080       19 IF(NTH.GT.1)GO TO 33
0081          NTH=1
0082          GO TO 26
0083       33 ITWO=0
0084       20 NTH=NTH/2
0085          ITWO=ITWO+1
0086          IF(NTH.GE.2)GO TO 20
0087          NTH=2**ITWO
0088       26 IASR=SR/NTH
0089          ASR=IASR
0090          WRITE(1,114)ASR
0091      114 FORMAT(/"ACTUAL SAMPLING RATE IS",X,F7.1," CYCLES/MIN.")
0092          LABF(38)=IASR
0093          CALL EXEC(1,1148,IKAY,0)
0094          IF(NSKP.EQ.0)GO TO 39
0095          DO 27 I=1,NSKP
0096          CALL EXEC(1,1148,IKAY,0)
0097          IF(IEOF(12).LT.0)GO TO 1001
0098       27 CONTINUE
0099       39 DO 36 K=1,256
0100          Y(K)=0
0101       36 CONTINUE
0102          DO 41 K=1,32
0103          X1(K)=0.
0104          Y1(K)=0.
0105       41 CONTINUE
0106          DO 45 K=1,8
0107          DO 45 I=1,96
0108          MAX(K,I)=0
0109       45 CONTINUE
0110          SR=SR/60.
0111          FC=SR/(NTH#3)
0112          CALL BUTF(SR,FC,A,B)
```

216620

Program Listing A-2-1 FLOCT (cont.)

```
PAGE  0003  FLOCT      (FTN4--RELEASE 24177B--JULY, 1971)

0113          DO 28 I=1,NRECS
0114          CALL EXEC(1,114B,IRAY,2048)
0115          IF(IEOF(12).LT.0)GO TO 1001
0116          IF(IWRDS(12).EQ.0)GO TO 1002
0117          IF(IWRDS(12)/256*256.NE.IWRDS(12))GO TO 1002
0118          NC=IWRDS(12)/256
0119          IF(NC.NE.NCHA)GO TO 1003
0120       29 DO 30 J=1,NCHA
0121          DO 30 K=1,256
0122          JRAY(J,K)=IRAY((K-1)*NC+J)
0123          DO 30 L=5,8
0124          X1(J,L)=JRAY(J,L-4)
0125       30 CONTINUE
0126          DO 28 J=1,NCHA
0127          DO 43 L=1,4
0128          Y2(L)=Y1(J,L)
0129       43 CONTINUE
0130          DO 34 K=1,4
0131          Y(K)=A(1)*JRAY(J,K)+A(2)*X1(J,3+K)+A(3)*X1(J,2+K)+
0132         1 A(4)*X1(J,1+K)+A(5)*X1(J,K)+B(1)*Y2(3+K)+
0133         2 B(2)*Y2(2+K)+B(3)*Y2(1+K)+B(4)*Y2(K)
0134       34 CONTINUE
0135          DO 35 K=5,256
0136          Y(K)=A(1)*JRAY(J,K)+A(2)*JRAY(J,K-1)+A(3)*JRAY(J,K-2)+
0137         1 A(4)*JRAY(J,K-3)+A(5)*JRAY(J,K-4)+B(1)*Y(K-1)+
0138         2 B(2)*Y(K-2)+B(3)*Y(K-3)+B(4)*Y(K-4)
0139       35 CONTINUE
0140          DO 47 K=1,256
0141          IMAX=IFIX(Y(K))
0142          IMAX=IABS(IMAX)
0143          LMAX=MAX(J,I)
0144          IF(IMAX.LE.LMAX)GO TO 47
0145          MAX(J,I)=IMAX
0146       47 CONTINUE
0147          IMAX=MAX(J,I)
0148       46 DO 40 K=1,4
0149          X1(J,K)=JRAY(J,252+K)
0150          Y1(J,K)=Y(252+K)
0151       40 CONTINUE
0152          DO 38 K=1,256/NTH
0153          KRAY(K)=Y((K-1)*NTH+1)+0.5)
0154       38 CONTINUE
0155          LNGTH=256/NTH
0156          CALL DWRI(IFTRK,LNGTH,KRAY,I,J,1)
0157          CALL STPT(IFTRK,KRAY,LNGTH,I,J,IMAX)
0158       28 CONTINUE
0159          CALL PTAPE(12,-2,0)
0160          NRECS=NRECS/NTH
0161          LABF(39)=NRECS
0162          DO 44 K=1,NRECS
0163          LABF(K+39)=MAX(1,K)
0164       44 CONTINUE
0165          CALL DWRI(IFTRK,0,LABF(1),0,0,1)
0166          WRITE(1,113)NRECS
0167      113 FORMAT(/"NO. OF 256 SAMPLE RECORDS TRANSFERED IS  ",I3)
0168          STOP
```

216621

Program Listing A-2-1 FLOCT (cont.)

```
      PAGE  0004  FLOCT     (FTN4--RELEASE 2417/B--JULY, 1971)

0169   1000 WRITE(1,900)
0170    900 FORMAT(/"FILE NOT FOUND!!")
0171        GO TO 5
0172   1001 WRITE(1,901)
0173    901 FORMAT(/"EOF ENCOUNTERED, CHECK NO. OF RECORDS!!")
0174        CALL PTAPE(12,-3,0)
0175        GO TO 5
0176   1002 WRITE(1,902)
0177    902 FORMAT(/"*TAPE ERROR"/)
0178        CALL PTAPE(12,-2,0)
0179        GO TO 5
0180   1003 NCHA=IWRDS(12)/256
0181        WRITE(1,903)NCHA
0182    903 FORMAT(/"WRONG NO. OF CHANNELS!!"/"NO. OF CHANNELS IS ",I1)
0183        WRITE(1,904)
0184    904 FORMAT(/"DO YOU WISH TO CORRECT?  ")
0185        READ(1,106)IANS
0186        IF(IANS.EQ.2HNO)GO TO 29
0187        WRITE(1,107)
0188        READ(1,108)NCHA
0189        LABF(37)=NCHA
0190        GO TO 29
0191   1004 WRITE(1,907)
0192    907 FORMAT(/"END OF TAPE")
0193        CALL EXEC(3,414B)
0194        GO TO 5
0195        END
```

APPENDIX A-2 (cont.)

SUBROUTINE DWRI (IFTRK, LENGTH, NAME, NUM, ICHA, IFILE)

Description

Subroutine DRWI (Disc WRIte) is a subroutine designed to write data files from memory into one of three disc files. In addition a header record is created on disc containing the file name, number of channels, actual sampling rate, and number of data records contained in the file. The three disc files numbered 1, 2, and 3 are created to store input data, processed data, and display-formatted data respectively. The program listing and disc organization associated with DWRI is shown in Figure A-2-2. Each disc file consists of 96 disc tracks with the data stored in order of channel number. The maximum capacity of each of the three disc files is eight channels of data each containing 96 256-word records.

Subroutine input parameters:

1. IFTRK, the first available free track on disc.
2. LNGTH, the length of each data record.
3. NAME, the name of the memory array containing the data file.
4. ICHA, the number of a particular channel to be written onto disc.
5. IFILE, to specify disc file 1, 2, or 3.

```
PAGE  0001              (FTN4--RELEASE 24177B--JULY, 1971)

0001  FTN4,L
0002        SUBROUTINE DWRI(IFTRK,LNGTH,NAME,NUM,ICHA,IFILE)
0003        DIMENSION NAME(1,1)
0004        IF(LNGTH.NE.0)GO TO 1
0005        L=135
0006        ITOF=IFTRK+(IFILE-1)*33
0007        IOFF=0
0008        IWRDS=0
0009        GO TO 2
0010      1 INUM=NUM-1
0011        L=LNGTH
0012        ITNUM=L*INUM
0013        IWRDS=MOD(ITNUM,128)
0014        IRMDR=ITNUM-IWRDS
0015        ISTRS=IRMDR/128
0016        IOFF=MOD(ISTRS,48)
0017        ITOF=(ISTRS-IOFF)/48
0018        ITOF=ITOF+1+(ICHA-1)*4+IFTRK+(IFILE-1)*33
0019      2 CALL BWRIT(NAME,L,2,ITOF,IOFF,IWRDS)
0020        RETURN
0021        END

**  NO ERRORS
```

TRACK	SECTOR	IFILE	CHANNEL
IFTRK	0	1	FILE NAME 0 - 36
	37		37 = NO. OF CHANNELS
	38		38 = ACTUAL SAMPLING RATE
	39		39 = NO. OF RECORDS
IFTRK + 1	0		1
	2		-
	3		-
	4		-
	5		2
	-		-
	-		-
	-		-
	9		3
	-		-
	-		-
	-		-
	13		4
	-		-
	-		-
	-		-
	29		8
IFTRK + 33	0	2	

Figure A-2-2 Program listing of DWRI and table showing disc file organization.

APPENDIX A-2 (cont.)

SUBROUTINE STPT (IFTRK, NAME, LNGTH, NUMR, ICHA, MAX)

Description

Subroutine STPT (STore PloT) scales the amplitude of the values in a data file, generates a new file suitable for fast display on the computer CRT, and stores this new file on disc file 3. Because the vertical span of the CRT is only 256 points and because a maximum of 8 channels may be simultaneously displayed, each data file is scaled to have a maximum amplitude of 32. To display a data point on the system CRT a 16 bit word is output to the D/A converter. The most significant eight bits of this word define the vertical position of a display point and the least significant 8 bits define the horizontal position. Therefore, after the data values have been scaled the amplitude information is shifted into the most significant eight bits and values corresponding to the location of the data points in the 256-word record are added to the least significant 8 bits. The scaled display-formatted data file is stored in disc file 3 using subroutine DWRI. The subroutine is given in Program Listing A-2-2.

Subroutine input parameters:

1. IFTRK, the first available free track on disc.
2. NAME, the name of the memory array containing the data file.
3. LNGTH, the length of each data record.
4. NUMR, the number of a particular record to be stored on disc.
5. ICHA, the number of a particular channel to be stored on disc.
6. MAX, the maximum amplitude in the data file.

APPENDIX A-2 (cont.)

Subroutines required:

1. Subroutine DWRI

Program Listing A-2-2 STPT

```
        PAGE  0001              (FTN4--RELEASE 24177B--JULY, 1971)

0001  FTN4,L
0002        SUBROUTINE SIPT(IFTRK,NAME,LNGTH,NUMR,ICHA,MAX)
0003        DIMENSION NAME(1)
0004        MX=MAX
0005        IF(MAX.EQ.0)MX=32767
0006        N=256/LNGTH
0007        NN=NUMR-1
0008        IP=MOD(NN,N)
0009        DO 10 I=1,LNGTH
0010        IRY=NAME(I)
0011        NAME(I)=FLOAT(IRY)*32/MX
0012        IRY=NAME(I)
0013        IF(IRY.LE.31)GO TO 2
0014        NAME(I)=31
0015      2 IF(IRY.GT.-31)GO TO 1
0016        NAME(I)=-31
0017      1 NAME(I)=NAME(I)*256+I+IP*LNGTH-1
0018     10 CONTINUE
0019        CALL DWRI(IFTRK,LNGTH,NAME,NUMR,ICHA,3)
0020        RETURN
0021        END

**  NO ERRORS*
```

APPENDIX A-2 (cont.)

SUBROUTINE DREA (IFTRK, LENGTH, NAME, NUM, ICHA, IFILE)

Description

Subroutine DREA (Disc REAd) transfers data records from disc to memory arrays. It assumes the disc file has been formatted by DWRI as described above. The main difference between DREA and DWRI is the direction of data flow. The subroutine is given in Program Listing A-2-3.

Subroutine input parameters:

IFTRK, LENGTH, NAME, NUM ICHA and IFILE as described for subroutine DWRI.

Program Listing A-2-3 DREA

```
        PAGE  0001                (FTN4--RELEASE 24177B--JULY, 1971)

0001   FTN4,L
0002         SUBROUTINE DREA(IFTRK,LNGTH,NAME,NUM,ICHA,IFILE)
0003         DIMENSION NAME(1)
0004         IF(LNGTH.NE.0)GO TO 1
0005         L=135
0006         ITOF=IFTRK+(IFILE-1)*33
0007         IOFF=0
0008         IWRDS=0
0009         GO TO 2
0010       1 INUM=NUM-1
0011         L=LNGTH
0012         ITNUM=L*INUM
0013         IWRDS=MOD(ITNUM,128)
0014         IRMDR=ITNUM-IWRDS
0015         ISTRS=IRMDR/128
0016         IOFF=MOD(ISTRS,48)
0017         ITOF=(ISTRS-IOFF)/48
0018         ITOF=ITOF+1+(ICHA-1)*4+IFTRK+(IFILE-1)*33
0019       2 CALL BREAD(NAME,L,2,ITOF,IOFF,IWRDS)
0020         RETURN
0021         END

**  NO ERRORS*
```

APPENDIX A-2 (cont.)

SUBROUTINE RDPT (IFTRK, NAME, NUMR, ICHA, LOC)

Description

Subroutine RDPT (ReaD PloT) transfers display-formatted data from disc to memory arrays. The length of the display record is fixed at 256 words. RDPT utilizes subroutine DREA to accomplish the disc read operation and then modifies the most significant 8 bits as a function of vertical location (LOC). Each data channel may be displayed in one of eight vertical positions depending on the value assigned to parameter LOC. A value of 1 positions the data channel at the top of the CRT while 8 positions the channel at the bottom. The subroutine is given in Program Listing A-2-4.

Input parameters:

1. IFTRK, NAME, NUMR, and ICHA as previously defined for STPT and DWRI.
2. LOC, location of the data channel on the CRT.

Program Listing A-2-4 RDPT

```
        PAGE  0001              (FTN4--RELEASE 241775--JULY, 1971)

0001  FTN4,L
0002        SUBROUTINE RDPT(IFTRK,NAME,NUMR,ICHA,LOC)
0003        DIMENSION NAME(1)
0004        CALL DREA(IFTRK,256,NAME,NUMR,ICHA,3)
0005        DO 10 I=1,256
0006        NAME(I)=NAME(I)+(223-(LOC-1)*64)*256
0007     10 CONTINUE
0008        RETURN
0009        END

**  NO ERRORS*
```

APPENDIX A-3

PROGRAM TDSPL (Time DiSPLay)

Description

Program TDSPL displays from one to eight channels of data on the HP 21 MX/E system's CRT and facilitates either low speed or high speed scanning of the complete data file. The sense switches control the program mode of operation. If sense switch 15 is set the record will slowly move across the CRT. If sense switch 14 is set the file is rapidly scanned on a 256-word record-by-record basis.

The data to be displayed must be previously placed on disc by FLOCT. Additional information about the program is provided by the flow chart of Figure A-3-1 and Program Listing A-3-1.

Required subroutines:

1. Subroutine GRID displays the grid on the CRT. Program Listing A-3-2 is a listing of subroutine GRID.
2. Subroutine RDPT
3. Subroutine DREA

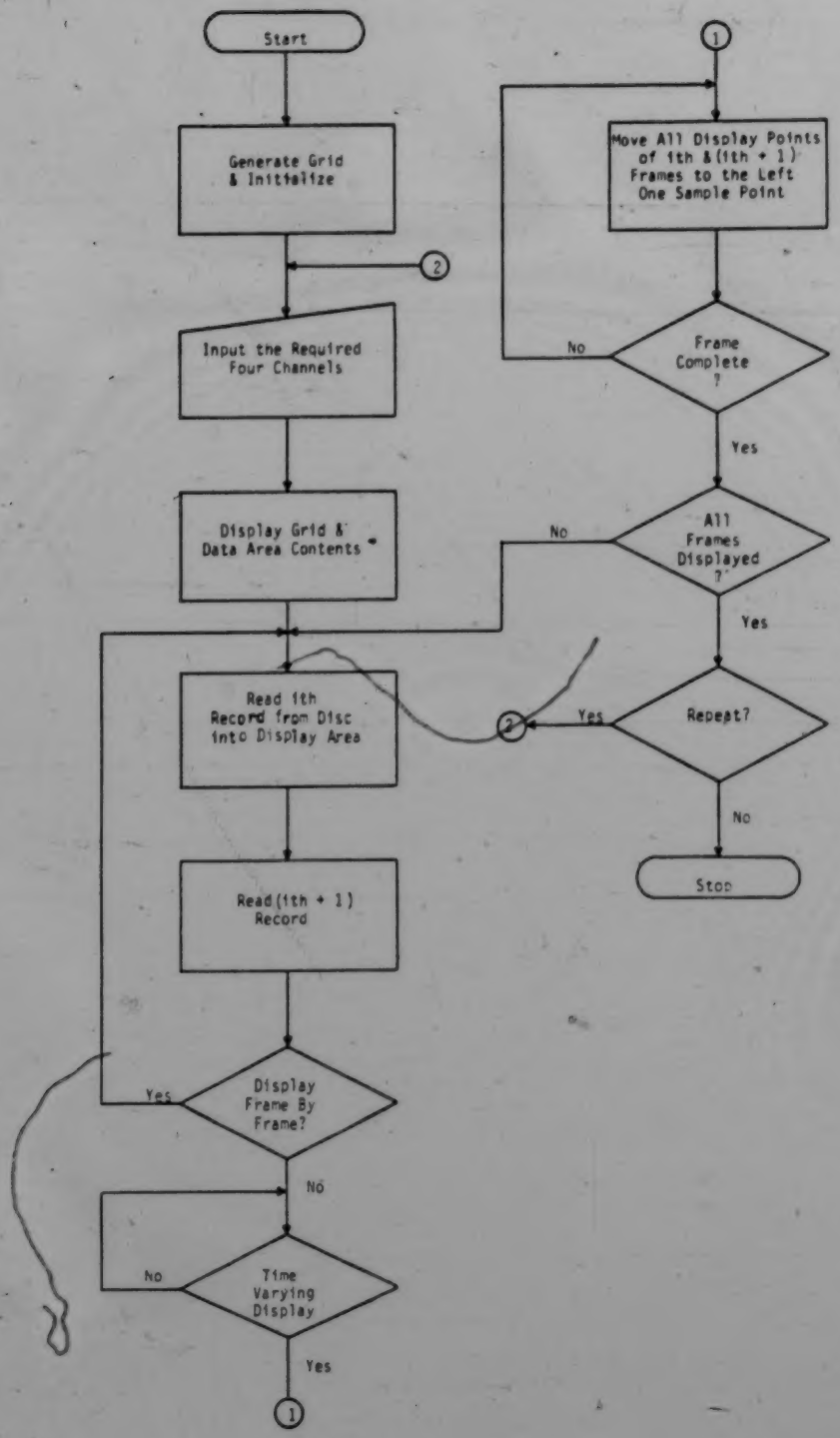

Figure A-3-1 Flow chart of TDSPL.

Program Listing A-3-1 TDSPL

```
     PAGE  0001            (FTN4--RELEASE 24177B--JULY, 1971)

0001  FTN4,L
0002        PROGRAM TDSPL
0003        DIMENSION JRAY(256,4),IGRID(2480),IRAY(256),LABF(135),ICH(4)
0004       1 ,KRAY(256,4)
0005        EQUIVALENCE (IGRID(1457),JRAY)
0006        CALL EXEC(17,IFTRK,ILTRK,ISIZE)
0007        CALL GRID(IGRID)
0008        CALL DREA(IFTRK,0,LABF,1,1,1)
0009      1 DO 10 I=1,4
0010        ICH(I)=0
0011       10 CONTINUE
0012        DO 11 I=1,1024
0013        JRAY(I)=0
0014       11 CONTINUE
0015        WRITE(1,100)
0016      100 FORMAT(/"INPUT THE REQUIRED FOUR CHANNELS! _")
0017        READ(1,*)(ICH(J),J=1,4)
0018        NRECS=LABF(39)
0019        DO 26 I=1,4
0020        ICHA=ICH(I)
0021        IF(ICHA.EQ.0)GO TO 15
0022       26 CONTINUE
0023       15 NCHA=I-1
0024        LTH=1456+NCHA*256
0025        IFST=0
0026        CALL EXEC(2,020111B,IGRID,LTH)
0027        DO 20 I=1,NRECS-1
0028       14 IF(IFST.GE.0)GO TO 12
0029        CALL DELAY(1000)
0030        CALL EXEC(3,11B)
0031        CALL EXEC(2,020111B,IGRID,LTH)
0032       12 DO 21 J=1,NCHA
0033        IC=ICH(J)
0034        CALL RDPT(IFTRK,IRAY,I,IC,J)
0035        DO 25 K=1,256
0036        JRAY(K,J)=IRAY(K)
0037       25 CONTINUE
0038       21 CONTINUE
0039        IF(NRECS.EQ.1)GO TO 30
0040        DO 19 J=1,NCHA
0041        ICHA=ICH(J)
0042        N=I+1
0043        CALL RDPT(IFTRK,IRAY,N,ICHA,J)
0044        DO 19 K=1,256
0045        KRAY(K,J)=IRAY(K)
0046       19 CONTINUE
0047       30 DO 24 L=1,256
0048       22 IST=ISSW(15)
0049        IFST=ISSW(14)
0050        IF(IFST.LT.0)GO TO 20
0051        IF(IST.LT.0)GO TO 22
0052        DO 23 J=2,256
0053        DO 23 K=1,NCHA
0054        JRAY(J-1,K)=JRAY(J,K)-1
0055       23 CONTINUE
0056        DO 24 K=1,NCHA
```

Program Listing A-3-1 (cont.)

```
      PAGE  0002  TDSPL     (FTN4--RELEASE 24177B--JULY, 1971)

0057          JRAY(256,K)=KRAY(L,K)-L+256
0058       24 CONTINUE
0059       20 CONTINUE
0060          WRITE(1,102)
0061      102 FORMAT(/"DO YOU WISH TO REPEAT? _")
0062          READ(1,103)IANS
0063          CALL EXEC(3,11B)
0064      103 FORMAT(A2)
0065          IF(IANS.EQ.2HYE)GO TO 1
0066          STOP
0067          END
```

Program Listing A-3-2 GRID

```
        PAGE  0001              (FTN4--RELEASE 24177B--JULY, 1971)

0001  FTN4,L
0002        SUBROUTINE GRID(IGRID)
0003        DIMENSION IGRID(1396)
0004      1 DO 10 I=1,256
0005        IGRID(I)=(I-1)*256+15
0006     10 CONTINUE
0007        DO 11 I=256,316,4
0008        DO 11 J=1,4
0009        IGRID(I+J)=(I-256)*1024+12+J
0010     11 CONTINUE
0011        DO 14 K=1,4
0012        I1=321+(K-1)*268
0013        I2=I1+239
0014        DO 12 I=I1,I2
0015        IGRID(I)=(223-64*(K-1))*256+I-305-(K-1)*268
0016     12 CONTINUE
0017        I1=560+(K-1)*268
0018        I2=I1+28
0019        DO 13 I=I1,I2,4
0020        DO 13 J=1,4
0021        IGRID(I+J)=(220-64*(K-1)+J)*256+8*(I-558-(K-1)*268)+32
0022     13 CONTINUE
0023     14 CONTINUE
0024        RETURN
0025        END

**  NO ERRORS*
```

APPENDIX A-4

SUBROUTINE PLOT (X, Y, YG, LABEL, NPLOT, NTR, IT)

Description

Subroutine PLOT produces an X-Y plot on the high speed printer of from one to four data arrays. The resolution of the plot is 16 units per inch in the horizontal direction and 12 units per inch in the vertical direction. The span of the plot is 50 by 100 units. When a single channel of data is to be plotted the subroutine provides the option of a normal plot or a bar graph. A flow chart of subroutine PLOT is provided in Figure A-4-1. A typical output for one data array is shown in Figure A-4-2 while a typical bar graph is shown in Figure A-6-2. Subroutine PLOT is given in Program Listing A-4-1.

Required input parameters:

1. X, an n x 4 array containing the horizontal coordinates for all data points.
2. Y, an n x 4 array containing from 1 to 4 sets of vertical coordinates.
3. YG, the maximum vertical amplitude of the plot. If this value is zero the plot is scaled such that the maximum vertical amplitude corresponds to the maximum data amplitude.
4. LABEL, an array containing up to 25 alphanumeric characters constituting the vertical label for the graph.
5. NPLOT, the number of data points in the arrays to be plotted.
6. NTR, the number of traces to be plotted.
7. IT, a parameter which determines if a single data array is to produce a normal or a bar graph.

APPENDIX A-4 (cont.)

If IT = ϕ, a normal graph is produced.

If IT = 1, a bar graph is generated.

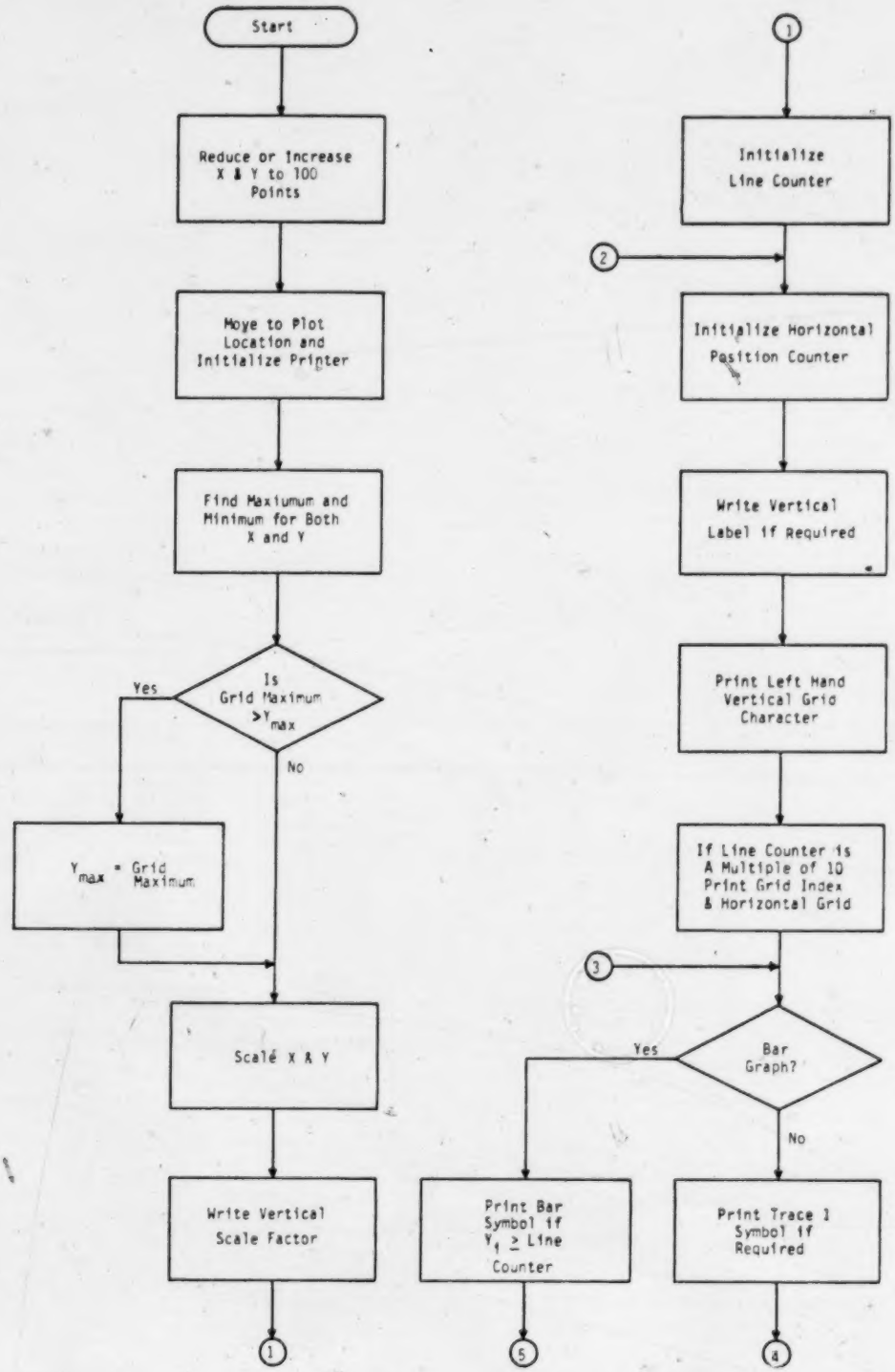

Figure A-4-1 Flow chart of PLOT.

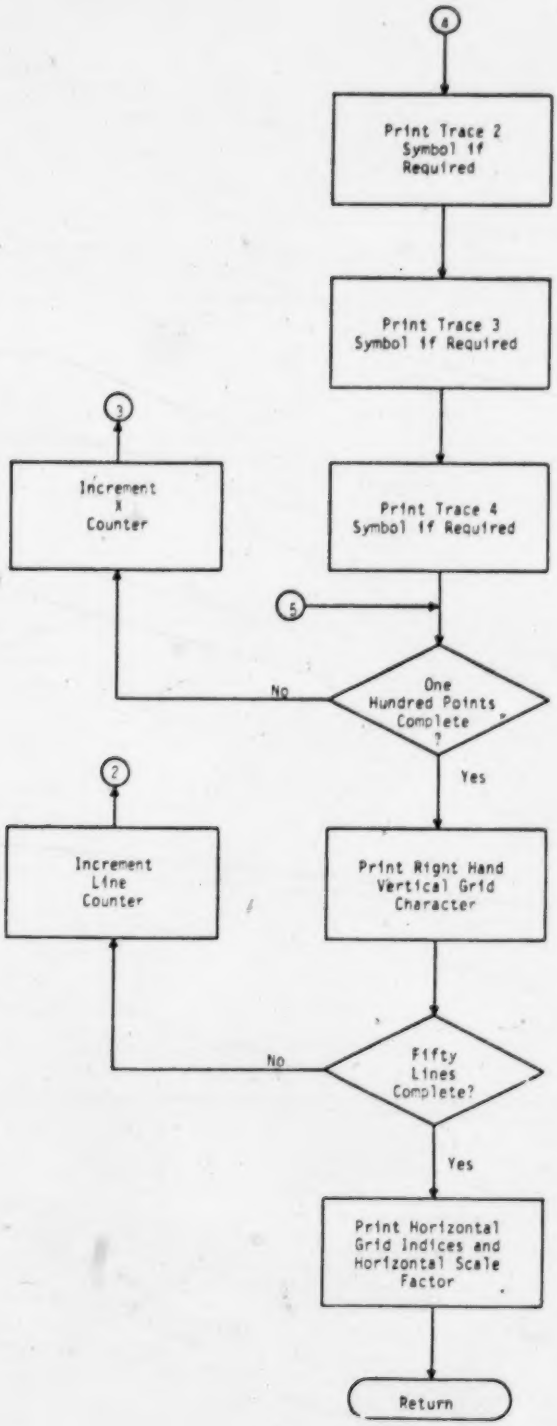

Figure A-4-1 Flow chart of PLOT (cont.).

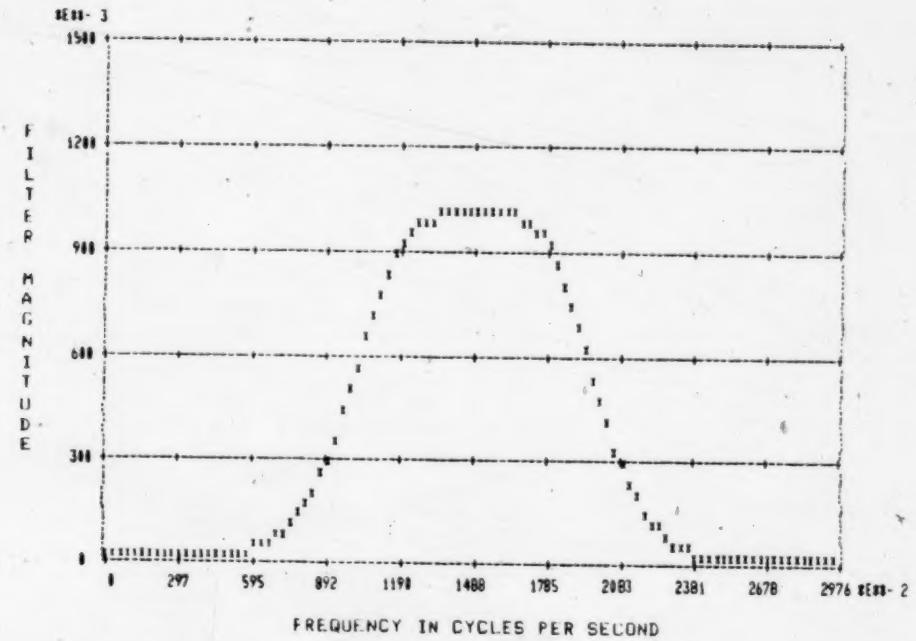

Figure A-4-2 Typical single channel output of subroutine PLOT.

Program Listing A-4-1 PLOT

```
PAGE  0001              (FTN4--RELEASE 24177B--JULY, 1971)

0001  FTN4,L
0002        SUBROUTINE PLOT(X,YY,YG,LABEL,NPLOT,NTR,IT)
0003        DIMENSION X(128),YY(128,4),Y(100,4),IL(100),LABEL(25),IS(5),L1(2
0004        DO 25 J=1,NTR
0005        DO 25 I=1,100
0006        II=IFIX(NPLOT*I/100.)
0007        Y(I,J)=YY(II+(J-1)*NPLOT)
0008     25 CONTINUE
0009        DO 26 I=1,100
0010        II=IFIX(NPLOT*I/100.)
0011        YY(I)=X(II)
0012        IF(I.LT.100.AND.I.NE.1)YY(I)=YY(I)+(X(II+1)-X(II))*(NPLOT*
0013       1 I/100.-II)
0014     26 CONTINUE
0015        DO 27 I=1,100
0016        X(I)=YY(I)
0017     27 CONTINUE
0018        WRITE(1,101)15446B,2H11
0019        WRITE(1,112)1HV
0020        WRITE(1,101)15446B,2H18
0021        WRITE(1,112)1HV
0022        ITAB=15461B
0023        IS(1)=1Hx
0024        IS(2)=1Ho
0025        IS(3)=1H+
0026        IS(4)=1H"
0027        IS(5)=77400B
0028        WRITE(1,100)ITAB,ITAB,ITAB
0029    100 FORMAT(20X,A2,4X,A2,6X,A2)
0030        WRITE(1,101)15446B,2H10
0031        WRITE(1,112)1HD
0032    101 FORMAT(2A2,"_")
0033        WRITE(1,101)15446B,2Hk2
0034        WRITE(1,112)1HS
0035        YMAX=-1.E+36
0036        YMIN=1.E+36
0037        XMAX=-1.E+36
0038        XMIN=1.E+36
0039        DO 50 I=1,100
0040        IF(X(I).GE.XMAX)XMAX=X(I)
0041        IF(X(I).LE.XMIN)XMIN=X(I)
0042     50 CONTINUE
0043        DO 51 I=1,100*NTR
0044        IF(Y(I).GE.YMAX)YMAX=Y(I)
0045        IF(Y(I).LE.YMIN)YMIN=Y(I)
0046     51 CONTINUE
0047        IF(YG.GT.YMAX)YMAX=YG
0048        NMIX=0
0049        NPLX=0
0050        XMX=XMAX
0051        XMN=XMIN
0052        XM=AMAX1(ABS(XMAX),ABS(XMIN))
0053        IF(XM.GT.9999.)GO TO 11
0054     13 IF(XM.GE.1000.)GO TO 14
0055        NMIX=NMIX+1
0056        XMX=XMX*10.

171358
```

Program Listing A-4-1 PLOT (cont.)

```
PAGE  0002  PLOT      (FTN4--RELEASE 24177B--JULY, 1971)

0057        XMN=XMN*10.
0058        XM=XM*10.
0059        GO TO 13
0060     11 NPLX=NPLX+1
0061        XMX=XMX/10.
0062        XMN=XMN/10.
0063        XM=XM/10.
0064        IF(XM.GT.9999.)GO TO 11
0065     14 MXX=IFIX(XMX)
0066        MNX=IFIX(XMN)
0067        DGX=(XMX-XMN)/100.
0068        NMIY=0
0069        NPLY=0
0070        YMX=YMAX
0071        YMN=YMIN
0072        YM=AMAX1(ABS(YMAX),ABS(YMIN))
0073        IF(YM.GT.9999.)GO TO 1
0074     3  IF(YM.GE.1000.)GO TO 4
0075        NMIY=NMIY+1
0076        YMX=10.*YMX
0077        YMN=YMN*10.
0078        YM=YM*10.
0079        GO TO 3
0080     1  NPLY=NPLY+1
0081        YMX=YMX/10.
0082        YMN=YMN/10.
0083        YM=YM/10.
0084        IF(YM.GT.9999.)GO TO 1
0085     4  MXY=IFIX(YMX)
0086        MNY=IFIX(YMN)
0087        DGY=(YMX-YMN)/50.
0088   112  FORMAT(A1)
0089        NT=10
0090        ITAB=4400B
0091        IF(NPLY.GT.0)WRITE(1,124)ITAB,ITAB,NPLY
0092   124  FORMAT(2A1,"*E**+",I2/)
0093        IF(NMIY.GT.0)WRITE(1,125)ITAB,ITAB,NMIY
0094   125  FORMAT(2A1,"*E**-",I2/)
0095        IRN=6400B
0096        DY=(YMAX-YMIN)/50.
0097        DO 20 I=1,50
0098        WRITE(1,104)ITAB
0099        LL=MOD(I,2)
0100        WRITE(1,101)15446B,2Hk0
0101        WRITE(1,104)1HS
0102        IF(LL.EQ.0)WRITE(1,104)LABEL(I/2)
0103        IF(LL.NE.0)GO TO 17
0104        IF(LABEL(I/2).EQ.0)WRITE(1,113)
0105     17 IF(LL.NE.0)WRITE(1,113)
0106   113  FORMAT(" ")
0107        WRITE(1,101)15446B,2Hk2
0108        WRITE(1,104)1HS
0109   104  FORMAT(A1," ")
0110        WRITE(1,104)ITAB
0111        IG=IFIX(MXY-(I-1)*DGY)
0112        IGG=MOD(I-1,10)
```

L71359

Program Listing A-4-1 PLOT (cont.)

```
PAGE  0003  PLOT      (FTN4--RELEASE 24177B--JULY, 1971)

0113          IF(IGG.EQ.0)WRITE(1,105)IG,ITAB
0114      105 FORMAT(I5,A1,"_")
0115          IF(IGG.NE.0)GO TO 21
0116          WRITE(1,116)
0117      116 FORMAT("+_")
0118          DO 10 J=1,NT
0119          WRITE(1,103)
0120      103 FORMAT("---------+_")
0121       10 CONTINUE
0122          WRITE(1,104)IRN
0123          WRITE(1,123)ITAB,ITAB,ITAB
0124      123 FORMAT(3A1," _")
0125       21 IF(IGG.EQ.0)GO TO 5
0126          WRITE(1,106)ITAB
0127      106 FORMAT(A1,":_")
0128          WRITE(1,104)IRN
0129          WRITE(1,123)ITAB,ITAB,ITAB
0130        5 DO 70 K=1,100
0131          IL(K)=1H
0132       70 CONTINUE
0133          Y1=YMAX-(I-1)*DY
0134          Y2=YMAX-I*DY
0135          DO 9 J=1,100
0136          GO TO(7,8)IT
0137        7 DO 60 K=NTR,1,-1
0138          IF(Y(J,K).LE.Y1.AND.Y(J,K).GT.Y2)IL(J)=IS(K)
0139          IF(Y(J,K).EQ.Y2)IL(J)=IS(K)
0140       60 CONTINUE
0141          GO TO 9
0142        8 IF(Y(J).GT.Y1)IL(J)=IS(5)
0143        9 CONTINUE
0144          IF(IGG.EQ.0)WRITE(1,107)IL
0145          IF(IGG.NE.0)WRITE(1,114)IL
0146      107 FORMAT(100A1)
0147      114 FORMAT(100A1,":")
0148          IF(IT.EQ.1)GO TO 20
0149          DO 19 J=1,1000
0150          DO 19 K=1,75
0151          CONTINUE
0152       19 CONTINUE
0153       20 CONTINUE
0154          WRITE(1,115)ITAB,ITAB,MNY,ITAB
0155      115 FORMAT(2A1,I5,A1," +_")
0156          DO 30 I=1,NT
0157          WRITE(1,103)
0158       30 CONTINUE
0159          WRITE(1,112)IRN
0160          WRITE(1,112)IRN
0161          WRITE(1,108)ITAB
0162      108 FORMAT(A1,"    _")
0163          DO 40 I=1,NT+1
0164          IG=IFIX(XMN+(I-1)*DGX*10.)
0165          WRITE(1,109)IG
0166      109 FORMAT(5X,I5,"_")
0167       40 CONTINUE
0168          IF(NPLX.GT.0)WRITE(1,110)NPLX
171360
```

Program Listing A-4-1 PLOT (cont.)

```
          PAGE  0004  PLOT       (FTN4--RELEASE 24177B--JULY, 1971)

0169          IF(NMIX.GT.0)WRITE(1,111)NMIX
0170      110 FORMAT(" *E**+",I2)
0171      111 FORMAT(" *E**-",I2)
0172          WRITE(1,101)15446B,2H*0
0173          WRITE(1,112)1HS
0174          WRITE(1,101)15446B,2H16
0175          WRITE(1,112)1HD
0176          RETURN
0177          END

**  NO ERRORS*
```

171361

APPENDIX A-5

PROGRAM FILTR (FILTeR)

Description

Program FILTR applies an eighth order bandpass filter to from one to eight channels of data stored on disc. The eighth order filter is obtained by cascading two identical fourth order filters which have been obtained from a bilinear transformation of a second order Butterworth equation. The difference equation for the filter is obtained from a subroutine BPASS for which the listing is given. Figure A-5-1 is a flow chart of program FILTR. The program is given in Program Listing A-5-1.

Required input parameters:

1. Upper and lower frequencies.
2. All other required information such as sampling rate, number of data channels, and record length is obtained from the data header record on disc.

Required subroutines:

1. DREA
2. DWRI
3. STPT
4. BPASS - see Program Listing A-5-2.

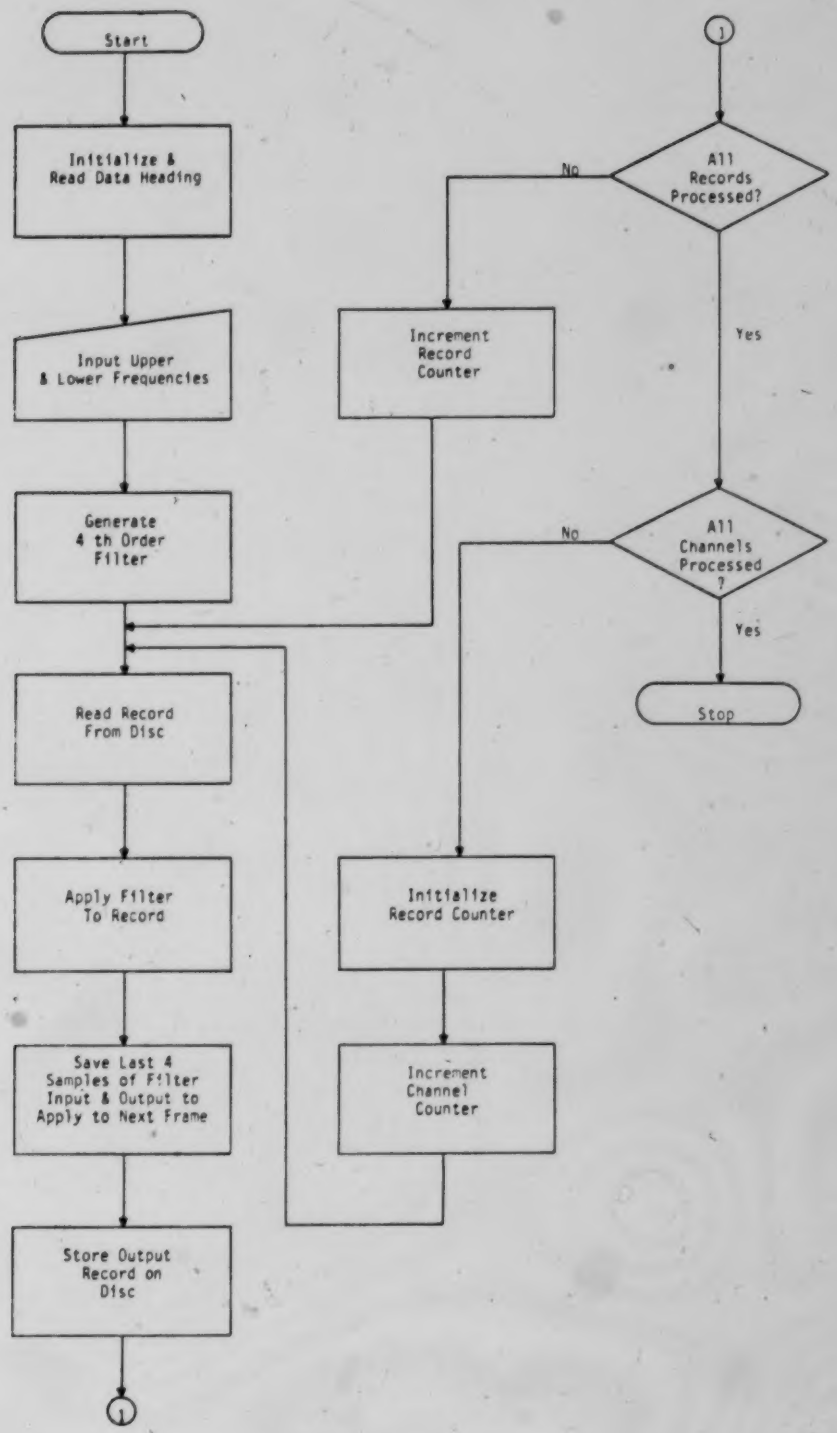

Figure A-5-1 Flow chart of program FILTR.

Program Listing A-5-1 FILTR

```
          PAGE  0001            (FTN4--RELEASE 24177B--JULY, 1971)

0001  FTN4,L
0002        PROGRAM FILTR
0003        DIMENSION LABF(135),A(5),B(5),Y(256),IX(256),IX1(8),Y1(8)
0004        EQUIVALENCE (IX1(5),IX),(Y1(5),Y)
0005        CALL EXEC(17,IFIRK,ILTRK,ISIZE)
0006        CALL DREA(IFIRK,0,LABF,1,1,1)
0007        SR= LABF(38)/60.
0008        NRECS=LABF(39)
0009        NCHA=LABF(37)
0010        WRITE(1,100)
0011    100 FORMAT(/"INPUT LOWER AND UPPER FREQUENCIES IN CYCLES/MIN. _")
0012        READ(1,*)LF,IHF
0013        ALF=LF/60.
0014        AHF=IHF/60.
0015        CALL BPASS(SR,ALF,AHF,A,B)
0016        DO 5 K=1,4
0017        IX1(K)=0
0018        Y1(K)=0
0019      5 CONTINUE
0020        DO 10 L=1,2
0021        DO 10 I=1,NCHA
0022        DO 10 J=1,NRECS
0023        MAX=0
0024        CALL DREA(IFIRK,256,IX,J,I,1)
0025        DO 11 K=1,4
0026        Y(K)=A(1)*IX(K)+A(2)*IX1(3+K)+A(3)*IX1(2+K)+
0027       1 A(4)*IX1(1+K)+A(5)*IX1(K)+B(1)*Y1(3+K)+
0028       2 B(2)*Y1(2+K)+B(3)*Y1(1+K)+B(4)*Y1(K)
0029     11 CONTINUE
0030        DO 12 K=5,256
0031        Y(K)=A(1)*IX(K)+A(2)*IX(K-1)+A(3)*IX(K-2)+
0032       1 A(4)*IX(K-3)+A(5)*IX(K-4)+B(1)*Y(K-1)+
0033       2 B(2)*Y(K-2)+B(3)*Y(K-3)+B(4)*Y(K-4)
0034     12 CONTINUE
0035        DO 13 K=1,4
0036        IX1(K)=IX(252+K)
0037        Y1(K)=Y(252+K)
0038     13 CONTINUE
0039        DO 14 K=1,256
0040        IX(K)=Y(K)
0041        IM=IABS(IX(K))
0042        IF(IM.LT.MAX)GO TO 14
0043        MAX=IM
0044     14 CONTINUE
0045        CALL DWRI(IFIRK,256,IX,J,I,1)
0046        IF(L.EQ.1)GO TO 10
0047        CALL STPT(IFIRK,IX,256,J,I,MAX)
0048     10 CONTINUE
0049        STOP
0050        END

**  NO ERRORS*
```

Program Listing A-5-2 BPASS

```
        PAGE  0001              (FTN4--RELEASE 24177B--JULY, 1971)

0001  FTN4,L
0002        SUBROUTINE BPASS(SR,F1,F2,A,B)
0003        DIMENSION A(5),B(5)
0004        T=1./SR
0005        W1=6.2832*F1
0006        W2=6.2832*F2
0007        D=COS((W2-W1)*T/2.)/SIN((W2-W1)*T/2.)
0008        D1=SQRT(TAN(W1*T/2.)*TAN(W2*T/2))
0009        D2=2.*ATAN(D1)
0010        E=2*COS(D2)
0011        Z0=D**2+1.4142136*D+1.
0012        Z1=-2.*E*D**2-1.4142136*E*D
0013        Z2=(E**2+2.)*D**2-2.
0014        Z3=-2.*E*D**2+1.4142136*E*D
0015        Z4=D**2-1.4142136*D+1.
0016        A(1)=1./Z0
0017        A(2)=0.
0018        A(3)=-2./Z0
0019        A(4)=0.
0020        A(5)=A(1)
0021        B(1)=-Z1/Z0
0022        B(2)=-Z2/Z0
0023        B(3)=-Z3/Z0
0024        B(4)=-Z4/Z0
0025        RETURN
0026        END

**  NO ERRORS*
```

APPENDIX A-5 (cont.)

PROGRAM DCAC

Description

Program DCAC determines the average or dc value of each channel of a data file on disc, and then removes this value by subtraction. The program is given in Program Listing A-5-3.

Required input parameters: None.

Subroutines required:

1. DREA
2. DWRI
3. STPT

Program Listing A-5-3 DCAC

```
      PAGE  0001              (FTN4--RELEASE 24177B--JULY, 1971)

0001  FTN4,I
0002        PROGRAM DCAC
0003        DIMENSION LABF(135),Y(256),IX(256),A(8)
0004        CALL EXEC(17,IFTRK,ILTRK,ISIZE)
0005        CALL DREA(IFTRK,0,LABF,1,1,1)
0006        SR= LABF(38)/60.
0007        NRECS=LABF(39)
0008        NCHA=LABF(37)
0009        DO 12 I=1,NCHA
0010        DO 12 J=1,NRECS
0011        CALL DREA(IFTRK,256,IX,J,I,1)
0012        DO 12 K=1,256
0013        A(I)=A(I)+IX(K)
0014     12 CONTINUE
0015        DO 5 K=1,NCHA
0016        A(K)=A(K)/(NRECS*256)
0017      5 CONTINUE
0018        DO 10 I=1,NCHA
0019        DO 10 J=1,NRECS
0020        MAX=0
0021        CALL DREA(IFTRK,256,IX,J,I,1)
0022        DO 11 K=1,256
0023        Y(K)=IX(K)-A(I)
0024     11 CONTINUE
0025        DO 14 K=1,256
0026        IX(K)=Y(K)
0027        IM=IABS(IX(K))
0028        IF(IM.LT.MAX)GO TO 14
0029        MAX=IM
0030     14 CONTINUE
0031        CALL DWRT(IFTRK,256,IX,J,I,1)
0032        IF(L.EQ.1)GO TO 10
0033        CALL STPT(IFTRK,IX,256,J,1,MAX)
0034     10 CONTINUE
0035        STOP
0036        END

**  NO ERRORS*
```

APPENDIX A-6

PROGRAM PSPT (Power SPecTrum)

Description

Program PSPT produces single or multiple power spectra for up to 8 channels of data stored on disc. The complete data file may be divided into n segments with power spectra produced for each segment. The power spectra are obtained from the application of the fast fourier transform to each 256 word record in a data segment. The power spectrum for each segment is an average of the power spectra obtained from the records in the segment. The magnitudes of the power spectra are output on the teleprinter using subroutine PLOT. The flow chart of program PSPT is given in Figure A-6-1 and a typical output is shown in Figure A-6-2. The program is given in Program Listing A-6-1.

Required input data:

1. Number of channels.
2. Whether or not absolute magnitudes are required as an output.
3. The number of segments into which the data record is to be divided.
4. The number of times the output data is to be smoothed using a moving average filter.
5. The number of plot points to be surpressed at the low frequency end of the spectrum.

Subroutines required:

1. IFFT - the fast fourier transform subroutine written by Dr. Z. Koles, U. of A.
2. DREA

3. PLOT

4. SMTH - a moving average filter. See Program Listing A-6-2.

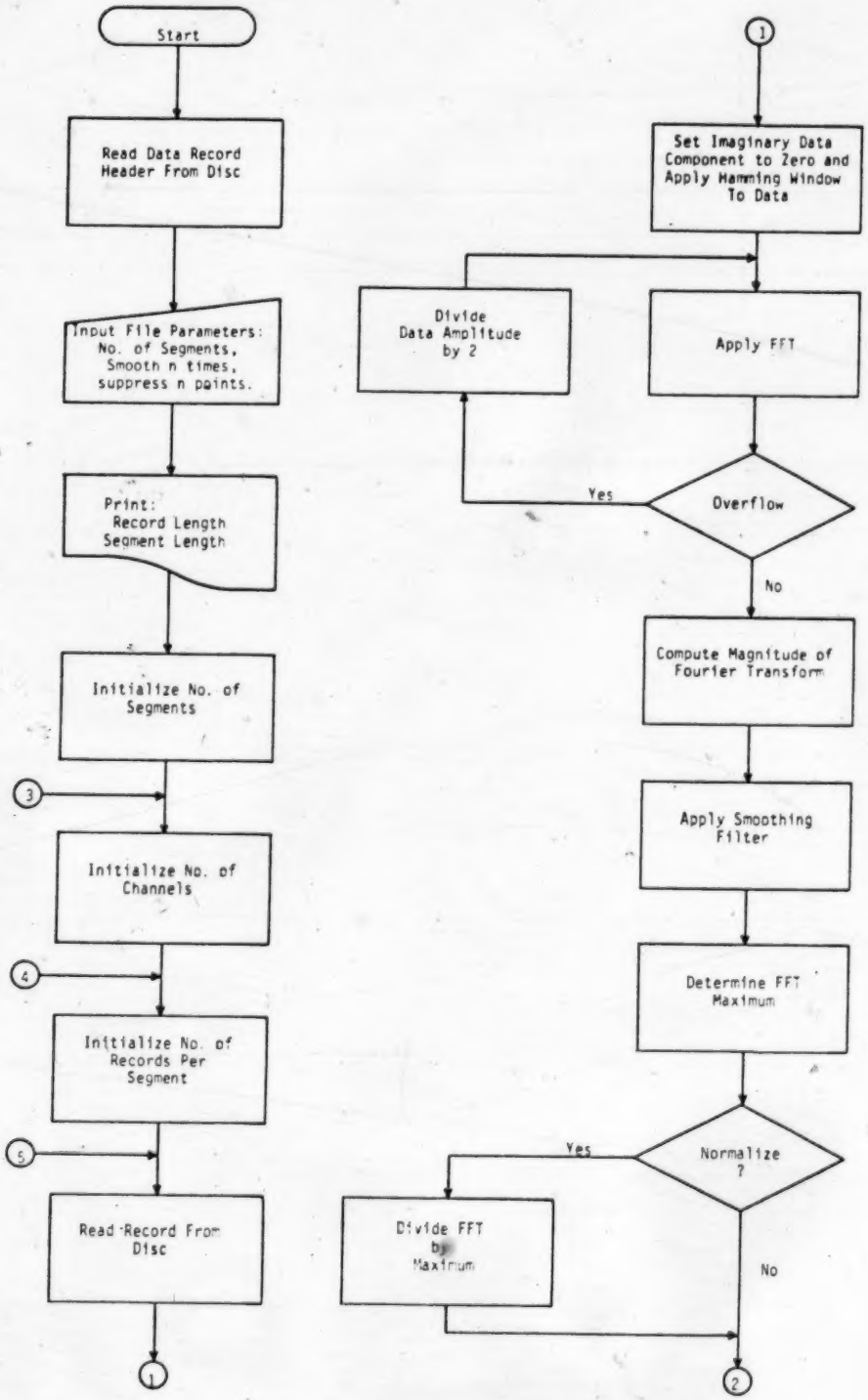

Figure A-6-1 Flow chart of program PSPT.

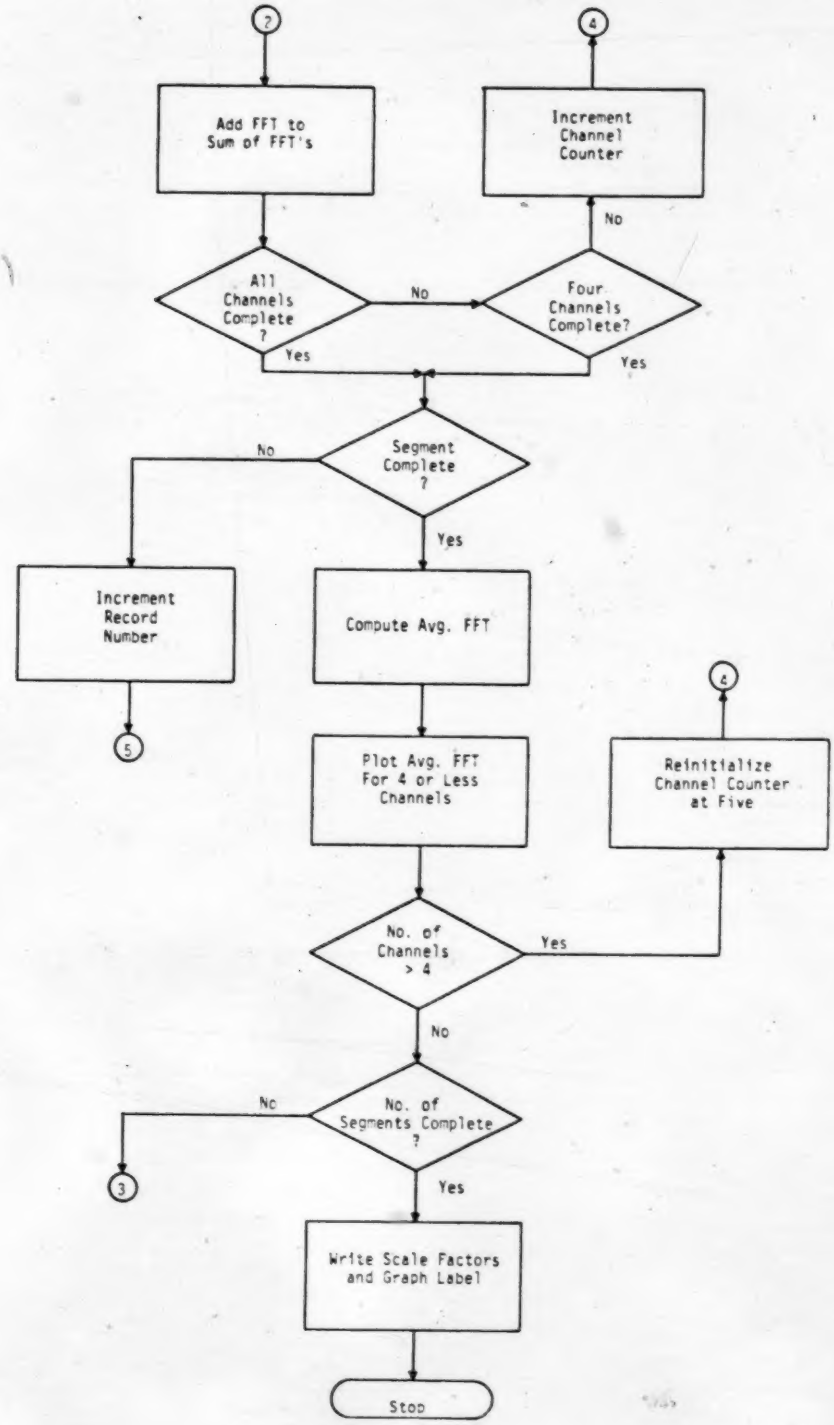

Figure A-6-1 Flow chart of program PSPT (cont.).

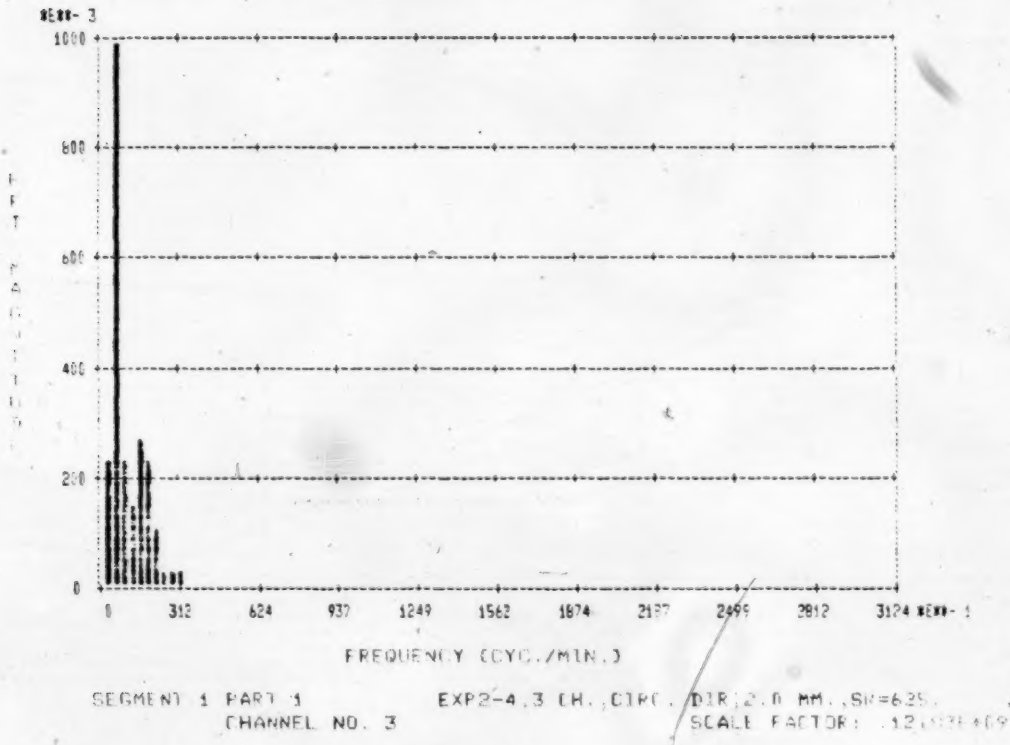

Figure A-6-2 Typical single channel output from program PSPT.

Program Listing A-6-1 PSPT

```
PAGE  0001          (FTN4--RELEASE 241778--JULY, 1971)

0001  FTN4,L
0002        PROGRAM PSPT
0003        DIMENSION LABF(135),ICH(8),Y(128,8),ISINES(65),IP(4),
0004       1 JRAY(256),IR(256),IM(256),NFLOW(8),YM(8),X(128),IESC(9),
0005       2 LABEL(50)
0006        DATA LABEL/18*1H ,1HF,1HF,1HT,1H ,1HM,1HA,1HG,1HN,1HI,1HT,1HU,
0007       1 1HD,1HE/
0008        DATA IESC/15446B,2Hk2,2HS ,2H18,2H11,2HV ,2HD ,2Hk0,2H16/
0009        CALL EXEC(17,IFTRK,ILTRK,ISIZE)
0010        CALL DREA(IFTRK,0,LABF,1,1,1)
0011        IWIDTH=100
0012      1 WRITE(1,100)
0013     100 FORMAT(/"INPUT THE REQUIRED CHANNELS? _")
0014        READ(1,*)(ICH(I),I=1,8)
0015        DO 10 I=1,8
0016        IF(ICH(I).EQ.0)GO TO 11
0017       10 CONTINUE
0018       11 NCHA=I-1
0019        NRECS=LABF(39)
0020        SR=LABF(38)/60.
0021       13 WRITE(1,101)
0022     101 FORMAT(/"DO YOU WANT ABSOLUTE MAGNITUDES? _")
0023        READ(1,102)ISC
0024     102 FORMAT(A2)
0025        IF(ISC.EQ.2HNO)GO TO 12
0026        IF(ISC.NE.2HYE)GO TO 13
0027       12 WRITE(1,104)
0028     104 FORMAT(/"NO OF SEGMENTS? _")
0029        READ(1,*)NSEG
0030        IF(NSEG.LE.0)GO TO 12
0031        IF(NSEG.GT.NRECS)NSEG=NRECS
0032        ISEG=NRECS/NSEG
0033       14 WRITE(1,105)
0034     105 FORMAT(/"SMOOTH N TIMES? _")
0035        READ(1,*)NFILT
0036        IF(NFILT.LT.0)GO  TO 14
0037       15 WRITE(1,113)
0038     113 FORMAT(/"SUPPRESS PLOT POINTS? _")
0039        READ(1,*)NSUP
0040        IF(NSUP.LT.0)GO TO 15
0041        NPLOT=128
0042        SEGL=(60./LABF(38))*256*ISEG
0043        LREC=SEGL*NSEG
0044        LSEG=SEGL
0045        MSEG=SEGL/60.
0046        MREC=LREC/60.
0047        ISECR=MOD(LREC,60)
0048        ISECS=MOD(LSEG,60)
0049        WRITE(1,107)MREC,ISECR
0050     107 FORMAT(/"RECORD LENGTH=",X,I3,X,"MINUTES",X,I3,X,"SECONDS")
0051        WRITE(1,108)MSEG,ISECS
0052     108 FORMAT(/"SEGMENT LENGTH=",X,I3,X,"MINUTES",X,I3,X,"SECONDS")
0053        DO 29 M=1,NSEG
0054        IF(NCHA.GT.4)GO TO 17
0055        ITIMES=NCHA
0056        GO TO 18
```

216280

Program Listing A-6-1 PSPT (cont.)

```
PAGE  0002  PSPT       (FTN4--RELEASE 24177B--JULY, 1971)
 0057      17 ITIMES=4
 0058      18 N=1
 0059         ISND=1
 0060         IAGAIN=1
 0061      20 DO 23 I=1,8
 0062         YM(I)=0.
 0063         DO 23 K=1,128
 0064         Y(K,I)=0.
 0065      23 CONTINUE
 0066         YMAX=0.
 0067         NT=0
 0068         DO 35 I=N,ITIMES
 0069         DO 22 J=1,ISEG
 0070         NFLOW(I)=0
 0071         ISET=1
 0072         CALL DREA(IFTNK,256,JRAY,J,ICH(I),1)
 0073      34 DO 19 K=1,256
 0074         IM(K)=0
 0075         IR(K)=IFIX(JRAY(K)*(1.+SIN((K-1)*6.2832/255.-1.5708))/(16.*ISET)
 0076      19 CONTINUE
 0077         NT=NT+1
 0078         CALL IFFT(IR,IM,ISINES,256,NT,0,IFL)
 0079         IF(IFL.EQ.0)GO TO 21
 0080         NFLOW(I)=NFLOW(I)+1
 0081         ISET=ISET*2
 0082         GO TO 34
 0083      21 SET=ISET**2
 0084         DO 22 K=1,128
 0085         Y(K,1)=Y(K,I)+SET*(FLOAT(IR(K))**2+FLOAT(IM(K))**2)
 0086      22 CONTINUE
 0087         Y(1,I)=0.
 0088         IF(NFILT.LE.0)GO TO 24
 0089         DO 25 K=1,NFILT
 0090      25 CALL SMTH(Y(2,1),127)
 0091      24 IF(NSUP.LT.1)GO TO 26
 0092         DO 27 K=1,NSUP
 0093      27 Y(K,I)=0.
 0094      26 DO 35 K=1,128
 0095         Y(K,I)=Y(K,I)/ISEG**2
 0096         IF(Y(K,I).GE.YM(I))YM(I)=Y(K,I)
 0097      35 CONTINUE
 0098         DO 28 I=N,ITIMES
 0099         IF(YM(I).GE.YMAX)YMAX=YM(I)
 0100      28 CONTINUE
 0101         IF(ISC.EQ.2HYE)GO  TO 30
 0102         YMAX=1.
 0103         DO 31 I=1,8
 0104         IF(YM(I).EQ.0)YM(I)=1.E36
 0105         DO 32 K=1,128
 0106         Y(K,I)=Y(K,I)/YM(I)
 0107         IF(Y(K,I).GT.1)Y(K,I)=1.
 0108      32 CONTINUE
 0109      31 CONTINUE
 0110      30 S=FLOAT(LABF(3B))/256.
 0111         DO 33 I=1,128
 0112         X(I)=(I-1)*S
```

216281

Program Listing A-6-1 PSPT (cont.)

```
PAGE  0003  PSPT       (FTN4--RELEASE 24177B--JULY, 1971)

0113      33 CONTINUE
0114         NTR=4
0115         IF(NCHA.LE.4)NTR=NCHA
0116      60 IT=1
0117         IF(NTR.EQ.1)IT=2
0118         CALL PLOT(X,Y(512*(ISND-1)+1),1.5,LABEL,128,NTR,IT)
0119         WRITE(1,109)M,ISND,(LABF(I),I=1,36)
0120     109 FORMAT(18X,"SEGMENT",I2," PART ",I1,10X,36A2)
0121         IF(NTR.EQ.1)GO TO 40
0122         WRITE(1,110)(ICH(I),I=1,4),21000B
0123     110 FORMAT(30X,"CH.",I2," x",8X,"CH.",I2," o",8X,"CH.",I2," +",
0124        1 8X,"CH.",I2," ",A1)
0125         WRITE(1,111)(NFLOW(I),I=N,ITIMES)
0126     111 FORMAT(14X,"   OVERFLOWS:   ",4(I3,12X))
0127         WRITE(1,112)(YM(I),I=N,ITIMES)
0128     112 FORMAT(14X,"  SCALE FACTORS: ",4(E10.5,5X))
0129      40 IF(NTR.EQ.1)WRITE(1,151)ICH(1),NFLOW(1),YM(1)
0130     151 FORMAT(28X,"CHANNEL NO. ",I1,4X,"OVERFLOWS: "I3,4X,
0131        1 "SCALE FACTOR: ",E10.5)
0132         N=5
0133         ITIMES=NCHA
0134         IAGAIN=-IAGAIN
0135         ISND=ISND+1
0136         IF(IAGAIN.LT.0.AND.NCHA.GT.4)GO TO 20
0137      29 CONTINUE
0138         WRITE(1,150)IESC(1),IESC(5),IESC(6)
0139     150 FORMAT(3A2)
0140         STOP
0141         END

**  NO ERRORS*
```

Program Listing A-6-2 SMTH

```
PAGE  0001          (FTN4--RELEASE 24177B--JULY, 1971)

0001          SUBROUTINE SMTH(X,NPTS)
0002          DIMENSION X(3)
0003          A=X(1)
0004          B=X(2)
0005          C=X(3)
0006          X(1)=.5*(A+B)
0007          DO 20 J=2,NPTS-1
0008          X(J)=(A+2.*B+C)*.25
0009          A=B
0010          B=C
0011       20 C=X(J+2)
0012          X(NPTS)=.5*(A+B)
0013          RETURN
0014          END
```

APPENDIX A-7

PROGRAM PHSE (PHaSE)

Description

Program PHSE uses zero-crossing techniques to determine cycle-to-cycle frequencies and relative phase shifts of any two data channels stored on disc. The frequencies and relative phase shift are plotted as a function of cycle number using the subroutine PLOT. Linear regression analysis is applied to the arrays of phase angles and frequencies to produce equations describing changes in these parameters as a function of cycle number. A flow chart of program PHSE is shown in Figure A-7-1 and a typical output is shown in Figure A-7-2. The program is given in Program Listing A-7-1.

Required input data:

1. The numbers of the two channels to be processed.
2. All remaining data is obtained from the data header record on disc.

Subroutines required:

1. DREA
2. PLOT
3. LFIT (Linear FIT) - a subroutine to do linear regression analysis. See Program Listing A-7-2.

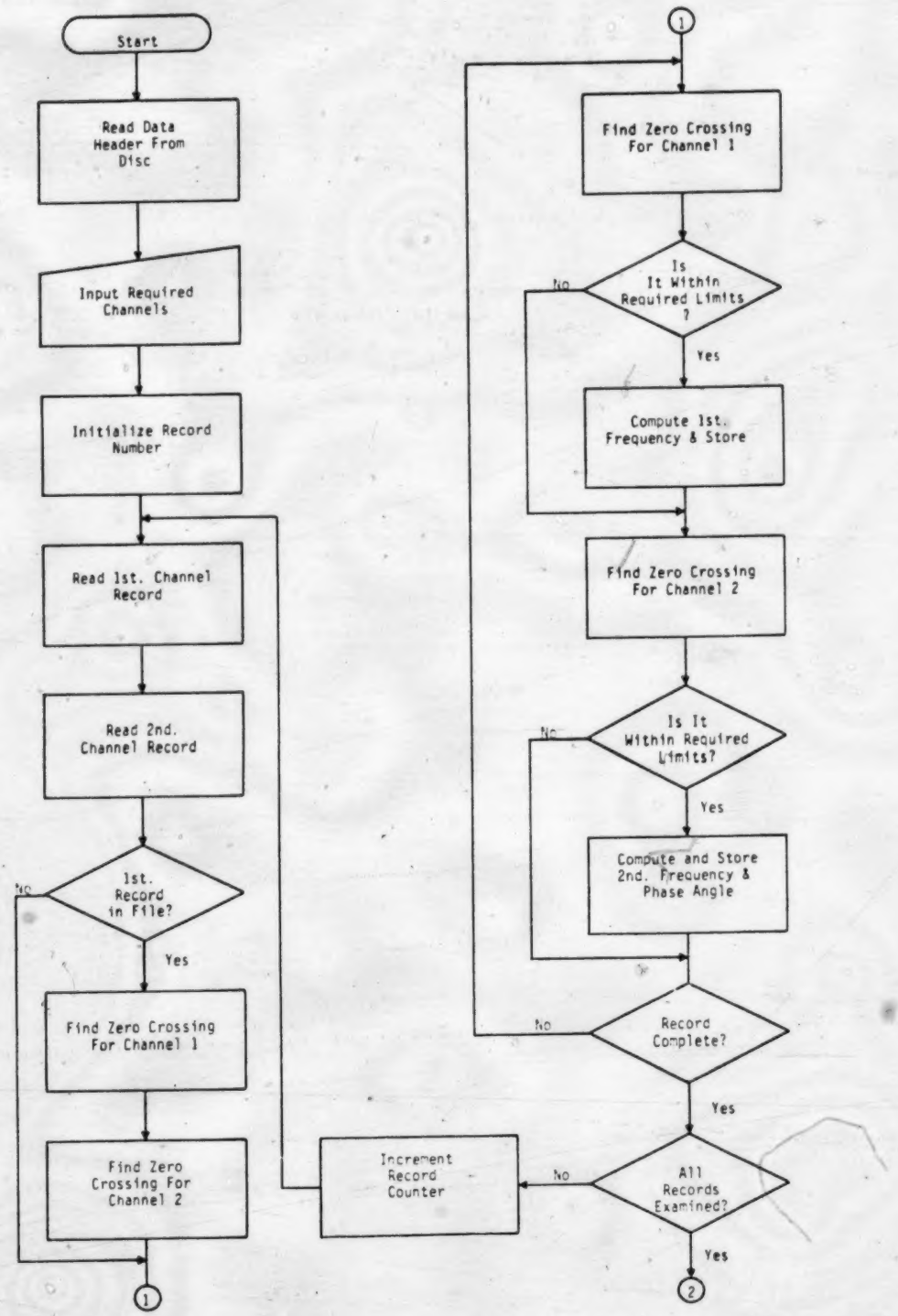

Figure A-7-1 Flow chart of program PHSE.

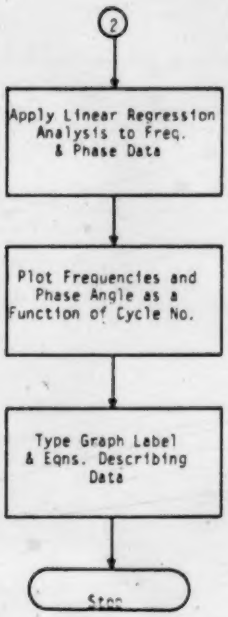
2
Apply Linear Regression Analysis to Freq. & Phase Data
Plot Frequencies and Phase Angle as a Function of Cycle No.
Type Graph Label & Eqns. Describing Data
Stop

Figure A-7-1 Flow chart of program PHSE (cont.).

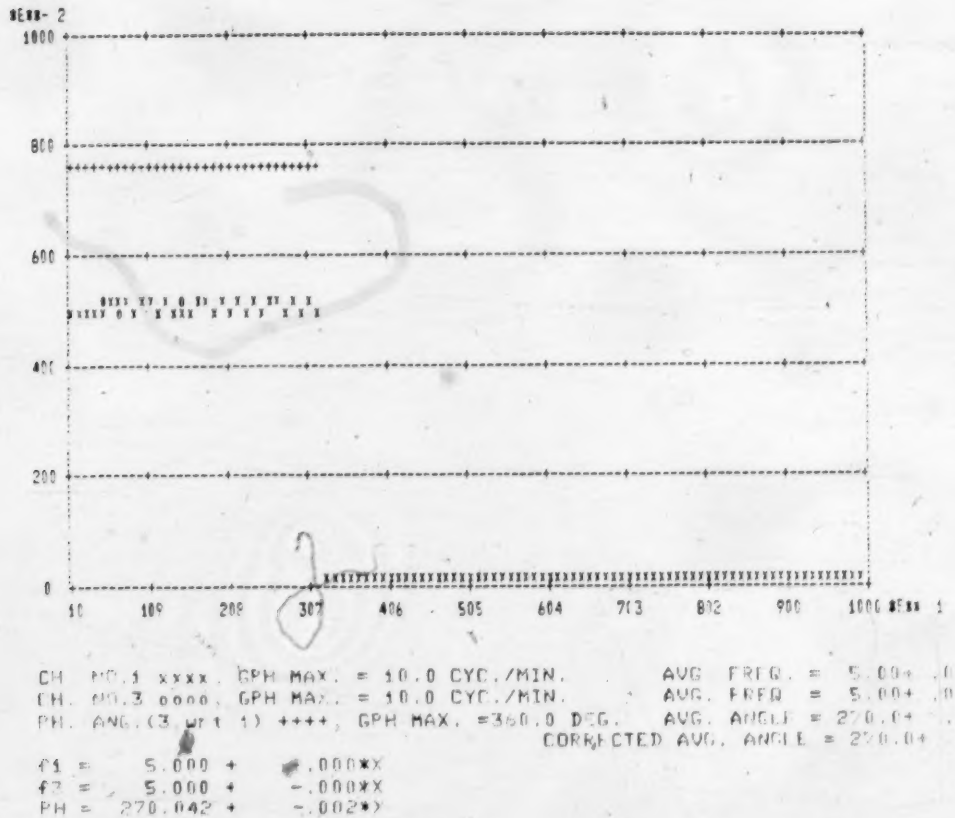

Figure A-7-2 Typical output from the program PHSE.

Program Listing A-7-1 PHSE

```
PAGE  0001              (FTN4--RELEASE 24177B--JULY, 1971)

0001  FTN4,L
0002        PROGRAM PHSE
0003        DIMENSION IESC(9),LABF(135),JRAY(256),KRAY(256),Y(100,3),F1(100)
0004       1 F2(100),PH(100),LABEL(25),X(100),CPH(100)
0005        DOUBLE PRECISION AF1,SD1,AF2,SD2,APH,SD3,ACPH,SD4
0006        DATA IESC/15446B,2Hk2,2HS ,2H18,2H11,2HV ,2HD ,2Hk0,2H16/
0007        CALL EXEC(17,IFTRK,IL,IS)
0008        CALL DREA(IFTRK,0,LABF,1,1,1)
0009        SR=LABF(38)/60.
0010        DT=1./SR
0011        NRECS=LABF(39)
0012        WRITE(1,100)
0013    100 FORMAT(/"INPUT THE REQUIRED CHANNELS! _")
0014        READ(1,*)ICH1,ICH2
0015        T=0.
0016        II1=0
0017        T1=0.
0018        T2=0.
0019        TP=0.
0020        J=1
0021        K=1
0022        L=1
0023        IP=0
0024        DO 10 M=1,NRECS
0025        CALL DREA(IFTRK,256,JRAY,M,ICH1,1)
0026        CALL DREA(IFTRK,256,KRAY,M,ICH2,1)
0027        II=1
0028       IF(M.NE.1)GO TO 11
0029        DO 12 I=2,256
0030        ISN1=ISIGN(1,JRAY(I-1))
0031        ISN2=ISIGN(1,JRAY(I))
0032        IF(ISN2.NE.ISN1.AND.JRAY(I).GT.0)GO TO 13
0033     12 CONTINUE
0034     13 T1=(FLOAT(JRAY(I))/(FLOAT(JRAY(I))-FLOAT(JRAY(I-1))))*DT
0035        II=1
0036     11 DO 20 I=II,256
0037        IF(I.NE.1)GO TO 14
0038        ISN1=ISIGN(1,IC1)
0039        GO TO 15
0040     14 ISN1=ISIGN(1,JRAY(I-1))
0041     15 ISN2=ISIGN(1,JRAY(I))
0042        IF(ISN2.NE.ISN1.AND.JRAY(I).GT.0)GO TO 16
0043        GO TO 17
0044     16 IF(I.GT.1)IC1=JRAY(I-1)
0045        IF(II1.EQ.0)GO TO 18
0046        T=T-DT*(FLOAT(JRAY(1))/(FLOAT(JRAY(I))-FLOAT(IC1)))
0047        F1(K)=60./(T-T1)
0048        IF(F1(K).GT.30.)GO TO 70
0049        AVF1=F1(K)
0050        IF(K.GT.3)AVF1=(F1(K-1)+F1(K-2)+F1(K-3))/3.
0051        IF(F1(K).GE.(1.5*AVF1))GO TO 70
0052        IP=1
0053        IF(F1(K).LT.(.67*AVF1))GO TO 18
0054        K=K+1
0055        IF(K.GT.100)GO TO 25
0056     18 T1=T
```

171318

Program Listing A-7-1 PHSE (cont.)

```
PAGE  0002  PHSE       (FTN4--RELEASE 24177B--JULY, 1971)

0057      70 T=T+DT*(FLOAT(JRAY(I))/(FLOAT(JRAY(I))-FLOAT(IC1)))
0058         IT1=1
0059      17 IF(I.NE.1)GO TO 19
0060         ISN1=ISIGN(1,IC2)
0061         GO TO 1
0062      19 ISN1=ISIGN(1,KRAY(I-1))
0063       1 ISN2=ISIGN(1,KRAY(I))
0064         IF(ISN2.NE.ISN1.AND.KRAY(I).GT.0)GO TO 2
0065         GO TO 3
0066       2 IF(I.GT.1)IC2=KRAY(I-1)
0067         T=T-DT*(FLOAT(KRAY(I))/(FLOAT(KRAY(I))-FLOAT(IC2)))
0068         IF(T2.EQ.0)GO TO 4
0069         F2(L)=60./(T-T2)
0070         IF(F2(L).GT.30.)T=T+DT*(FLOAT(KRAY(I))/(FLOAT(KRAY(I))-
0071        1 FLOAT(IC2)))
0072         IF(F2(L).GT.30.)GO TO 3
0073         AVF2=F2(L)
0074         IF(L.GT.3)AVF2=(F2(L-1)+F2(L-2)+F2(L-3))/3.
0075         IF(F2(L).GE.(1.5*AVF2))T=T+TD*(FLOAT(KRAY(I))/(FLOAT(KRAY(I))
0076        1 -FLOAT(IC2)))
0077         IF(F2(L).GE.(1.5*AVF2))GO TO 3
0078         IF(F2(L).LT.(.67*AVF2))GO TO 4
0079         L=L+1
0080         IF(L.GT.100)GO TO 25
0081       4 T2=T
0082         T=T+DT*(FLOAT(KRAY(I))/(FLOAT(KRAY(I))-FLOAT(IC2)))
0083         TP=T2-T1
0084         IF(TP.EQ.0)GO TO 3
0085         PH(J)=(TP*F1(K-1)/60.)*360.
0086         IP=0
0087         J=J+1
0088         IF(J.GT.100)GO TO 25
0089       3 T=T+DT
0090      20 CONTINUE
0091         IC1=JRAY(256)
0092         IC2=KRAY(256)
0093      10 CONTINUE
0094      25 IF(F1(K).GT.30.)F1(K)=30.
0095         IF(F2(L).GT.30.)F2(L)=30.
0096         AF1=0.
0097         SD1=0.
0098         L=L-1
0099         K=K-1
0100         J=J-1
0101         DO 30 I=1,K
0102         AF1=AF1+F1(I)
0103         SD1=SD1+F1(I)**2
0104      30 CONTINUE
0105         CALL LFIT(F1,K,A01,A11)
0106         AF1=AF1/K
0107         SD1=SD1/K
0108         SD1=DABS(SD1-AF1**2)
0109         SD1=DSQRT(SD1)
0110         AF2=0.
0111         SD2=0.
0112         DO 40 I=1,L
```

171319

Program Listing A-7-1 PHSE (cont.)

```
PAGE  0000  PHSE      (FTN4--RELEASE 24177B--JULY, 1971)

0113          AF2=AF2+F2(I)
0114          SD2=SD2+F2(I)**2
0115       40 CONTINUE
0116          CALL LFIT(F2,L,A02,A12)
0117          AF2=AF2/L
0118          SD2=SD2/L
0119          SD2=DABS(SD2-AF2**2)
0120        * SD2=DSQRT(SD2)
0121          SD3=0.
0122          DO 50 I=1,J
0123          APH=APH+PH(I)
0124          SD3=SD3+PH(I)**2
0125       50 CONTINUE
0126          APH=APH/J
0127          SD3=SD3/J
0128          SD3=DABS(SD3-APH**2)
0129          SD3=DSQRT(SD3)
0130          ACPH=0.
0131          SD4=0.
0132          DO 28 I=1,J
0133          CPH(I)=PH(I)
0134          IF(APH.LT.90..AND.PH(I).GT.270.)CPH(I)=PH(I)-360.
0135          IF(APH.GT.270..AND.PH(I).LT.90.)CPH(I)=PH(I)+360.
0136          ACPH=ACPH+CPH(I)
0137          SD4=SD4+CPH(I)**2
0138        7 IF(PH(I).GE.0)GO TO 28
0139          PH(I)=PH(I)+360.
0140          GO TO 7
0141       28 CONTINUE
0142          CALL LFIT(CPH,J,A03,A13)
0143          ACPH=ACPH/J
0144          SD4=SD4/J
0145          SD4=DABS(SD4-ACPH**2)
0146          SD4=DSQRT(SD4)
0147          F1MX=0.
0148          F2MX=0.
0149          FMX=0.
0150          PHMX=0.
0151          DO 59 I=1,J
0152          IF(PH(I).GE.PHMX)PHMX=PH(I)
0153       59 CONTINUE
0154          MXPH=300
0155          FMAX=0.
0156          IF(PHMX.GT.45.)GO TO 55
0157          PHMX=45.
0158          GO TO 56
0159       55 IF(PHMX.GT.90.)GO TO 58
0160          PHMX=90.
0161          GO TO 56
0162       58 IF(PHMX.GT.180.)GO TO 57
0163          PHMX=180.
0164          GO TO 56
0165       57 IF(PHMX.GT.360)GO TO 54
0166           PHMX=360.
0167          GO TO 56
0168       54 MXPH=MXPH+100
```

171320

Program Listing A-7-1 PHSE (cont.)

```
PAGE  0004  PHSE       (FTN4--RELEASE 24172B--JULY, 1971)

0169          IF(PHMX.GT.MXPH)GO TO 54
0170          PHMX=MXPH
0171       56 DO 60 I=1,K
0172          IF(F1(I).GE.F1MX)F1MX=F1(I)
0173       60 CONTINUE
0174          DO 61 I=1,L
0175          IF(F2(I).GE.F2MX)F2MX=F2(I)
0176       61 CONTINUE
0177          IF(F2MX.GE.F1MX)GO TO 62
0178          FMX=F1MX
0179          GO TO 66
0180       62 FMX=F2MX
0181       66 FMAX=FMAX+10.
0182          IF(FMX.GT.FMAX)GO TO 66
0183          FMX=FMAX
0184       63 DO 64 I=1,100
0185          PH(I)=PH(I)*FMX/PHMX
0186       64 CONTINUE
0187          MX=MAX0(J,K,L)
0188          DO 65 I=1,100
0189          X(I)=I
0190          Y(I)=F1(I)
0191          Y(I+100)=F2(I)
0192          Y(I+2*100)=PH(I)
0193       65 CONTINUE
0194      104 FORMAT(3A2)
0195          IBS=4137B
0196          CALL PLOT(X,Y,FMX,LABEL,100,3,1)
0197          WRITE(1,110)IESC(1),IESC(9),IESC(7)
0198      110 FORMAT(3A2," ")
0199          WRITE(1,105)(LABF(I),I=1,36)
0200      105 FORMAT(16X,36A2)
0201          WRITE(1,101)ICH1,FMX,AF1,IBS,SD1
0202      101 FORMAT(16X,"CH. NO.",I1," xxxx, GPH MAX. =",F5.1,
0203         1 " CYC./MIN.",7X,"AVG. FREQ. =",F6.2,"+",A2,F4.2,
0204         2 " CYC./MIN.")
0205          WRITE(1,103)ICH2,FMX,AF2,IBS,SD2
0206      103 FORMAT(16X,"CH. NO.",I1," oooo, GPH MAX. =",F5.1,
0207         1 " CYC./MIN.",7X,"AVG. FREQ. =",F6.2,"+",A2,F4.2,
0208         2 " CYC./MIN.")
0209      102 FORMAT(16X,"PH. ANG.(",I1," wrt ",I1,") ++++, GPH",
0210         1 " MAX. =",F5.1," DEG.",3X,"AVG. ANGLE =",F6.1,"+",
0211         2 A2,F4.1," DEG.")
0212          WRITE(1,102)ICH2,ICH1,PHMX,APH,IBS,SD3
0213          WRITE(1,106)ACPH,IBS,SD4
0214      106 FORMAT(54X,"CORRECTED AVG. ANGLE =",F6.1,"+",A2,F4.1,
0215         1 " DEG.")
0216          WRITE(1,107)ICH1,A01,A11
0217      107 FORMAT(16X,"f",I1," = ",F8.3," + ",F8.3,"*X")
0218          WRITE(1,108)ICH2,A02,A12
0219      108 FORMAT(16X,"f",I1," = ",F8.3," + ",F8.3,"*X")
0220          WRITE(1,109)A03,A13
0221      109 FORMAT(16X,"PH = ",F8.3," + ",F8.3,"*X")
0222          WRITE(1,110)IESC(1),IESC(9),IESC(7)
0223          WRITE(1,104)IESC(1),IESC(5),IESC(6)
0224          STOP

171321
```

Program Listing A-7-2 LFIT

```
        PAGE  0001              (FTN4--RELEASE 24177B--JULY, 1971)

0001  FTN4,L
0002        SUBROUTINE LFIT(X,NUM,A0,A1)
0003        DIMENSION X(1)
0004        SX=0.
0005        SN=0.
0006        SNS=0.
0007        SXN=0.
0008        DO 10 I=1,NUM
0009        SX=SX+X(I)
0010        SN=SN+I
0011        SNS=SNS+I**2
0012        SXN=SXN+X(I)*I
0013     10 CONTINUE
0014        A0=(SX*SNS-SN*SXN)/(NUM*SNS-SN**2)
0015        A1=(NUM*SXN-SN*SX)/(NUM*SNS-SN**2)
0016        RETURN
0017        END

** NO ERRORS*
```

APPENDIX A-8

PROGRAM XCORR (Cross CORRelation)

Description

Program XCORR computes the cross-correlation of two data channels stored on disc. If the two specified channels are the same an auto-correlation is obtained. The normalized correlation versus delay time is plotted on the teleprinter using subroutine PLOT. Also if the correlation function is cyclic, its frequency and relative phase shift are determined from the function's zero crossings. The flow chart of XCORR is given in Figure A-8-1 and a typical output is shown in Figure A-8-2. The program is given in Program Listing A-8-1.

Required input data:

1. The numbers of the channels to be processed. If the two channel numbers are the same, the autocorrelation of that channel is produced.
2. All remaining data is obtained from the header record on disc.

Subroutines required:

1. DREA
2. PLOT

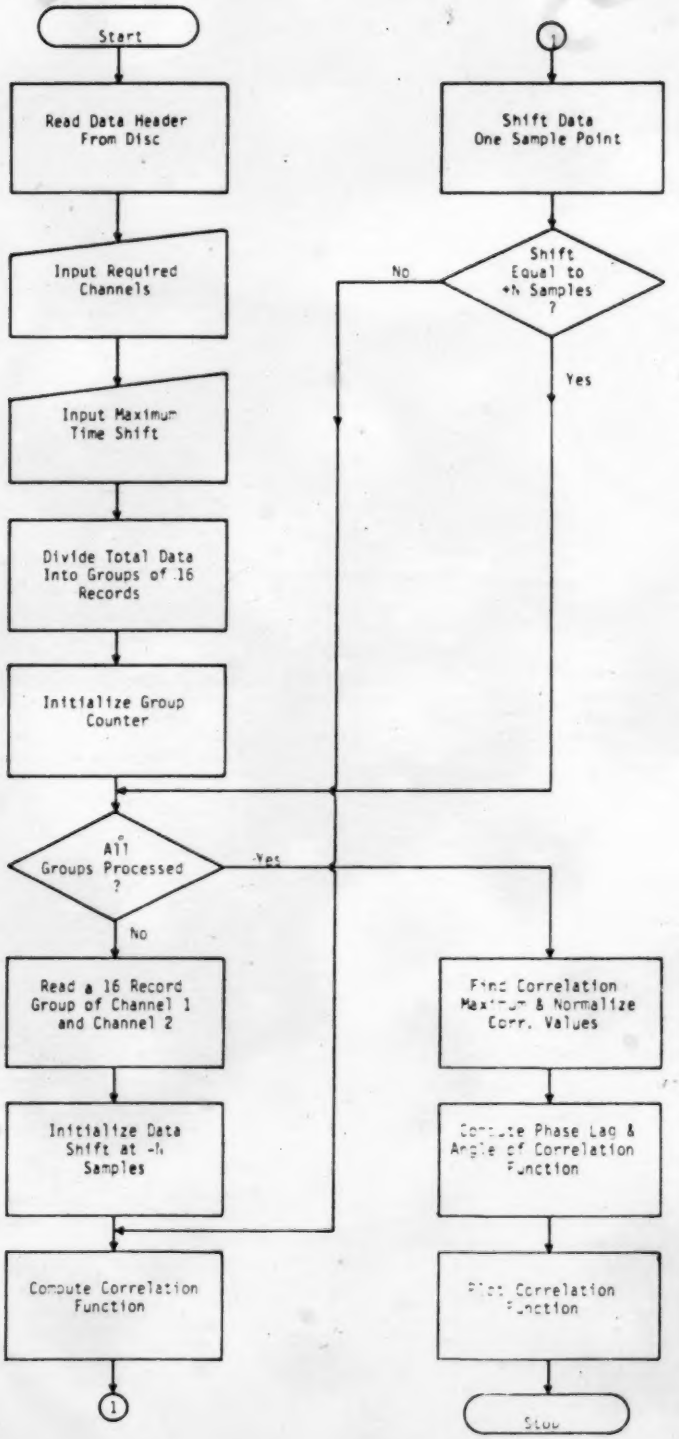
Start
Read Data Header From Disc
Input Required Channels
Input Maximum Time Shift
Divide Total Data Into Groups of 16 Records
Initialize Group Counter
All Groups Processed ?
Yes
No
Read a 16 Record Group of Channel 1 and Channel 2
Initialize Data Shift at -h Samples
Compute Correlation Function
1
Shift Data One Sample Point
Shift Equal to +h Samples ?
No
Yes
Find Correlation Maximum & Normalize Corr. Values
Compute Phase Lag & Angle of Correlation Function
Plot Correlation Function
Stop

Figure A-8-1 Flow chart of program XCORR.

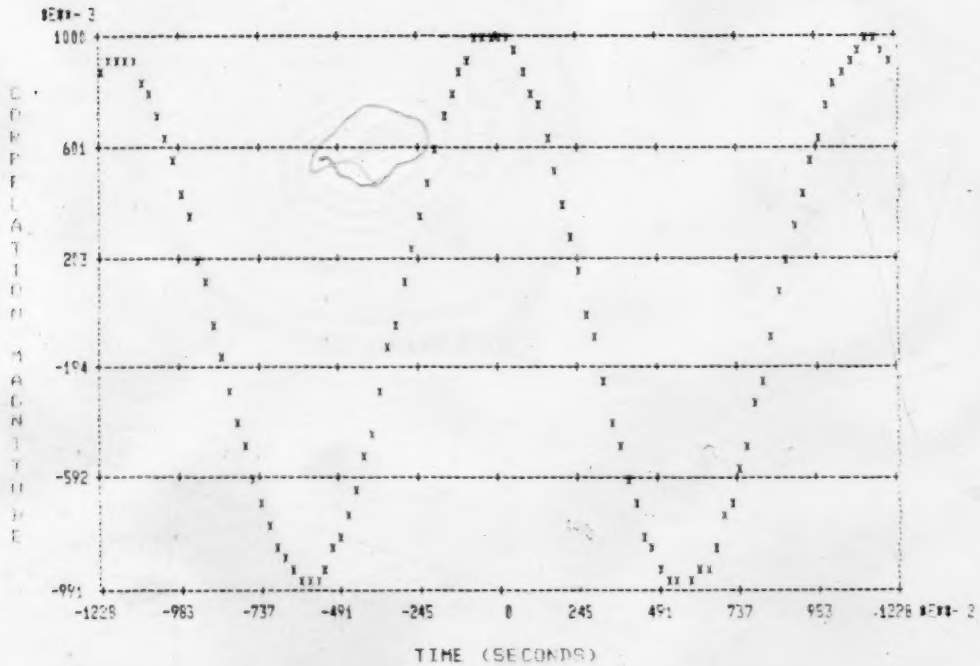

CH. 1 RELATIVE TO CH. 2 EXP2-4 3 CH. CIRC DIR.2.0 MM.,SP=4.25.
% SHIFT = 6.25 FREQ. = 5.19 CYCLES/MIN. PHASE = -2.95 DEGREES
MAXIMUM CORRELATION AMPLITUDE IS .350558E+11

Figure A-8-2 Typical output of program XCORR.

Program Listing A-8-1 XCORR

```
PAGE  0001              (FTN4--RELEASE 24177B--JULY, 1971)

      FTN4,
            PROGRAM XCORR
            DIMENSION IX(4224),IY(4224),C(257),X(257),LABEL(25),
           1 LABF(135),IESC(9)
            EQUIVALENCE (Y,IY),(X,IX)
            DATA IESC/15446B,2Hk2,2HS ,2HEB,2H11,2HV ,2HD ,2Hk0,2H16/
            DATA LABEL/2*1H ,1HC,1HO,1HR,1HR,1HE,1HL,1HA,1HT,1HI,1HO,
           1 1HN,1H ,1HM,1HA,1HG,1HN,1HI,1HT,1HU,1HD,1HE/
            CALL EXEC(17,IFTRK,ILTRK,ISIZE)
            CALL DREAD(IFTRK,0,LABF,1,1,1)
            SR=LABF(38)/60.
            NRECS=LABF(39)
            NCHA=LABF(37)
            DO 15 I=1,4224
            IX(I)=0
            IY(I)=0
         15 CONTINUE
            DO 19 I=1,257
            C(I)=0.
         19 CONTINUE
          1 WRITE(1,100)
        100 FORMAT(/"INPUT THE REQUIRED CHANNELS?  ")
            READ(1,*)ICH1,ICH2
            IF(ICH1.GT.NCHA)GO TO 1
            IF(ICH2.GT.NCHA)GO TO 1
            WRITE(1,101)
        101 FORMAT(/"INPUT MAXIMUM TIME SHIFT IN SECONDS?  ")
            READ(1,*)TMAX
            N=IFIX(TMAX*SR/2.)*2
            IF(N.LE.128)GO TO 2
            N=128
            TMAX=N/SR
            WRITE(1,102)TMAX
        102 FORMAT(/"MAXIMUM TIME SHIFT REDUCED TO ",F7.1," SECONDS")
          2 LNGTH=4096
            IST=129
            IST=129
            NREM=MOD(NRECS,16)
            NTIME=(NRECS-NREM)/16
            IF(NTIME.NE.0)GO TO 3
          4 LNGTH=NREM*256
            NTIME=1
            NREM=0
          3 DO 20 J=1,NTIME
            IREC=(J-1)*16+1
            CALL DREAD(IFTRK,LNGTH,IX(1ST),IREC,ICH1,1)
            CALL DREAD(IFTRK,LNGTH,IY(1SY),IREC,ICH2,1)
            DO 10 I=-N,N
            DO 16 K=1,LNGTH+128
            IIX=I+K
            IF(IIX.LE.0)GO TO 16
            IMAX=LNGTH+128
            IF(IIX.GT.IMAX)GO TO 16
            C(N+1+I)=C(N+1+I)+FLOAT(IY(K))*FLOAT(IX(I+K))
        16 CONTINUE
        10 CONTINUE
```

171558

Program Listing A-8-1 XCORR (cont.)

```
PAGE  0002  XCORR      (FTN4--RELEASE 24177B--JULY, 1971)

0057          DO 20 K=1,128
0058          IX(K)=IX(LNGTH+K)
0059          IY(K)=IY(LNGTH+K)
0060       20 CONTINUE
0061          IF(NREM.NE.0)GO TO 4
0062          N=2*N
0063        6 YMAX=0
0064          DO 13 I=1,N+1
0065          AY=ABS(C(I))
0066          IF(AY.GT.YMAX)IMAX=I
0067          IF(AY.GT.YMAX)YMAX=AY
0068       13 CONTINUE
0069          DO 14 I=1,N+1
0070          C(I)=C(I)/YMAX
0071          X(I)=(I-N/2.-1)/SR
0072       14 CONTINUE
0073          NPER=0
0074          PER=0.
0075          DIR=1.
0076          DO 21 I=1,N
0077          SN1=SIGN(1.,C(I))
0078          SN2=SIGN(1.,C(I+1))
0079          IF(SN1.EQ.SN2)GO TO 21
0080          IF(C(I+1).LT.C(I))DIR=-1.
0081          T1=(C(I+1)/(C(I+1)-C(I)))*DIR/SR
0082          GO TO 22
0083       21 CONTINUE
0084       22 DO 23 J=I+1,N
0085          SN1=SIGN(1.,C(J))
0086          SN2=SIGN(1.,C(J+1))
0087          IF(SN1.EQ.SN2)GO TO 23
0088          IF(SN2.NE.DIR)GO TO 23
0089          T2=(C(J+1)/(C(J+1)-C(J)))*DIR/SR
0090          PER=T1+(J-I)/SR-T2+PER
0091          NPER=NPER+1
0092          GO TO 24
0093       23 CONTINUE
0094          GO TO 25
0095       24 I=J
0096          T1=T2
0097          GO TO 22
0098       25 F=(FLOAT(NPER)/PER)*60.
0099          TMX=(FLOAT(IMAX)-N/2.-1)/SR
0100          PHAS=360.*TMX*NPER/PER
0101          RATIO=YMAX*100./(256*LABF(39)*60./LABF(38))
0102          CALL PLOT(X,C,0.,LABEL,N+1,1,1)
0103          WRITE(1,104)
0104      104 FORMAT(42X,"TIME (SECONDS)")
0105          WRITE(1,105)ICH1,ICH2,(LABF(I),I=1,36)
0106      105 FORMAT(/20X,"CH. ",I1," RELATIVE TO CH. ",I1,5X,36A2)
0107          WRITE(1,107)RATIO,F,PHAS
0108      107 FORMAT(20X,"% SHIFT =",F5.2,3X,"FREQ. =",F5.2," CYCLES/MIN.",
              1 3X,"PHASE =",F7.2," DEGREES")
0110          WRITE(1,108)YMAX
0111      108 FORMAT(20X,"MAXIMUM CORRELATION AMPLITUDE IS ",E12.6)
0112          WRITE(1,103)IESC(1),IESC(5),IESC(6)
```

171559

Program Listing A-8-1 XCORR (cont.)

```
PAGE  0003  XCORR      (F1N4--RELEASE 24177B--JULY, 1971)

0113      103 FORMAT(3A2)
0114          STOP
0115          END

** NO ERRORS*
```

APPENDIX A-9

PROGRAM MAIN

Program MAIN is a master program which permits the researcher to process up to eight data files using any or all of the previously described programs. The input files are read from magnetic tape and are specified on the basis of their file numbers. The file length, number of records to be skipped at the beginning of each file, and the sample data reduction rates are input for all eight files. The programs can be applied twice to the same set of data files. Program MAIN provides a list of the available programs and requests the order in which these programs are to be applied to the data in each of two processing applications. An input order of zero indicates that a particular program is not to be applied. Program MAIN outputs each program name and awaits two sequence numbers, one for each processing pass through the data files. The following is a typical output followed by the required sequence numbers:

PROGRAM:	1st. 2nd
FLOCT	1, 1
DCAC	0, 2
FILTR	0, 3
PSPT	2, 0
PHSE	0, 5
XCORR	0, 4

The above set of sequence numbers will result in programs FLOCT followed by PSPT being applied to all specified data files (a maximum

of 8 files) during the first processing pass. During the second pass programs FLOCT, DCAC, FILTR, XCORR, and PHSE will be applied to the data in the order listed. Program FLOCT will always be first in the sequence unless only one file is to be processed and it already exists on disc.

Required input parameters:

1. Number of files (a maximum of 8).
2. Specific file numbers.
3. File lengths (number of 256-word records).
4. Skip sequence (number of records to be skipped at the beginning of each file).
5. Two sample reduction rates (one for each pass).
6. Input sample rate.
7. Number of channels.
8. Number of segments for fourier analysis.
9. Maximum time delay for cross-correlation.
10. Digital filter cutoff frequencies.
11. Two sequence numbers for each program.

Programs and subroutines required are:

1. FLOCT
2. DCAC
3. FILTR
4. PSPT
5. PHSE
6. XCORR
7. DREA
8. DWRI
9. STPT
10. RDPT
11. PLOT
12. IFFT
13. SMTH
14. BPASS
15. LFIT

Program MAIN is given in Program Listing A-9-1.

Program Listing A-9-1 MAIN

```
PAGE  0001              (FTN4--RELEASE 24177B--JULY, 1971)

0001  FTN4,L
0002        PROGRAM MAIN
0003        DIMENSION ISEQ(6,2),JFILE(8),NS(2),LOCT(3),IDCAC(3),IFILT(3),
0004       1 IPSPT(3),IPHSE(3),IXCOR(3)
0005        COMMON LABF(135),IFILE,ICH1,ICH2,NRC(8),NSK(8),NTH,NSEC,FL,FH
0006        DATA LOCT/2HLO,2HCT,2H5 /,IDCAC/2HDC,2HAC,2H5 /,IFILT/2HFI,
0007       1 2HLT,2H5 /,IPHSE/2HPH,2HSE,2H5 /,IXCOR/2HXC,2HOR,2H5 /,
0008       1 IPSPT/2HPS,2HPT,2H5 /
0009        WRITE(1,100)
0010    100 FORMAT(/"NO. OF FILES? _")
0011        READ(1,*)NFILES
0012        WRITE(1,113)
0013    113 FORMAT(/"INPUT FILE NUMBERS!! ")
0014        READ(1,*)(JFILE(I),I=1,NFILES)
0015        WRITE(1,103)
0016    103 FORMAT(/"INPUT RECORD LENGTHS! _")
0017        READ(1,*)(NRC(I),I=1,NFILES)
0018        WRITE(1,102)
0019    102 FORMAT(/"RECORD SKIP SEQUENCE!! ")
0020        READ(1,*)(NSK(I),I=1,NFILES)
0021        WRITE(1,106)
0022    106 FORMAT(/"INPUT TWO SAMPLE REDUCTION RATES!! _")
0023        READ(1,*)NS(1),NS(2)
0024        WRITE(1,114)
0025    114 FORMAT(/"INPUT SAMPLE RATE!! ")
0026        READ(1,*)SR
0027        WRITE(1,115)
0028    115 FORMAT(/"INPUT NO. OF CHANNELS!! _")
0029        READ(1,*)NC
0030        WRITE(1,121)
0031    121 FORMAT(/"INPUT NO. OF SEGMENTS!! _")
0032        READ(1,*)NSG
0033        WRITE(1,122)
0034    122 FORMAT(/"INPUT MAXIMUM TIME DELAY!! _")
0035        READ(1,*)TMAX
0036        WRITE(1,104)
0037    104 FORMAT(/"INPUT TWO SEQUENCE NUMBERS OPPOSITE EACH PROGRAM!!"///
0038        WRITE(1,105)15446B,2HdD,15446B,2HdA
0039    105 FORMAT(2A2,"PROGRAM:",6X,"1ST.,2ND.",2A2//)
0040        WRITE(1,107)
0041    107 FORMAT(1X,"FLOCT",11X,"_")
0042        READ(1,*)ISEQ(1,1),ISEQ(1,2)
0043        WRITE(1,108)
0044    108 FORMAT(1X,"DCAC",12X,"_")
0045        READ(1,*)ISEQ(2,1),ISEQ(2,2)
0046        WRITE(1,109)
0047    109 FORMAT(1X,"FILTR",11X,"_")
0048        READ(1,*)ISEQ(3,1),ISEQ(3,2)
0049        WRITE(1,110)
0050    110 FORMAT(1X,"PSPT",12X,"_")
0051        READ(1,*)ISEQ(4,1),ISEQ(4,2)
0052        WRITE(1,111)
0053    111 FORMAT(1X,"PHSE",12X,"_")
0054        READ(1,*)ISEQ(5,1),ISEQ(5,2)
0055        WRITE(1,112)
171737 0056    112 FORMAT(1X,"XCORR",11X,"_")
```

Program Listing A-9-1 MAIN (cont.)

```
PAGE  0002  MAIN      (FTN4--RELEASE 24177B--JULY, 1971)

0057        READ(1,*)ISEQ(6,1),ISEQ(6,2)
0058        WRITE(1,125)15446B,2H11,2HV
0059        IFILE=0
0060        DO 10 I=1,NFILES
0061        DO 20 J=1,2
0062        NTH=NS(J)
0063        FL=1.
0064        FH=SR*.67/(2.*NTH)
0065        DO 20 K=1,6
0066        DO 20 L=1,6
0067        IS=ISEQ(L,J)
0068        IF(IS.NE.K)GO TO 20
0069        GO TO(1,2,3,4,5,6),L
0070      1 IFILE=JFILE(I)-IFILE
0071        ICH1=I
0072        NSEG=IFIX(SR)
0073        CALL EXEC(8,LOC1)
0074        NCHA=LABF(37)
0075        IF(NC.LT.NCHA)NCHA=NC
0076        IFILE=JFILE(I)
0077        GO TO 20
0078      2 CALL EXEC(8,IDCAC)
0079        WRITE(1,118)
0080    118 FORMAT(/15X,"DCAC COMPLETED")
0081        GO TO 20
0082      3 CALL EXEC(8,IFILT)
0083        WRITE(1,119)FL,FH
0084    119 FORMAT(/15X,"FILTR COMPLETED WITH BAND PASS ",E12.3," TO ",
0085       1 E12.3," CYCLES/MIN.")
0086        GO TO 20
0087      4 NSEG=NSG
0088        WRITE(1,120)
0089    120 FORMAT(/15X,"PSPT INITIATED!!")
0090        FH=LABF(38)*.67/2.
0091        ISEG=LABF(39)/NSEG
0092        SEGL=(60./LABF(38))*256*ISEG
0093        LREC=SEGL*NSEG
0094        LSEG=SEGL
0095        MSEG=SEGL/60.
0096        MREC=LREC/60.
0097        ISECR=MOD(LREC,60)
0098        ISECS=MOD(LSEG,60)
0099        WRITE(1,123)MREC,ISECR
0100    123 FORMAT(/15X,"RECORD LENGTH =",X,I3,X,"MINUTES",X,I3,X,"SEC.")
0101        WRITE(1,124)MSEG,ISECS
0102    124 FORMAT(/15X,"SEGMENT LENGTH =",X,I3,X,"MINUTES",X,I3,X,"SEC.")
0103        NCHA=LABF(37)
0104        IF(NC.LT.NCHA)NCHA=NC
0105        DO 21 N=1,NCHA
0106        ICH1=N
0107        CALL EXEC(8,IPSPT)
0108        WRITE(1,125)15446B,2H11,2HV
0109    125 FORMAT(3A2)
0110     21 CONTINUE
0111        GO TO 20
0112      5 WRITE(1,116)
```

171738

Program Listing A-9-1 MAIN (cont.)

```
PAGE  0003  MAIN      (FTN4--RELEASE 2417/B--JULY, 1971)

0113     116 FORMAT(/15X,"PHSE INITIATED!!")
0114         DO 22 N=1,NCHA
0115         ICH1=N
0116         ICH2=N+1
0117         IF(N.EQ.NCHA)ICH2=1
0118         CALL EXEC(8,IPHSF)
0119         WRITE(1,125)15446B,2H11,2HV
0120      22 CONTINUE
0121         GO TO 20
0122       6 TEMP=FL
0123         FL=TMAX
0124         WRITE(1,117)
0125     117 FORMAT(/15X,"XCORR INITIATED!!")
0126         N=IFIX(TMAX*LABF(38)/120.)*2
0127         IF(N.GT.128)TMAX=128.*60./LABF(38)
0128         WRITE(1,126)TMAX
0129     126 FORMAT(/15X,"MAXIMUM TIME SHIFT IS ",F7.1)
0130         DO 23 N=1,NCHA
0131         ICH1=N
0132         ICH2=N+1
0133         IF(N.EQ.NCHA)ICH2=1
0134         CALL EXEC(8,IXCOR)
0135         WRITE(1,125)15446B,2H11,2HV
0136      23 CONTINUE
0137         FL=TEMP
0138      20 CONTINUE
0139      10 CONTINUE
0140         STOP
0141         END

**  NO ERRORS*
```

APPENDIX B

The modified Krebs-Ringer solution used in this work had the following composition:

Sodium	144.0 mM/liter
Potassium	5.4 mM/liter
Calcium	2.5 mM/liter
Magnesium	1.2 mM/liter
Chloride	128.8 mM/liter
Bicarbonate	22.0 mM/liter
Phsophate	1.2 mM/liter
Glucose	10.1 mM/liter